The Pennsylvania State University

Communications and Space Sciences Laboratory

University Park, Pennsylvania

Final Report

Office of Naval Research

N00014-86-K-0677

Submitted by

A. J. Ferraro, The Pennsylvania State University

Alfred Y. Wong, University of California, Los Angeles

K. Papadopoulos, Science Applications International Corporation

Introduction

The contract period for the University Research Initiative was from September 15, 1986 to September 30, 1989. The Pennsylvania State University served as the prime contractor with A. J. Ferraro as Principal Investigator; subcontracts were awarded to the University of California at Los Angeles (A. Y. Wong) and S.A.I.C. (D. Papadopolous). Reports of these subcontractors are attached to this final report. Support from the Geophysical Institute (J. V. Olson) was provided by a separate ONR contract and a final report was submitted earlier. A broad definition of the tasks of the above institutions are:

Penn State - Develop the science utilizing the HIPAS facility.

U.C.L.A. - Operation of the HIPAS facility for cooperative experiments.

S.A.I.C. - develop theoretical concepts related to ionospheric modification.

Geophysical Institute - Provide information on the development of electrojet current events.

There were four experimental campaigns established during this contract covering the period

June 15-25, 1987
October 13-23, 1987
July 11-22, 1988
July 12- Aug. 8, 1989

The performance summary of the HIPAS facility is described in detail in the U.C.L.A. attachment to this final report.

Overview

The broad research objective of this program has been to investigate unique concepts for generating ULF, ELF and VLF using the ionosphere as the "wireless" antenna. The "Wireless Antenna" or HF demodulation experiment was demonstrated by A. J. Ferraro in 1980 using the Arecibo Observatory's heating facility. Modulation of the dynamo current system at that latitude was the major source for the "wireless" antenna.

Some of the major experimental accomplishments are

- Excellent quality of generated ELF and VLF signals .
- Determination of D-region electron density profiles at high latitudes for large sunspot numbers.
- slow beam steering to examine the structure of the electrojet current system mapped down into the D-region
- determination of electrojet activity from ELF/VLF polarization characteristics
- created multiple VLF ionospheric sources (two-element VLF arrays)
- Fast beam steering - the painting technique; a potential method of increasing ELF power.
- Short range field measurements in Alaska with the Penn State Mobile Van.
- Demonstrated the stability of the current system to support bi-phase PSK and Quad-phase PSK to increase data rates.

Based upon the July 1988 campaign it was estimated that the ELF power produced by HIPAS for one spot exceeded one milliwatt 80% of

the time. This figure was arrived at by taking 2000 Hz data and scaling to 100 Hz.

Geomagnetic and Solar Conditions during the HIPAS Campaigns

Attached are summarized data for the solar flux and earth's magnetic field. One can refer to these to estimate the ionospheric conditions during the experiment times that some campaigns were conducted during the increasing active phase of the solar cycle.

AGARD Symposium

Attached is a preprint of a paper presented at the Spring 1990, Electromagnetic Wave Propagation Panel Symposium held in Bergen, Norway.

List of Titles and Abstracts of Key Scientific Achievements

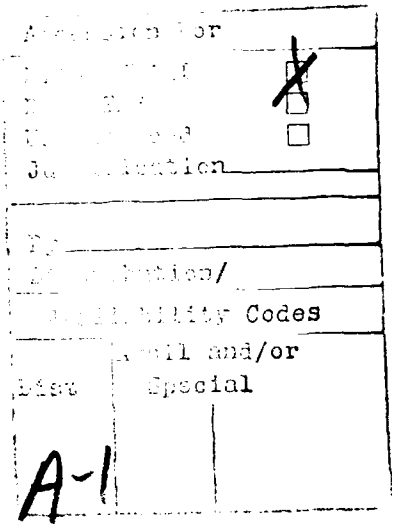

October 1987

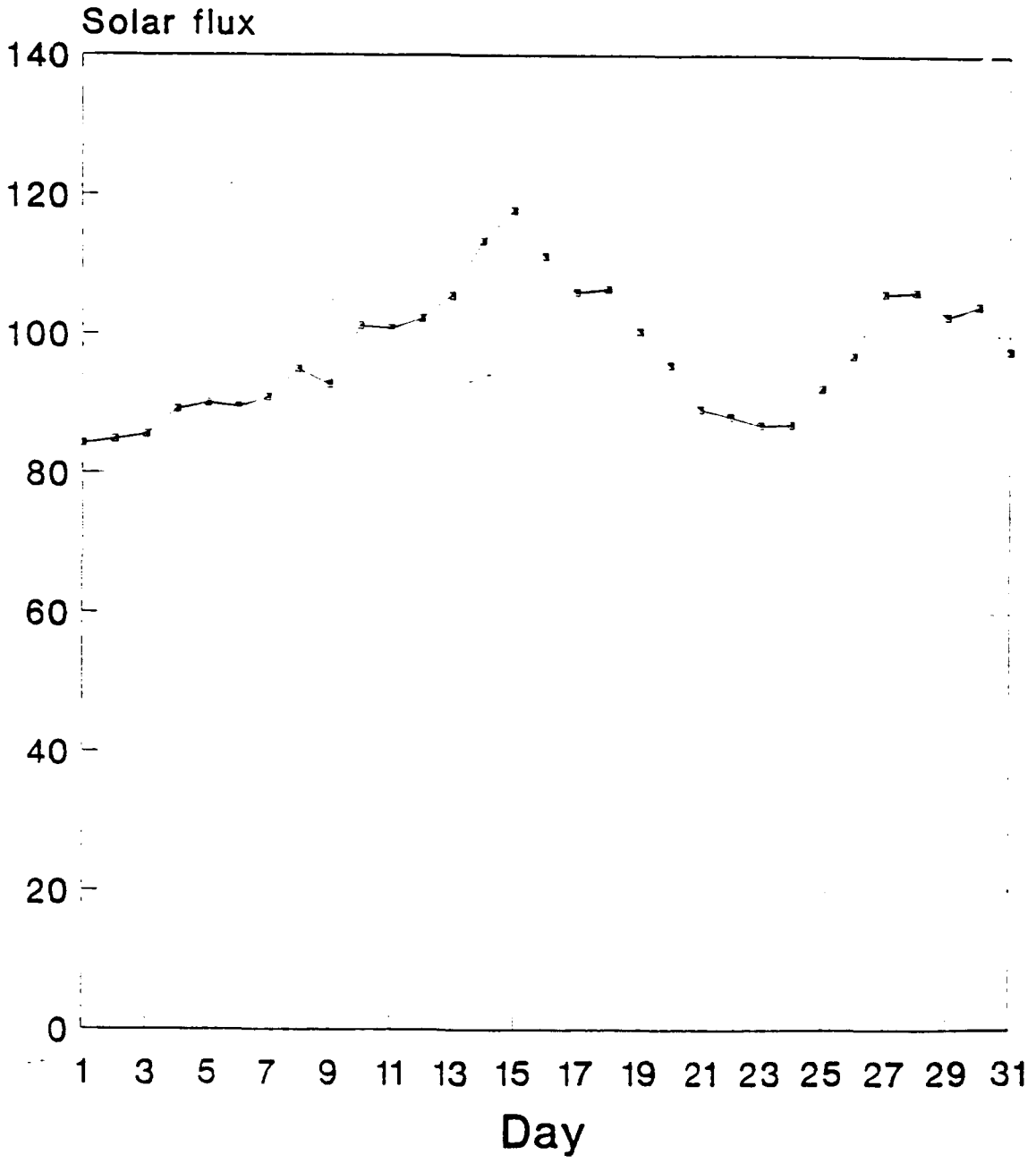

Ottawa 10.7 cm solar flux for October 1987. The measurements are adjusted to 1 AU, measured at 17:00 UTC daily and expressed in units of 10^{-22} watts/m^2/hertz. Data taken from the National Geophysical Data Center.

July 1988

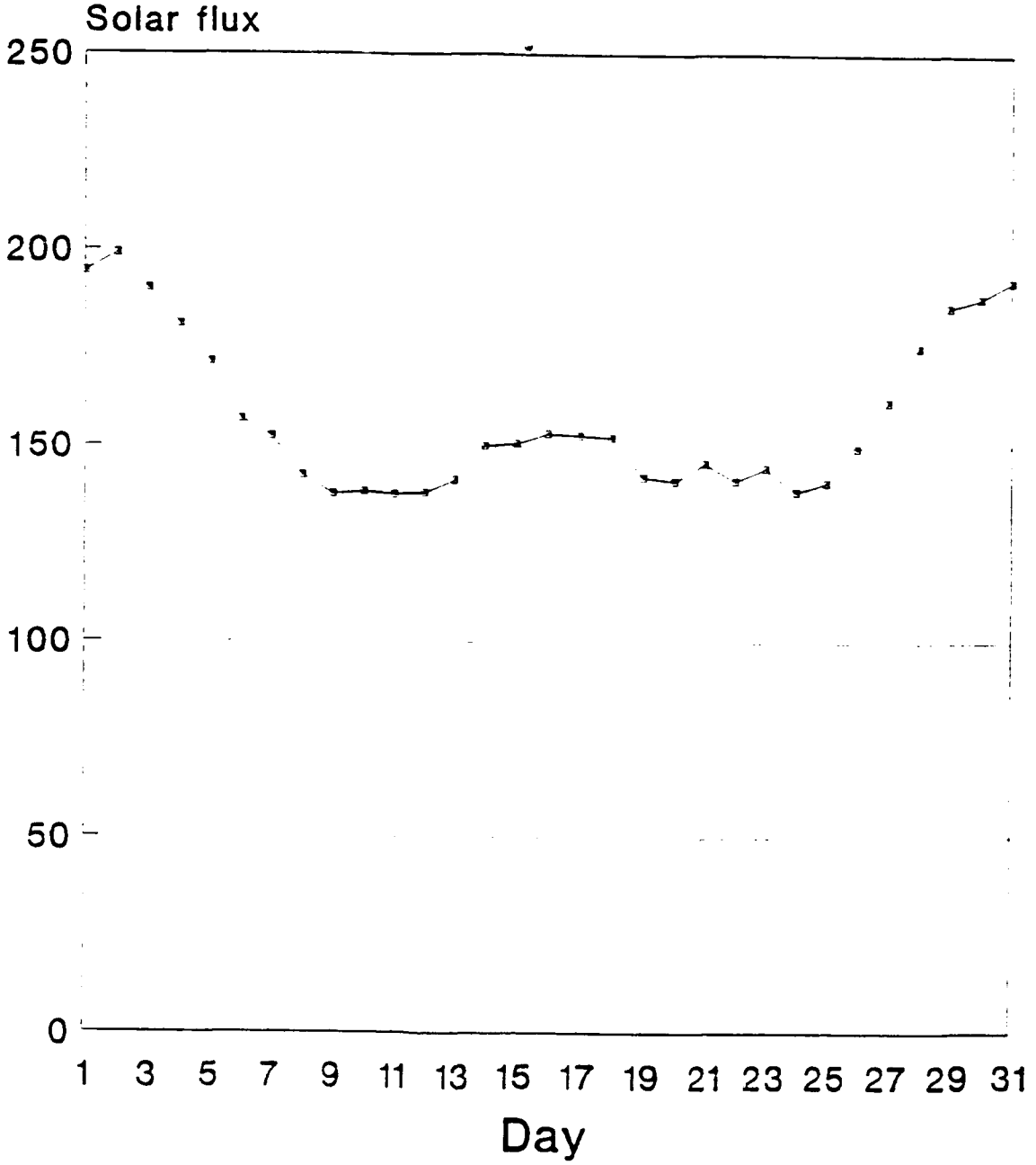

Ottawa 10.7 cm solar flux for July 1988. The measurements are adjusted to 1 AU, measured at 17:00 UTC daily and expressed in units of 10^{-22} watts/m^2/hertz. Data taken from the National Geophysical Data Center.

October 1987

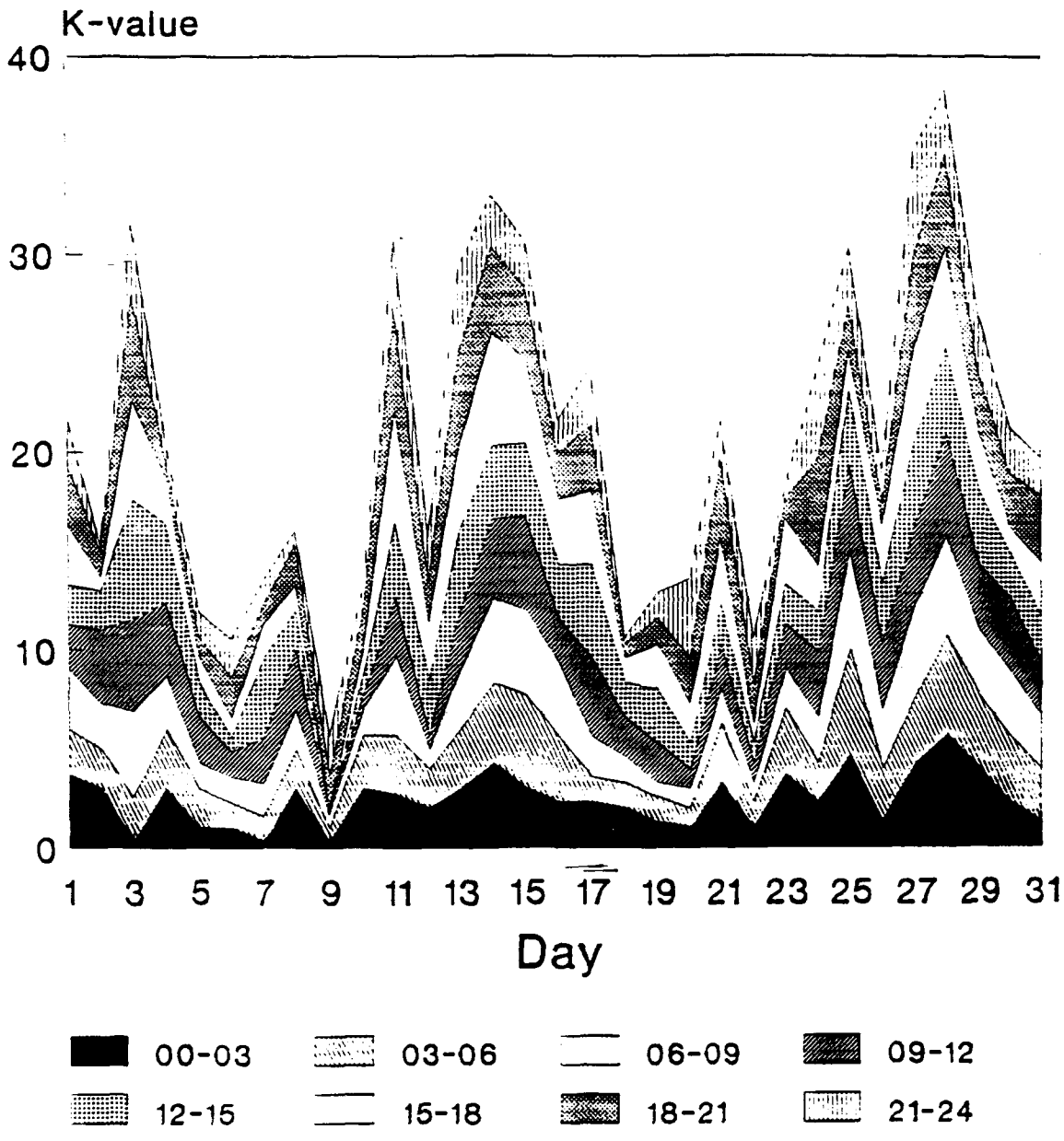

Planetary K indices for October 1987. Each shaded area shows 3-hour range. Data taken from the National Geophysical Data Center.

July 1988

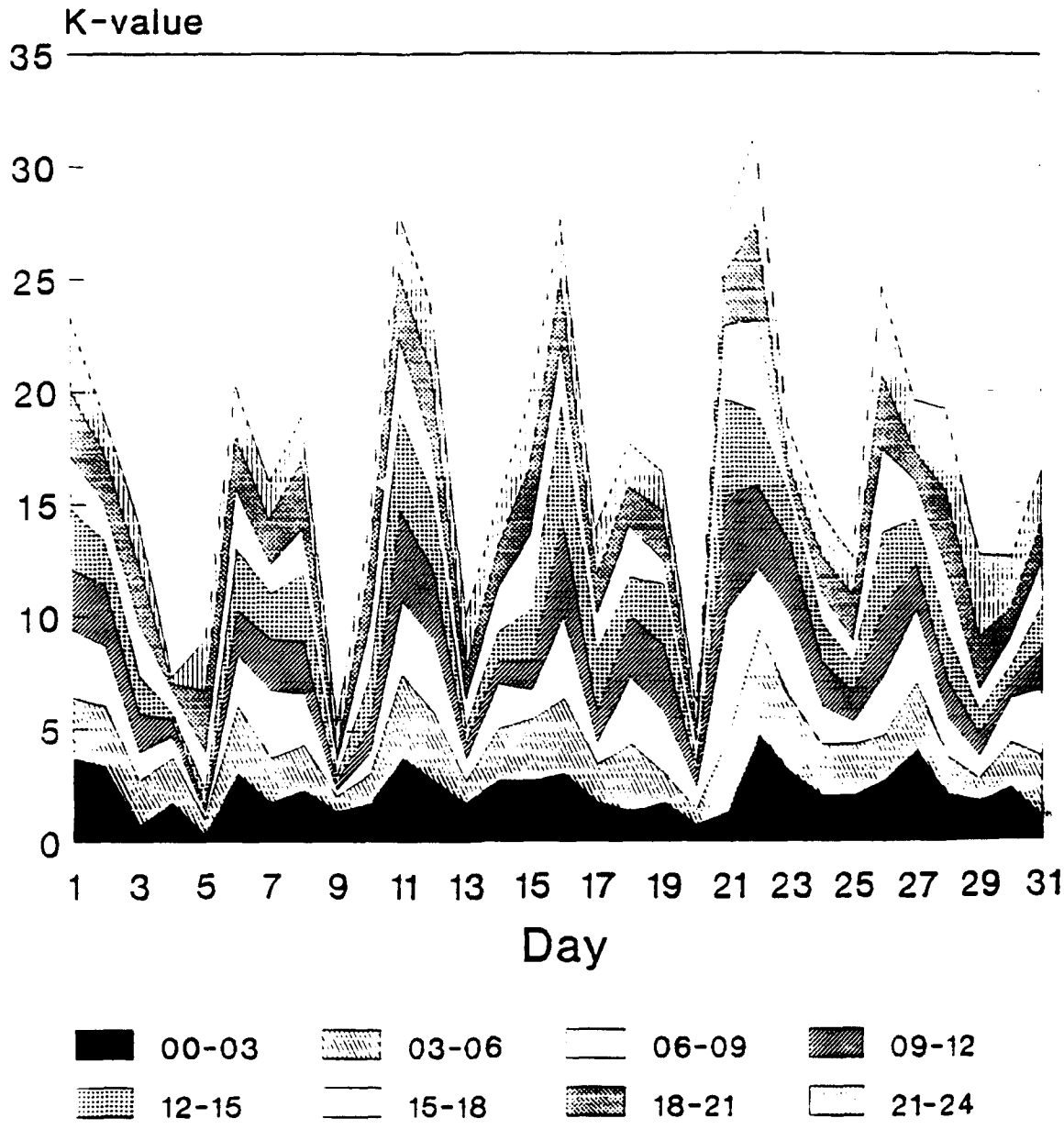

Planetary K indices for July 1988. Each shaded area shows 3-hour range. Data taken from the National Geophysical Data Center.

An Experimental Method to Determine the Phase Height of an Artificially Created Ionospheric ELF/VLF Source

This report describes the design and operation of a system which can determine the phase height of extremely long wavelength electromagnetic emissions from natural ionospheric currents which have been modulated by radio wave heating. Previously, experimental campaigns at Arecibo have utilized collocated heater transmitters and ionospheric signal receivers which greatly simplifies the task of determining a phase relationship between the heater modulation wave and the received signal wave. However, future experiments envision extensive portable receiver operation at sites quite remote and distant from the heater transmitter.

A low cost portable system is developed. The system consists of two stages for operation at the HIPAS heater site and the receiver site. Prior to an experimental session the two systems are compared to determine an initial phase relationship. One system then provides the modulation to the heater wave while the other provides a reference signal at the receiver site. A programmable frequency synthesizer is also incorporated into the system which will coexist with the existing equipment controllers.

A function relating signal phase shift to source phase height is developed for the general case of an oblique incidence heater beam. This function is reduced for the considered case of a normal incidence heater beam. Selected source phase height results from an experimental campaign at HIPAS are presented to illustrate the systems performance in actual use (figures attached).

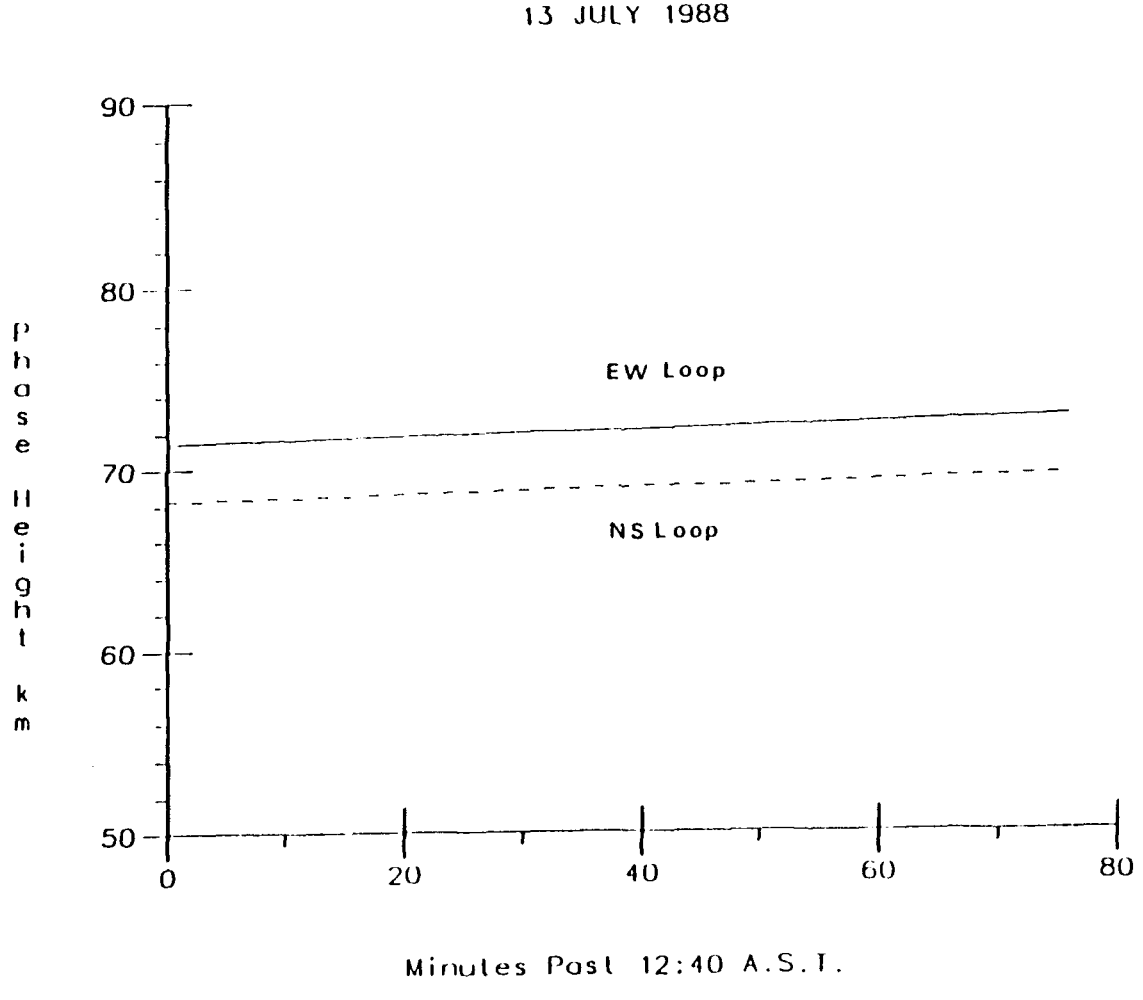

Phase height 13 July 1988 @ 12:40 A.S.T.

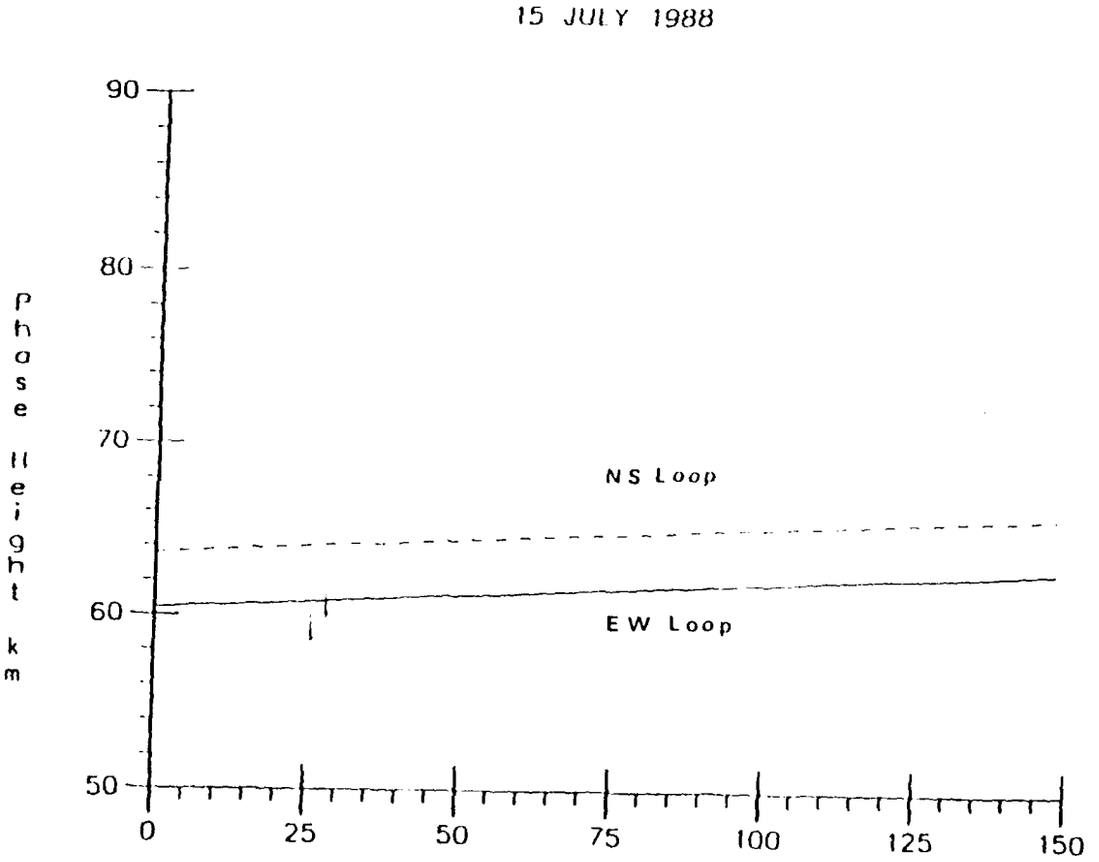

Phase height 15 July 1988 @ 24:40 A.S.T.

An Investigation of the Obliquely Downgoing ELF/VLF Generated Waves During Ionospheric Modification Heating Experiments at High Latitudes

This document has reported on a series of ionospheric modification heating experiments conducted at the High Power Auroral Simulation (HIPAS) facility near Fairbanks, Alaska over a period of 2 years from June 1987 to August 1989. Particular emphasis is devoted to the study of the polarization of the electric field of the obliquely downgoing ELF/VLF electromagnetic waves generated by irradiation of the heated volume from a high power modulated HF wave.

A single slab model of the ionosphere has been chosen to simplify the solution of the Booker quartic which is used to compute the wave path and direction. The ELF/VLF source is simulated by two horizontal current sources; one in the east-west direction, and one in the north-south direction due to modulation of the electrojet which flows at an altitude of 100 km to 110 km. The waves resulting from these two orthogonal sources are superimposed on the ground to give the tilt angle and ellipticity of the incoming waves which are the parameters being measured.

The polarization ellipse gives a very good indication of the presence of an electrojet event. The polarimeter is sensitive even with weak ELF/VLF returns. During all the experiments, it is able to provide instantaneous visual information on the ground and can provide guidance as to the scientific measurement schedule during campaigns. When pulsations were first encountered, it showed a very distinct signature. This is a big advantage over the

magnetogram records which are not immediately available during the course of the experiments.

It has been shown that the polarimeter is a viable part of the ELF/VLF scientific program in furnishing diagnostics. It can also provide a rough estimate of electron density and collision frequency. For certain electron densities and collision frequencies, the tilt angle of the polarization ellipse is shown to track the angular displacement of the horizontal source current. This allows the angular direction of the source current to be determined.

The attached figure shows the tilt angle of the polarization ellipse versus source angular displacement. For a reasonable range of electron collision frequencies the expected observed tilt does track the source angular displacement. For those cases, the observed ground level polarization is a reasonable indicator of current direction flow in the ionosphere.

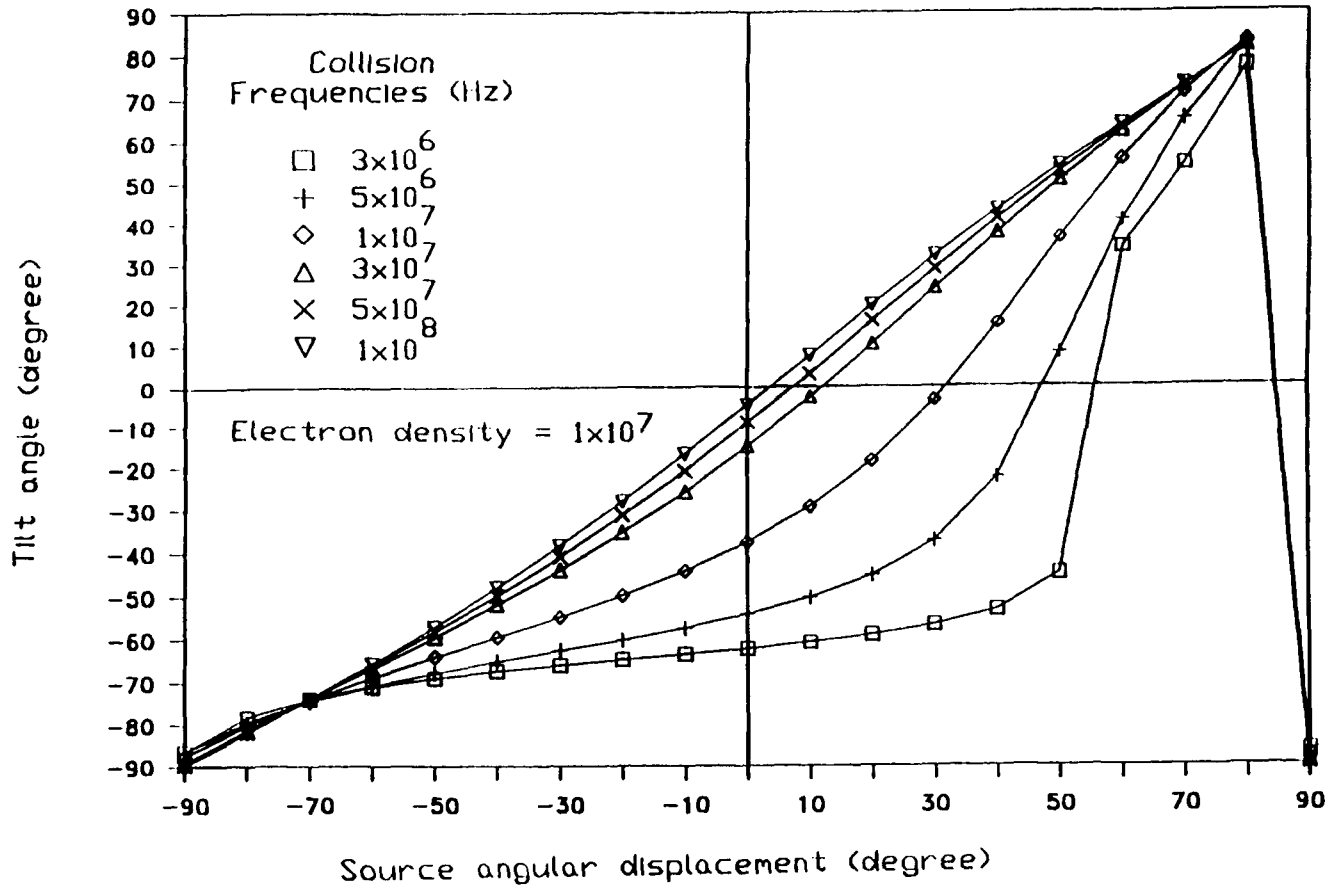

Tracking of tilt angle for electron density of $1\times10^{7}(m^{-3})$

An Investigation of the Polar Electrojet Current System Using Radio Wave Heating of the Lower Ionosphere

The HIgh Power Auroral Stimulation (HIPAS) heating facility has been used to modulate D-region ionospheric currents at high latitudes, producing extremely low frequency (ELF) radio wave emissions. The behavior of these ionospheric currents can be deduced from a comprehensive study of the ELF signals received at a local field site. This document examines the relationship between the ELF magnetic field strength measured on the ground and the intensity of an overhead electrojet current. The mapping of the polar electrojet current from the E region down through the D region, where it can then be modulated by the heater beam, is investigated. A finite difference solution to the electrojet mapping problem is presented in which arbitrary conductivity profiles can be specified. Results have been obtained using a simple Cowling model of the electrojet. These results indicate that for an electrojet flowing at an altitude of 100 km with a scale size in excess of 100 km, the mapping of the horizontal current density can be completely characterized in terms of the Pedersen and Hall conductivities. This indicates that the mapping becomes independent of scale sizes which exceed 100 km. The downward mapping of the electrojet current and associated electric field in the presence of ionospheric conductivity irregularities has been studied. It was demonstrated that D region conductivity irregularities do not significantly change the downward mapping of ionospheric electric fields. However, these conductivity irregularities were found to have a major influence upon the

downward mapping of ionospheric currents. A promising new diagnostic technique, for studying ionospheric D region currents, has been implemented using the HIPAS facility. This technique involves HF beam steering for localized ELF generation in the mapped region below electrojets. Beam steering has been used to deduce the strength and current distribution of the polar electrojet, and for charting the movements of overhead currents. The attached figure shows ELF relative field strength for a conical scan. The dashed curve is expected ELF return from a uniform current sheet while the solid curve is due to the actual overhead current distribution. The difference between these two curves is a measure of the horizontal variation in current density. The next figure is a deduced ionospheric current map showing current density strengths over the region of conical scan.

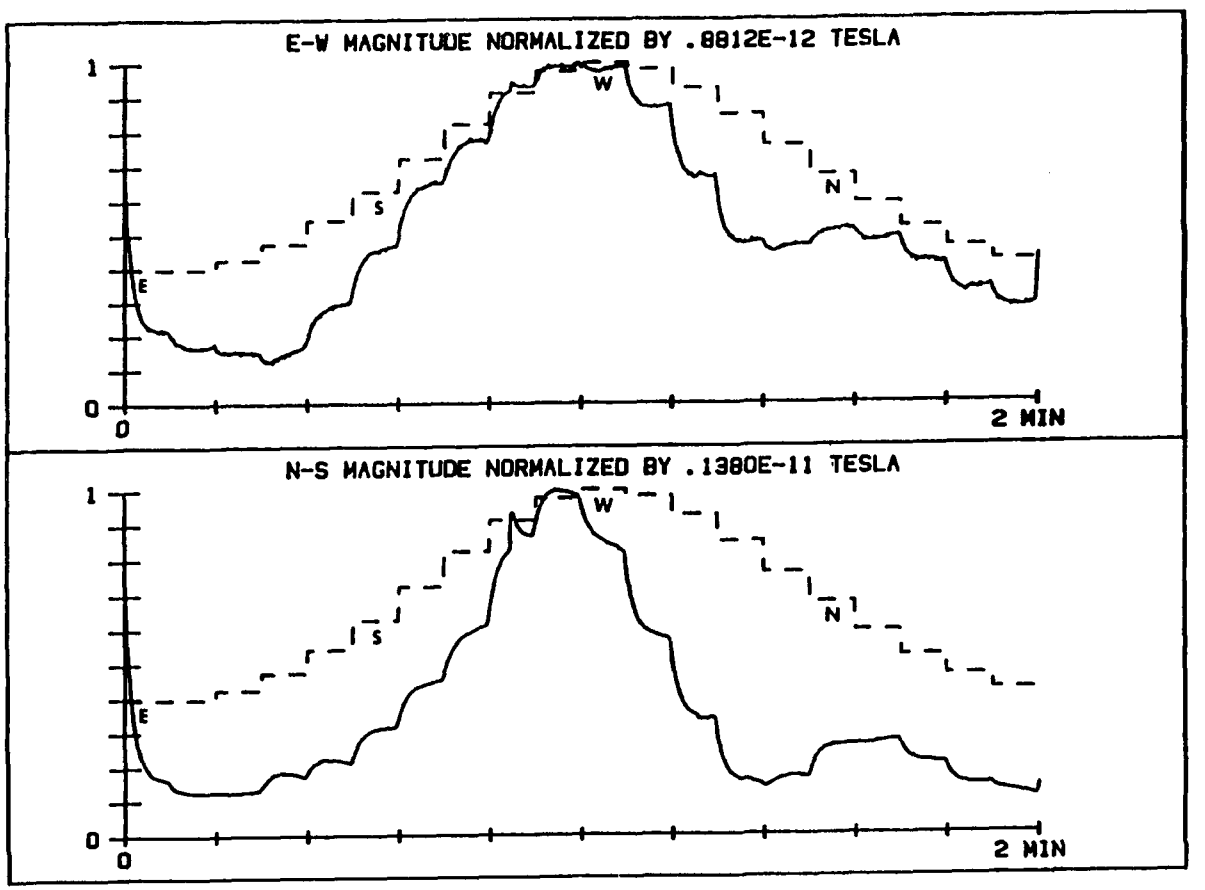

Conical scan magnitude data. The data file was CNSCAN21.29, the start time was 04:52:00, and the date recorded was 7/21/88.

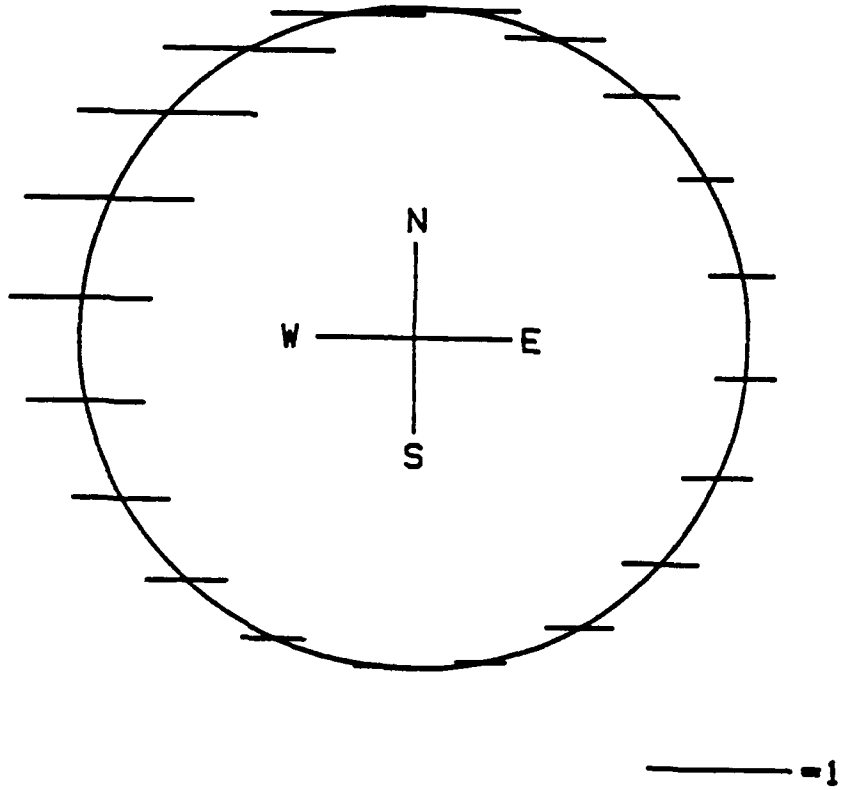

Ionospheric current map

Determination of D-region Electron Densities Using the Stepped Frequency Technique with Ionospheric Heating

This document describes a new technique for deriving D-region electron densities from the Extremely Low Frequency (ELF) signals produced by heating of the D-region of the ionosphere. A catalog approach was employed in this technique. A class of exponential density models were used to create a catalog of transmission coefficients deduced from the full wave theory, and stored in a file. The electron density profiles were derived by searching the catalog with the transmission coefficient extracted from the locally received ELF signals and selecting the best fit model to the observation. In particular, the degree of electron density ionization of the D-region at high latitudes can be studied. The heating facility near Fairbanks, Alaska, known as the HIPAS facility was used for this work. In this document the theory of electron density synthesis is described, results of actual ELF data presented, and preliminary electron density profiles determined. A new future ionospheric measurement technique FDTD is discussed.

Attached are figures giving examples of stepped frequency data and derived D-region electron densities.

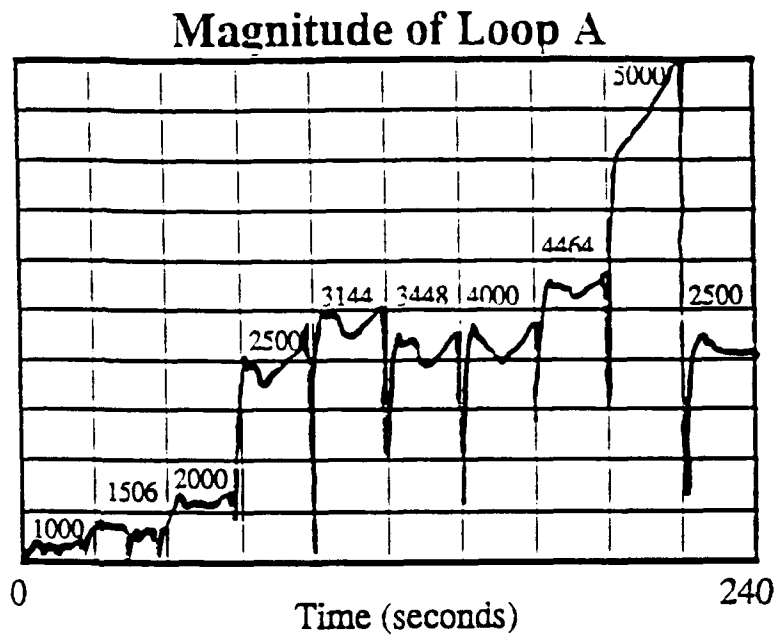

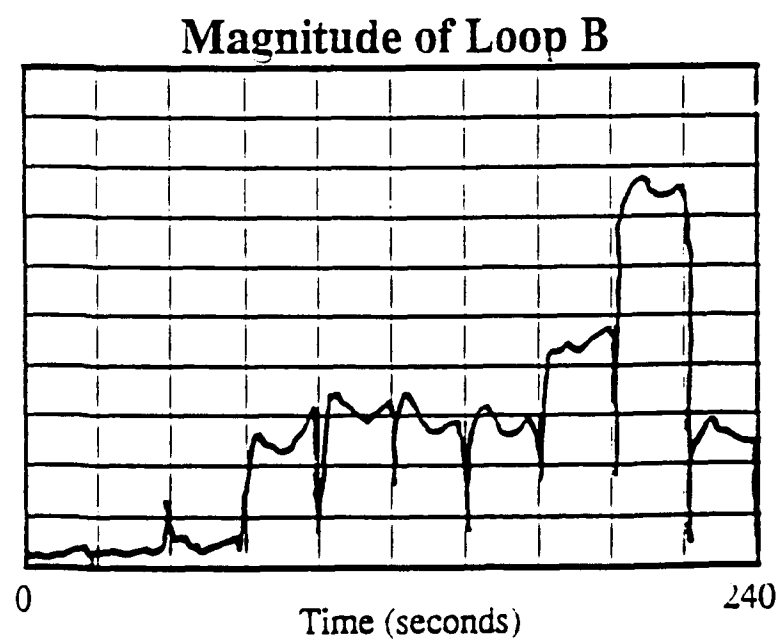

Example of stepped data. A sample of the magnitude of received high band stepped frequency data taken at HIPAS on 10/14/87 at 17:08 to 17:12 A.S.T..

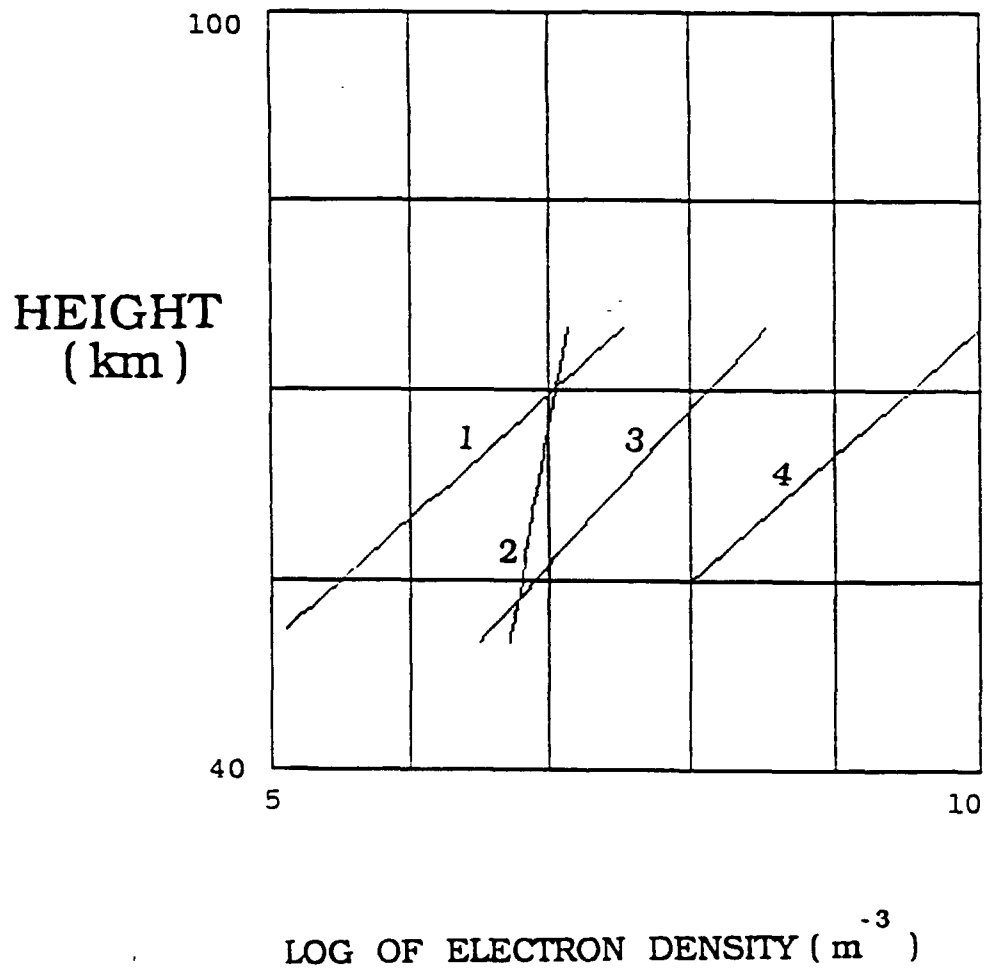

Electron density profiles. 1. Mitro-Rowe density profile; 2. density profile for 17:28:00 of 10/14/87 AKT; 3. density profile for early morning of 10/16/87 AKT; 4. density model used by Barr.

Development of a Diagnostic System for Ionospheric Modification Studies at High Latitudes

This report describes the design and operation of a diagnostic system for the study of extremely long wavelength electromagnetic emissions from natural ionospheric currents which have been modulated by radio wave heating. The ionosphere at high polar latitudes is complex in structure and dynamic in behavior, particularly during periods of auroral activity and geomagnetic disturbance. It also contains strong current systems which hold great potential, when properly modulated, as radiators of ULF, ELF, and VLF signals. Two experimental campaigns have been conducted to investigate the generation and reception of signals produced through modulated ionospheric heating from the High Power Auroral Stimulation transmitters near Fairbanks, Alaska.

The diagnostic system includes a dual-channel receiver capable of operation at frequencies below 8 kHz, and companion microcomputers for real-time data acquisition and processing. Software has been developed to control data collection, analysis, and storage in a "user-friendly" fashion; several configurations and operational modes provide maximum flexibility under a variety of experimental conditions. Specific provisions are made for coherent demodulation and high-speed digital sampling of incoming signals.

Additional computer control the transmitter modulating frequency and receiver tuning. These permit synchronized, operation of the transmitter and receiver sites according to a preselected schedule, reducing the need for manual intervention and

permitting rapid reselection of operating frequency. Selected results from the experimental campaigns are presented to illustrate the system's capabilities and performance in actual use.

A more detailed discussion is allocated to this report since the receiver plays an important role in developing the science.

Loop Antennas

Loop antennas are simple to construct and provide stable operation in all climates. With the addition of capacitive loading, the resonant frequency of the antenna system may be lowered to obtain voltage amplification of the output signal and improved selectivity. A center-tap allows connection to balanced transmission line, and the azimuthal pattern variation lends itself well to measurement of wave direction and polarity. Three types of loop antennas are available for use with the reconfigurable receiving system.

The first set of loops was used in previous experimental campaigns, and each consists of 200 turns of number 14 wire (center-tapped) upon a 1 meter diameter wooden form. The coils have a measured DC resistance of approximately 7 ohms and an inductance of .075 henry with a self-resonant frequency near 8000 Hz. For calibration, a single-turn loop of 0.5 m diameter is mounted coaxially at a distance of 0.5 m. The drive signal is applied through a 50 ohm series resistor, and the current in the calibration coil is obtained by measurement of the voltage drop across the resistor. Mathematical formula provide a relationship for the mutual inductance between two coaxial loops used for calibration.

The considerable size and weight of these units necessitated an attempt to simplify the logistics and expenses involved in transportation of the receiver system. A second set of loop antennas was constructed with 800 turns, of number 28 wire upon 0.5 m diameter wooden forms. The product of the number of turns and loop cross-sectional area was not altered, in order to achieve electrical operation comparable with the original units. The redesigned antenna could be easily carried by one person, eliminating the need for special packaging and handling.

Following construction of wooden coil forms and scramble-wound center-tapped loops, the DC resistance was measured as 98 ohms and the inductance as 0.3 henry. In order to simplify the calibration process, a single-turn calibration loop was wound directly on top of the receiving loop itself; instead of the complicated mutual-inductance expression referred to above, the new design could now be treated as an ideal transformer. Frequency response measurements revealed that these loops resonated at approximately 1200 Hz due to the increased inductance and self-capacitance of the smaller design. As expected, the increased resistance of a greater number of turns would with smaller wire also reduced the Q factor.

For ULF reception below 10 Hz, several loop antennas of 20,000 turns upon a mu-metal core were obtained from geophysical researchers at the University of Texas. At these very low frequencies, calibration is performed in an incident magnetic field produced by the rotation of a motor-driven precision bar magnet. Although a very long and slender core having a large ratio of length to diameter will maximize the permeability, several factors

render this approach impractical. These include the mechanical integrity of the resulting structure, the effect of elastic strains upon the core's magnetic properties, and possible desentization by the earth's geomagnetic field. The latter is due to magnetic saturation of the core reducing the effective permeability, yielding an antenna sensitivity which varies greatly with geographic orientation.

In order to minimize these effects, the length to diameter ratio is chosen to be much smaller than the theoretical optimum, forcing the effective core permeability to be dependent solely upon this factor. The ULF loop antennas satisfy the criteria for a "geometry limited" design which performs in a stable and predictable manner.

Antenna Tuning and Transmission Line Interconnection

The loop antenna may be treated as a parallel LC tank circuit, and its resonant frequency lower by an increase in capacitance through the external addition of parallel capacitors. The mu-metal core ULF antenna is operated with a single capacitor across its terminals at all times, but the air-core ELF/VLF receiving loops are tuned to the specific resonant frequency of interest.

The original technique, developed for earlier experimental campaigns, utilized a large rotary switch at the antenna site which sequentially connected preselected sets of mylar and silver mica fixed capacitors. Assembly of these capacitor combinations was largely trial-and-error, necessitating measurement of frequency response following each modification. Operation was limited to pretuned channels, and manual selection of the proper switch

setting was necessary. Since the tuning assembly was remotely located at the antenna loop, adjustment required the dispatch of an operator.

Although originally acceptable, this method became increasingly unwieldy when a comprehensive program of stepped frequency measurements was begun. The ability to rapidly retune the antennas was required in order to permit operation on multiple frequencies within a short span of time; otherwise, the dynamic nature of the ionosphere would preclude valid comparison of results obtained at different frequencies. The rotary switch tuning box was replaced by a relay switching unit which contains a binary sequence of sixteen composite capacitors connected in parallel through relay contacts. A 16-bit binary number is placed upon the relay control lines; each energized relay switches in a capacitance twice that of the preceding (less significant) bit position. The resultant combination can synthesize any required value, limited in range by a maximum of all capacitors simultaneously in-circuit and limited in resolution by the capacitance of the initial increment.

The total capacitance at the tuning unit terminals is equal to the product of the binary value upon the control inputs, and the capacitance associated with the least significant bit position. As built, the base unit is approximately 20 pf, and the maximum value available is approximately 1.31 uf. These values permit tuning of the 1 m diameter loops over an approximate range of 800 Hz to 8000 Hz, and the 0.5 m diameter loops over 200 Hz to 1200 Hz. In order to ensure a monotonic sequence without missing values, the

capacitance associated with each bit position was carefully trimmed on an impedance bridge equipped with a digital readout.

Equipment Control at Transmitter and Receiver Sites

The primary functions of the main data processing system are real-time data acquisition, analysis, display, and storage; in actual operation, a minimum amount of processor time remains for the performance of other tasks. The video display and keyboard are dedicated to instantaneous display of incoming data and interactive operator communications. The assignment of additional functions would then prove detrimental to the overall system operation. Further, 32 bits of parallel output are required for control of each synthesizer's frequency, and 16 bits are used to set the antenna loading for each tuned loop; as equipped, the 8088-based system lacked this extensive parallel input-output capacity.

For these reasons, two Apple II computers used in earlier experimental campaigns were restored to service as equipment controllers for the transmitter and receiver sites. Serial ports are available on the multifunction board in the data processing computer to establish communications links with these systems, and an adequate parallel interface capability was provided by existing Apple II peripheral circuit cards which had seen use in prior data acquisition systems. Although the operation of the Apple II computers under control of the interpreted Applesoft BASIC language is not particularly fast, it proved sufficient to meet the demands of controlling the attached devices with fractional second accuracy, marking a significant improvement over purely manual methods.

The Apple II computer systems utilize the Synertek 6502 microprocessor operating at a clock speed of 1.023 MHz, with 48 kilobytes of random access memory. Integral video display circuitry provides the 24 line by 40 character monochrome text mode used in this application. Peripheral cards attach to an eight slot expansion bus; unlike the IBM PC-XT design which permits addressing of expansion cards independently of slot position, the Apple II motherboard contains address decoding circuitry which usually requires assignment of a specific edge connector to each interface card.

Since all recording of experimental data is performed on the 8088-based data processor, only the software for equipment control need be resident on the Apple II system. Adequate disk storage is provided by a 5.25 inch single-sided single-density floppy disk drive capable of recording 143 kilobytes per volume. The disk controller card resides in slot 6 of the Apple II expansion bus.

Slot 5 contains a Prometheus VERSAcard multifunction board, which includes an RS-232 serial port, parallel printer port and real-time clock/calendar. Although it physically occupies a single position on the bus, the timekeeping hardware is logically addressed as slot 1, and the printer port as slot 7; these connectors become unusable for other peripheral cards. Further, slot 0 is reserved for access to additional read-only memory containing software enhancements. As a result, only slots 2, 3, and 4 remain available for installation of parallel interface cards, which proves sufficient for the existing receiver configuration but severely limits future expansion.

Design and Operation of Data Acquisition Interface Unit

Three modes of operation were envisioned for the diagnostic reception of ULF, ELF, and VLF emissions. In Mode 1, the incoming ELF or VLF signal is demodulated by the lock-in analyzer; the resulting in-phase and quadrature outputs are digitized at a rate far below that necessary for direct sampling of the baseband signal, and recorded on disk storage. Mode 2 provides high-speed digitization of the ELF or VLF signal prior to demodulation, requiring DMA operation to achieve the necessary throughput of values between the data acquisition board and random access memory. Mode 3 is intended for reception at ULF frequencies, which allow digitization of both the baseband signal and demodulator outputs at speeds comparable to those of Mode 1.

Data Collection and Recording Loop

Digitized data is placed in a data buffer as it is collected by the interrupt-driven background task. Two separate areas are allocated for alternate use to prevent lost information during the time required for recording. The buffers serve as shared memory for interprocess communication between multiple tasks, and ASYST provides predefined words which permit examination of the current buffer status from the foreground program.

The main program continuously monitors the active buffer, in order to update the displayed percentage of data accumulated. Every 10th set of I and Q measurements is extracted from the buffer as available for calculation of the corresponding magnitudes and phases; these are plotted on the graphic display to form a dynamic

representation of the incoming signal. More frequent screen updates are difficult to attain with the computing power found in the present equipment configuration. Further, a graphics presentation containing more detail would likely be of little value when displayed with the limited resolution video hardware currently in use. Plotting every tenth point has been found to give satisfactory results in actual experimental operation.

The foreground task also monitors the keyboard for activity during every iteration of the acquisition loop. If a keypress is detected, then the addition of points to the magnitude and phase plots is suspended and appropriate action is taken. Upon completion of the interactive command, the display is updated as quickly as possible in order to correctly reflect the data resident in the active buffer.

Unfortunately, ASYST permits only data acquisition operations to be concurrently multitasked; all other functions such as operator communication through the keyboard/display and disk file access must be handled in a preemptive manner due to the non-reentrancy of the disk operating system. Should too much time elapse before completion of command entry, it is possible for both buffers to become overwritten, destroying data which has been collected but not yet recorded on disk.

When a buffer is completely filled with data, the foreground routine detects that a switch to the alternate data area has occurred. It then writes the collected data to disk storage and clears the dynamic display areas before repeating the entire procedure on the other buffer. A flag variable, modified by an

interactive user command, is tested after each data file is written; if set, the acquisition loop is terminated and control is returned to the ASYST interpreter.

Although the transmitter modulator itself contains waveshaping circuitry intended to limit the high-frequency content of input signals, care must be taken to avoid rapid transients which can cause damage to the output stages of the power amplifiers. For this reason, modulation is typically removed from the transmitter when the synthesizer frequency is manually changed from its front-panel switches; remote synthesizer control in binary format, however, ensures amplitude continuity and allows the frequency to be reselected under full-power operating conditions.

Fairbanks Receiver Site

The receiver system was located in a wooded area immediately adjacent to the Elvey Building, which houses the Geophysical Institute on the campus of the University of Alaska at Fairbanks. The electronic and computer equipment was set up in a trailer which housed support circuitry for the Institute's induction magnetometers and earth current sensors. This allowed convenient access to the magnetometer outputs for digitization and storage by the receiver's data acquisition system.

All loop antennas were placed approximately 20 m from the trailer in order to minimize interference pickup by the sensitive receivers. An orthogonal layout was used to eliminate the manual rotation performed in prior experimental campaigns for determining the orientation of the modulated current system. For convenience, the loop antenna positions are referred to as "A" and "B". The

plane of the "A" loops is along the north-south axis with maximum sensitivity to signals produced by currents flowing in an east-west direction. Conversely, the "B" loops display maximum sensitivity to signals generated by currents aligned in a north-south direction. These designations are carried throughout the remainder of the dual-channel receiver system. Figure 23 is a photograph of the air-core loop antennas as deployed for the October, 1987 experimental campaign.

The 1 m diameter loop antennas were used for reception at frequencies between 800 Hz and 8000 Hz, while the 0.5 m loops were used at frequencies between 200 Hz and 1200 Hz. Extreme care was taken to prevent inadvertent phase reversals throughout the receiver system, with regard to the winding sense of the pickup and calibration coils as well as the balanced transmission line interconnections.

During the October campaign, routine testing controlled by the FRQSWP.001 software revealed a drop in the frequency response of the large (1 meter diameter) loop antennas near 1200 Hz. This anomaly is due to absorption in the self-resonant circuit formed by the adjacent small (0.5 meter diameter) loops, which were disconnected during the tests; indeed, the small loops were known to resonate at approximately 1200 Hz based on measurements made at the time of construction. Accordingly, operational procedure now requires that the small loop antennas be short-circuited at their terminal posts when not connected to the remainder of the system, in order to prevent unsatisfactory receiver performance in this frequency range.

Tuning of Loop Antennas

Once the receiver system has been set up, the loop antennas must be tuned for resonance at the anticipated operating frequencies. The ASYST program TUNING.001 is used to determine the optimum tuning unit capacitance settings for each loop. A strong signal is coupled into the receiving loop from the associated calibration coil, and the capacitive loading is progressively adjusted by computer control until maximum signal level is detected on the lock-in analyzer.

Upon completion of the tuning process, FRQSWP.001 is executed to measure the bandwidth and Q value at each center frequency. Unlike the adaptive tuning routine which varies capacitance while maintaining a constant excitation frequency, the response measurement program sweeps the calibration coil drive frequency in order to locate the -3 dB points of the amplitude transfer function at a specific loading.

Remote Sensing of ELF Signals in a Penn State Mobile Receiving Van for —the Purposes of Evaluating Communications Applications

One of the problems to be evaluated, during the 1990 summer heating campaign at the HIPAS Facility in Alaska, was the ability of the ELF signals created by ionospheric heating to be injected into the earth-ionosphere waveguide. If distant communications were to be achieved, it was necessary to know if the ELF signals were ducting through this waveguide or being radiated out of the heated region in some other direction. ELF signals had to be received with reasonable strength at locations farther than the 25 miles separating the transmitter from the fixed Penn State receiving station located near the Geophysical Institute at the University of Alaska, Fairbanks (U of AF).

A single channel Penn State VLF/ELF/ULF receiving system was mounted in a 26 foot mobile van and driven to locations ranging from 130 miles to 387 miles from the heated volume in an attempt to determine the signal strength at each of the locations. The receiver located near the U of AF was receiving the same signals during the experiment to allow for a correction to the variation of the signal amplitudes received at the mobile van in order to compensate the variations in ionospheric activity. As shown in the attached map, all of the sites were located along a line that is nearly magnetic south from the HIPAS facility.

The transmitter at HIPAS was modulated with the ELF carrier frequency as in normal ELF generation experiments. This ELF modulation was further modified by turning the modulation on and

off (Amplitude Modulation, AM), Quadrature Phase Shift Keying (QPSK) modulation or CW (continuously modulated with a constant amplitude of the ELF frequency). Another method of modulating the radiated ELF signal strength and phase was by rotating the beam of the HF signal in a circular path tilted 30 degrees off vertical. This method was coined "conical scan" and caused a change in signal path and the region of the ionosphere that was being heated; thus, causing a variation in phase and amplitude to be detected at the receiver. Plots attached show a typical signal amplitude and phase received during QPSK modulation and the next figure shows the amplitude and phase variations caused by conical scanning the beam as noted above. Both of these plots are derived from received data taken at the Cantwell, AK location.

The results of the remote experiment indicate that the ELF signals are being injected into the earth-ionosphere waveguide as predicted. Furthermore, the two station reception (PSU at U of AF and remote receiver) allows for correction of the radiated signal strength due to ionospheric variations. This correction coupled with the measurements taken at various distances from HIPAS permit the calculation of the attenuation of the ELF signal as it travels along the waveguide.

REMOTE EXPERIMENT
ALASKA MAP

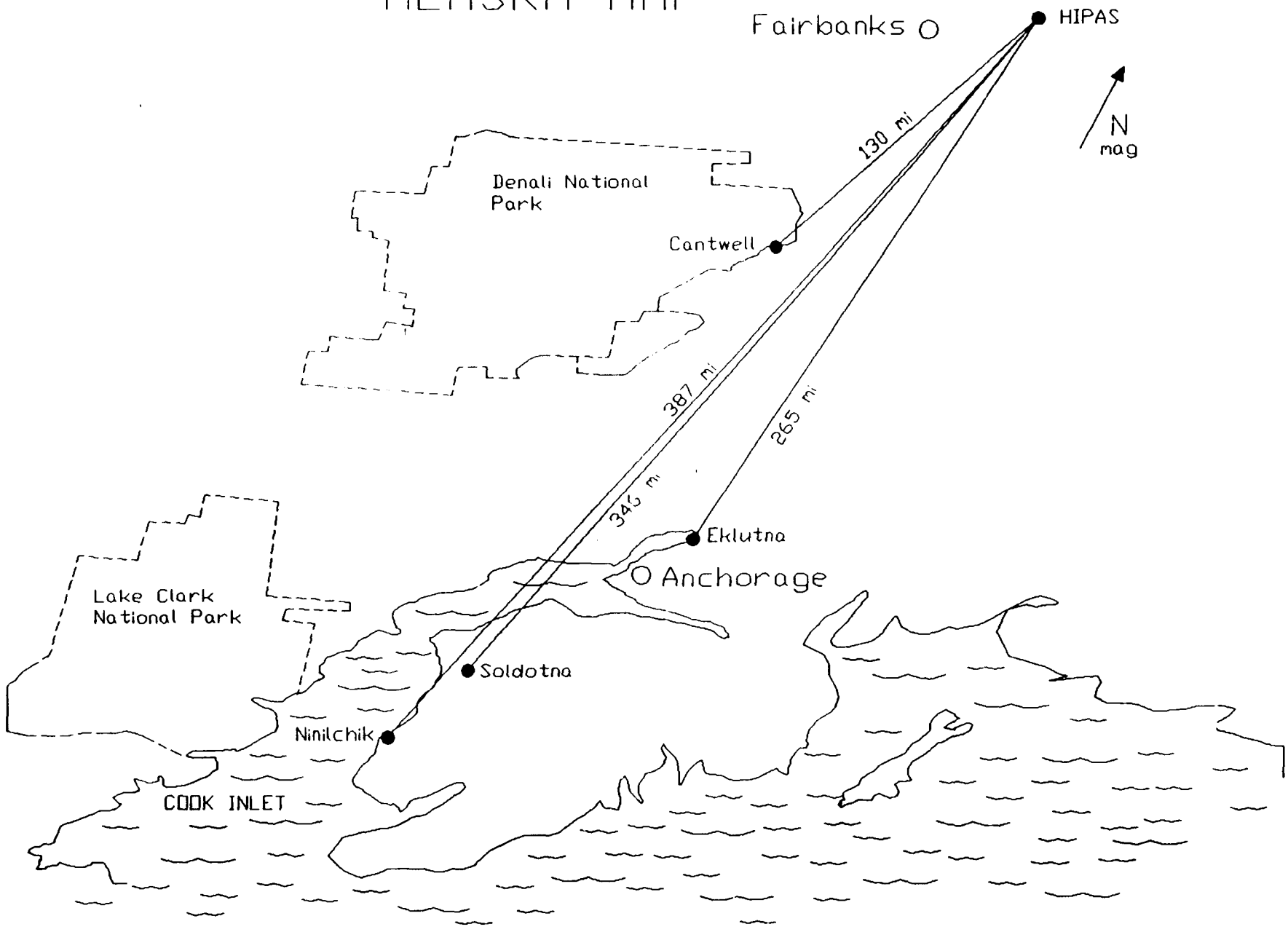

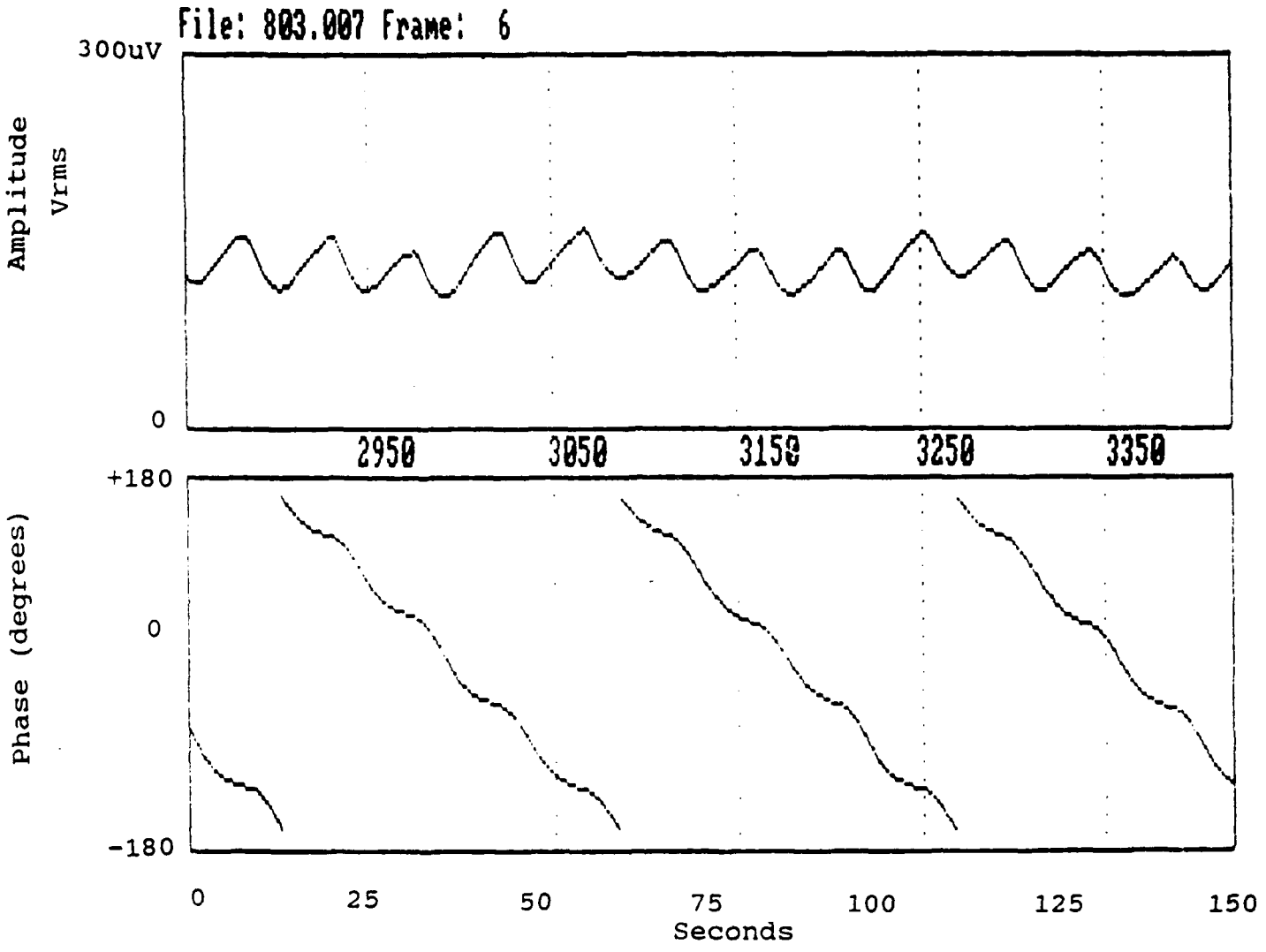

23:02:06L

RECEIVED 2Khz QPSK DATA
3 AUGUST 1989 - CANTWELL, AK

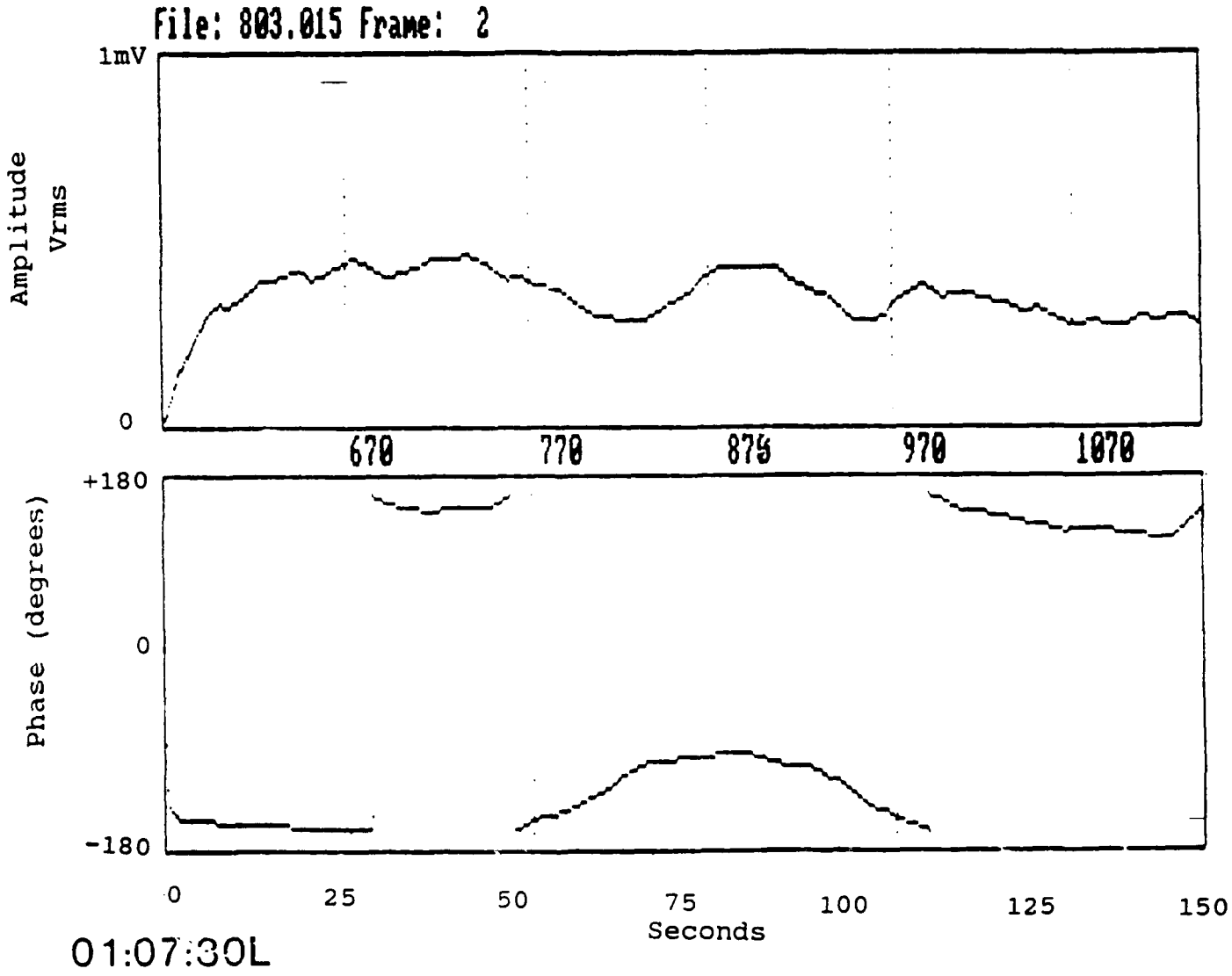

RECEIVED 2Khz CONICAL SCAN DATA
4 AUGUST 1989 - CANTWELL, AK

Publications for Past Five Years (Prime Contractor only)

Ferraro, A. J., Generation of Extremely Low Frequency Radio Waves by High Frequency Heating of the Lower Ionosphere, Naval Research Reviews, Four/V XXXVI, 1985.

Lunnen, R. J., A. J. Ferraro, H. S. Lee, R. Allshouse and K. Carroll, Detection of Local and Long-Path VLF/ELF Radiation from Modulated Ionospheric Current System, Radio Sci., 20, May-June 1985.

Ferraro, A. J. and D. H. Werner, Steerable ELF/VLF Radiation Produced by an Array of Ionospheric Dipoles Generated from HF Heating, IEEE Transactions on Antennas and Propagation, AP-35, No. 9, Sept. 1987.

Ferraro, A. J. and H. S. Lee, Measurements of Extremely Low Frequency Signals from Modulation of the Polar Electrojet Above Fairbanks, AK, IEEE Transactions on Antennas and Propagation, Vol. 37, No. 6, 1989.

Werner, D. H. and A. J. Ferraro, Cosine Pattern Synthesis for Single and Multiple Main Beam Uniformly Spaced Linear Arrays, IEEE Transaction on Antennas and Propagation, Vol. 37, No. 11, 1989.

Ferraro, A. J. and P. J. Li, Determination of D-Region Electron Densities from the ELF Frequency Stepping Experiment; accepted in Radio Science for a 1990 Special Issue.

Lee, H. S., A J. Ferraro and J. V. Olson, Detection and Characterization Geomagnetic Pulsations Using HF Ionospheric Heating; accepted in Radio Science for a 1990 Special Issue.

Baker, M. R., T. W. Collins, H. S. Lee and A .J. Ferraro, A Diagnostic System for the Study of Extremely Long Wavelength Emission Produced by Ionospheric Modification; accepted in Radio Science for a 1990 Special Issue.

Werner, D. H. and A. J. Ferraro, Mapping of the Polar Electrojet Current Down to Ionospheric D-Region Altitudes; accepted in Radio Science for a 1990 Special Issue.

Ferraro, A. J., Historical Review of Ionospheric Modification at the Communications and Space Sciences Laboratory; accepted in Radio Science for a 1990 Special Issue.

Mohd-Zain, A. and A. J. Ferraro, The Polarization Characteristics of ELF Generated Waves During Electrojet and Pulsation Events; accepted in Radio Science for a 1990 Special Issue.

Carroll, K. and A. J.Ferraro, Computer Simulation of ELF Injection in the Earth-Ionosphere Waveguide; accepted in Radio Science for a 1990 Special Issue.

Werner, D. H., A J. Ferraro and A. Albert, Implementation of an ELF/ULF Steerable Array of Ionospheric Dipoles Using the HIPAS Facility, accepted in Radio Science for a 1990 Special Issue.

Olson, J. V., A. J. Ferraro and H.S. Lee, Observation of ULF Pulsation Electric Fields in the D-Region Using the HIPAS Heater Facility; accepted in Radio Science for a 1990 Special Issue.

Research Awards or Honors:

1990 - Distinguished Professor

1989 -Fetter Fellow of Electrical Engineering

1988 -Fellow of the Institute of Electrical and Electronics Engineers

Distribution List

Addressee	DODAAD Code	Number of Copies
Scientific Officer	N00014	1
Administrative Contracting Officer (see Blk. 8 DD2222)	N66005	1
Director, Naval Research Laboratory, ATTN: Code 2627 Washington, D.C. 20375	N00173	6
Defense Technical Information Center, Bldg. 5, Cameron Station Alexandria, VA 22314	S47031	12

INVESTIGATION OF THE POLAR ELECTROJET CURRENT SYSTEM USING RADIO WAVE HEATING FROM A GROUND-BASED FACILITY

by
D. H. Werner, A. J. Ferraro
Communications and Space Sciences Laboratory
The Pennsylvania State University
University Park, PA, USA 16802
R. G. Brandt
Physics Division
Office of Naval Research
Arlington, VA, USA 22217-5000

The High Power Auroral Stimulation (HIPAS) heating facility has been used to modulate D region ionospheric currents at high latitudes, producing very low frequency (VLF) radio wave emissions. The behavior of these ionospheric currents can be deduced from a comprehensive study of the VLF signals received at a local field site. This paper examines the relationship between the VLF magnetic field strength measured on the ground and the intensity of an overhead electrojet current for the purpose of enhancing communications. The mapping of the polar electrojet current from the E region down through the D region, where it can then be modulated by the heater beam, is investigated. A finite difference solution to the electrojet mapping problem is presented in which arbitrary conductivity profiles can be specified. Results have been obtained using a simple Cowling model of the electrojet. These results indicate that for an electrojet flowing at an altitude of 110 km with a scale size in excess of 100 km, the mapping of the horizontal current density can be completely characterized in terms of the Pedersen and Hall conductivities. This indicates that the mapping becomes independent of scale sizes which exceed 100 km. A promising new diagnostic technique, for studying ionospheric D region currents, has been implemented using the HIPAS facility. This technique involves high frequency (HF) beam steering for localized VLF generation in the mapped region below electrojets. Beam steering has been used to estimate the strength and current distribution of the polar electrojet, and for charting the movements of overhead currents.

I. Introduction

The generation of ELF/VLF signals by modulation of the dynamo current system using the HF heating facility located near Arecibo, Puerto Rico, has been reported by Ferraro et al. [1] and Ferraro et al. [2]. Radiation from a heated and modulated equatorial electrojet current system was detected by Lunnen et al. [3]. Ionospherically produced signals resulting from periodic plasma heating of the polar electrojet current system have been studied by Stubbe et al. [4], Rietveld et al. [5], Rietveld et al. [6], and more recently by Ferraro et al. [7].

A series of ionospheric heating experiments have been conducted at the HIPAS facility near Fairbanks, Alaska, over a period of two years from June 1987 to August 1989. The transmitting system consists of eight individual HF heating transmitters which feed the eight antennas that comprise the HIPAS heating array. The HIPAS array has a total of eight crossed-dipoles, seven of which are equally spaced around the circumference of a 340 foot radius circle, with an eighth one situated at the center. Ionospheric heating is achieved by modulating the HF continuous wave output of the transmitter.

A reconfigurable ELF/VLF receiver was positioned 47 km west of HIPAS at a University of Alaska Geophysical Institute field site [8]. A polarimeter was set up at the receiving site in order to monitor the polarization characteristics of the incoming ELF/VLF signals at the ground. This polarimeter consisted of two orthogonal loop antennas, one with its plane oriented in the magnetic north-south direction and the other with its plane in the east-west direction. The components of the ELF/VLF signals which were intercepted by each of the tuned loops would undergo preamplification and filtering. Lock-in analyzers then extracted the in-phase (I) and quadrature (Q) components of the signals using narrowband coherent detection. The outputs of the lock-in analyzers were digitized by a data acquisition system for analysis, display, and storage via a microcomputer. Highly stable crystal frequency standards were used at both the transmitter and receiver locations to insure precise frequency coherence and sampling accuracy.

Experiments were carried out in which the HIPAS heater beam was conically scanned at an angle of 30° with respect to the vertical. The total time to complete one of these scans was two minutes. Some conical scanning VLF data is presented and interpreted in this paper.

II. The Downward Mapping of the Polar Electrojet Current

A simple Cowling model was used by Werner and Ferraro [9] to represent the polar electrojet current. The potential associated with an electrojet current was found to be

$$\Phi(x,y,z) = -\Phi_1 \sin(\beta_1 x + \beta_2 y)\, Z(z) \tag{1}$$

where

$$\beta_1 = \frac{2\pi}{\lambda_1} \tag{2}$$

$$\beta_2 = \frac{2\pi}{\lambda_2} \tag{3}$$

The parameters λ_1 and λ_2 are the spatial wavelengths in the geomagnetic east-west and north-south directions, respectively, of an electrojet flowing at an altitude of z_1. The spatial wavelengths determine scale size of an electrojet and are related by

$$\lambda_1 \sigma_1(z_1) = \lambda_2 \sigma_2(z_1) \tag{4}$$

The function Z(z) appearing in Eq. (1) is the solution of a boundary value problem characterized by

$$\frac{d}{dz}\left(\sigma_2 \frac{dZ}{dz}\right) - \beta_e^2 \sigma_1 Z = 0 \tag{5}$$

$$Z(0) = 0 \tag{6}$$

$$Z(z_1) = 1 \tag{7}$$

where

$$\beta_e = \frac{2\pi}{\lambda_e} = \sqrt{\beta_1^2 + \beta_2^2} \tag{8}$$

is the effective wave number of the electrojet. The generalized form of Ohm's law for a plasma in a magnetic field is used to relate the current density to the potential function given in Eq. (1),

$$J = -\sigma \nabla\Phi \tag{9}$$

where

$$\sigma = \begin{bmatrix} \sigma_1 & \sigma_2 & 0 \\ -\sigma_2 & \sigma_1 & 0 \\ 0 & 0 & \sigma_0 \end{bmatrix} \tag{10}$$

is the ionospheric conductivity tensor. The term σ_0 is known as the direct conductivity, σ_1 the Petersen conductivity, and σ_2 the Hall conductivity. An expression for the normalized magnitude of the horizontal current density is given by

$$\frac{J_\perp(z)}{J_\perp} = Z(z)\sqrt{\frac{\sigma_1^2(z) + \sigma_2^2(z)}{\sigma_1^2(z_1) + \sigma_2^2(z_1)}} \tag{11}$$

where

$$J_\perp = \beta\, \sigma_1(z_1)\Phi_1 \tag{12}$$

and

$$\tau = \frac{(\sigma_1^2 + \sigma_2^2)}{\sigma_1} \tag{13}$$

is the Cowling conductivity. The corresponding angle of the horizontal current density, measured in degrees south of west, is then

$$\phi_1(z) = \tan^{-1}\left[\frac{\sigma_2(z_1)\sigma_1(z) - \sigma_1(z_1)\sigma_2(z)}{\sigma_1(z_1)\sigma_1(z) + \sigma_2(z_1)\sigma_2(z)}\right] \tag{14}$$

The boundary value problem described by Eq. (5), Eq. (6), and Eq. (7) must be solved numerically, with the exception of a few special cases of the conductivities [9]. A finite difference scheme was used by Werner [10] to obtain a numerical solution to this boundary value problem. The ability to specify arbitrary conductivity profiles has been incorporated into the numerical mapping model. The differential equation Eq. (5) can be approximated at $z=z_i$ by the difference equation

$$\frac{Z_{i+1} - 2Z_i + Z_{i-1}}{h^2} - p(z_i)\frac{Z_{i+1} - Z_{i-1}}{2h} - r(z_i)Z_i = 0 \qquad 2 \le i \le N \tag{15}$$

with the boundary conditions

$$Z_1 = 0 \tag{16}$$

$$Z_{N+1} = \tag{17}$$

where

$$p(z_i) = \frac{\ln \sigma_2(z_{i+1}) - \ln \sigma_2(z_{i-1})}{2h} \tag{18}$$

$$r(z_i) = \beta_e^2 \frac{\sigma_1(z_i)}{\sigma_0(z_i)} \tag{19}$$

$$z_i = (i-1)h \quad \text{for} \quad i = 1, 2, \ldots, N+1 \tag{20}$$

$$h = \frac{z_t}{N} \tag{21}$$

Figure 1 shows some normalized horizontal current density profiles for the altitude range between 100 km and 60 km. Profiles for several different effective wavelengths are included (dashed curves), while the solid curve represents the profile to which the horizontal current density converges with $\lambda_e \to 100$ km. This curve is characterized by

$$\frac{J_1(z)}{J_1} \sim \sqrt{\frac{\sigma_1^2(z) + \sigma_2^2(z)}{\sigma_1^2(z_1) + \sigma_2^2(z_1)}} \quad \text{for} \quad z_1 > 100\,\text{km} \tag{22}$$

which only depends on the Hall and Petersen conductivities. The current density profiles of Figure 1 were obtained assuming the presence of an intense magnetic storm during sunspot maximum daytime conditions. An electrojet source height of 100 km was assumed in accordance with the results of Kamide and Brekke [11]. The ionospheric conductivity model corresponding to sunspot maximum daytime conditions was adopted from Hughes and Southwood [12].

III. The Ambient and Modulated D Region Current Densities

The VLF ionospheric source can be treated as an incremental volume element $\Delta x \Delta y \Delta z$ with a modulated horizontal current density of $|\Delta J_1|$ centered at the altitude of maximum heating. For typical experimental conditions, the extent of the effective radiating layer Δz is approximately 1 km and the layer is assumed to be centered at 70 km. The current density of the modulated ionosphere ΔJ can be related to the current density of the ambient ionosphere J_1 by

$$\Delta J = \left[\sigma(T_e)\sigma(T_\eta)^{-1} - I\right] J_0 \tag{23}$$

where

$$\Delta J = \Delta\sigma(T_e) E_0 \tag{24}$$

and

$$\Delta\sigma(T_e) = \sigma(T_e) - \sigma(T_\eta) \tag{25}$$

For a vertical geomagnetic field, the ambient (unprimed) and the heated (primed) conductivity tensors are given by

$$\sigma(T_\eta) \approx \sigma = \begin{bmatrix} \sigma_1 & \sigma_2 & 0 \\ -\sigma_2 & \sigma_1 & 0 \\ 0 & 0 & \sigma_0 \end{bmatrix} \tag{26}$$

and

$$\sigma(T_e) \approx \sigma' = \begin{bmatrix} \sigma'_1 & \sigma'_2 & 0 \\ -\sigma'_2 & \sigma'_1 & 0 \\ 0 & 0 & \sigma'_0 \end{bmatrix} \tag{27}$$

It follows from Eq. (23), Eq. (26), and Eq. (27) that

$$\sigma'\sigma^{-1} - I = \begin{bmatrix} \left(\frac{\sigma_1\sigma'_1 + \sigma_2\sigma'_2}{\sigma_1^2 + \sigma_2^2}\right) - 1 & \left(\frac{\sigma_1\sigma'_2 - \sigma_2\sigma'_1}{\sigma_1^2 + \sigma_2^2}\right) & 0 \\ -\left(\frac{\sigma_1\sigma'_2 - \sigma_2\sigma'_1}{\sigma_1^2 + \sigma_2^2}\right) & \left(\frac{\sigma_1\sigma'_1 + \sigma_2\sigma'_2}{\sigma_1^2 + \sigma_2^2}\right) - 1 & 0 \\ 0 & 0 & \frac{\sigma'_0}{\sigma_0} - 1 \end{bmatrix} \tag{28}$$

If we let

$$a_{11} = \left(\frac{\sigma_1\sigma'_1 + \sigma_2\sigma'_2}{\sigma_1^2 + \sigma_2^2}\right) - 1 \tag{29}$$

and

$$a_{12} = \left(\frac{\sigma_1\sigma'_2 - \sigma_2\sigma'_1}{\sigma_1^2 + \sigma_2^2}\right) \tag{30}$$

then the modulated horizontal current densities can be expressed in terms of the ambient horizontal current densities in the following way

$$\begin{bmatrix} \Delta J_x \\ \Delta J_y \end{bmatrix} = \begin{bmatrix} a_{11} & a_{12} \\ -a_{12} & a_{11} \end{bmatrix} \begin{bmatrix} J_x \\ J_y \end{bmatrix} \tag{31}$$

Using Eq. (31), it can be shown that the magnitude of the total horizontal ambient current density and the total horizontal modulated current density are related by

$$|J_0| = \frac{|\Delta J_0|}{\sqrt{a_{11}^2 + a_{12}^2}} \tag{32}$$

The horizontal modulated current density may be estimated from the intensity of the VLF magnetic field measured on the ground. The values of $\Delta\sigma$ are determined using ionospheric heating theory [13], [14]. The ambient horizontal current density can then be calculated from Eq. (32). Finally, the strength of the electrojet current J_0 can be found using the results of mapping theory Eq. (22). Figure 2 shows a block-diagram of the model developed to study the relationship between the VLF magnetic field intensity measured on the ground and the strength of the polar electrojet.

IV. Estimation of Electrojet Current Density

The Alaska meridian chain of magnetometers was used to confirm the presence of an electrojet over the HIPAS facility when heating experiments were in progress. The Alaska meridian chain consists of several flux-gate magnetometers located, approximately, along a line of constant geomagnetic longitude. Each magnetometer measures three components of the earth's vector magnetic field in a coordinate system in which the H-component represents magnetic north, the D-component represents magnetic east, and the Z-component points down towards the ground. In general, currents flow in the east-west direction in the high-latitude ionosphere.

Figures 3, 4, and 5 show the H-, D-, and Z-traces, respectively, for July 22, 1988 [15]. The magnetometer stations of greatest interest are Talkeetna (TLK) which is south of Fairbanks, and Fort Yukon (FYU) which is north of Fairbanks. At 0335 local time (1135 UT) on July 22, the HIPAS HF heater beam was being modulated at a 5 kHz rate in the vertical position. The corresponding B-field intensity measured on the ground was 0.68 pT. The magnetograms for this period indicated that there was a negative perturbation in the H-component measured at the FYU and TLK stations. There was no perturbation in the D-component measured at FYU and TLK. The Z-component was positive to the north (FYU) and negative to the south (TLK) of Fairbanks. These measurements indicate that there was a westward traveling electrojet present over Fairbanks during this time.

A VLF B-field intensity of 0.68 pT corresponds to a horizontal modulated current density of 9.25×10^{-3} A/km, assuming that the altitudes of maximum heating is 70 km. Papadopoulos et al. [14] evaluate the level of conductivity modulation at various ionospheric heights as function of incident HF power density. The values of $\Delta\sigma_0$ and $\Delta\sigma_1$ can be found from these curves assuming an altitude of 70 km and a maximum HF ground power for HIPAS of 1.6 MW. These modulated conductivity values used in conjunction with Eq. (32) imply that the horizontal ambient current density $|J_0|$ at a 70 km altitude was 2.56×10^{-4} A/km. If it is assumed that the electrojet was flowing at an altitude of 110 km and had an effective wavelength which exceeded 100 km, then Eq. (22) suggests that the strength of the electrojet J_0 must have been 5.1 A/km. This electrojet current density is within the range of values reported by Kamide and Brekke [11].

V. The Conical Scanning Experiment

A promising new diagnostic technique, for studying ionospheric D region currents, has recently been implemented at the HIPAS facility [16]. This technique permits a localized cross section of the ionosphere to be probed by steering the HF heater beam. The VLF signals resulting from this beam steering are monitored and recorded at a field site on the ground via a coherent detection scheme. This beam steering diagnostic technique was successfully demonstrated during a HIPAS ionospheric heating campaign which took place in July of 1988.

Scanning of the HIPAS heater beam in a conical fashion was investigated during the July 1988 campaign. The conical scan was primarily used for diagnostics of the ionospheric current system in the vicinity of the HIPAS facility. Under ideal conditions of a uniform overhead current, the signature of the VLF received on the ground resulting from a conical scan should exhibit a certain characteristic shape. Any deviation from this shape may indicate the movement of a current into the path of the conically scanning heater beam. Since the position of the heater beam is known, it is possible to use the conical scanning technique to pinpoint the geographic (or geomagnetic) location of the influxing current.

The geometry illustrating the conical scanning mode of operation is shown in Figure 6. The location of the receiver site is 47 km due west of the HIPAS facility, i.e. d=47 km and $\phi'=270^\circ$. The coelevation θ of the HIPAS heater beam is fixed at 30° while the azimuth ϕ of the beam is incremented 18° every 6 seconds with geographic east ($\phi=90^\circ$) as the starting point. This produces a conical scanning of the heater beam which traces out a circle in the ionosphere above HIPAS once every two minutes.

An incremental volume of current radiating in free space was adopted to model the VLF ionospheric source. The incremental current volume was chosen because it can be used as a basic unit to construct more complex radiating structures. The VLF source model relates the magnetic field strength measured on the ground to the strength of the modulated horizontal current density at the altitude of maximum heating. This elementary source model was used in the analysis of conical scan data.

Typical VLF magnitude and phase data obtained from a conical scan is shown in Figures 7 and 8, respectively. These measurements were made from 0558-0600 local time (1358-1400 UT) just prior to an electrojet event on July 21, 1988. The transition of the heater beam from a vertical position to the scanning mode is visible during the first few seconds of the conical scan data and should be disregarded. The frequency of VLF signals generated during the conical scanning experiment was 5 kHz.

The dashed curve appearing in Figure 7 represents the normalized field strength that would result from a uniform ionospheric current flowing at an altitude of 70 km.

The magnitude data is not exactly symmetrical indicating that heating by sidelobes may produce VLF radiation which interferes with the radiation generated by heating from the main beam. Figure 9 is a current map showing the relative intensity of the ionospheric currents associated with the E-W conical scan magnitude data of Figure 7. The length of each line segment in the current map is proportional to the ratio of the measured conical scan data to the theoretical values for a uniform current. If the length of the line segment is less than one unit, then the ionospheric current is weaker than that predicted by the uniform current model. And if the length of the line segment is greater than one unit, then the ionospheric current is stronger than that predicted by the uniform current model. The coordinates used for the current map are geomagnetic. Hence the current is strongest to the north-west of HIPAS, which is in agreement with magnetometer records of this period.

The results presented above suggest that conical scanning could be used for communications purposes as well as diagnostics. The heater beam could be adaptively steered to the region of the ionosphere where the strongest current was detected by a conical scan. This procedure could be repeated periodically to account for any changes in the location of the most intense current brought about by the dynamic polar ionosphere.

Figures 10 and 11 show the VLF magnitude and phase data resulting from a conical scan made during 0434-0436 local time (1234-1236 UT) on July 21, 1988. The magnitude data for this conical scan reveals that the strongest current was located to the geographic north-west of HIPAS. If this were an adaptive conical scan the heater beam would subsequently be parked at a coelevation of 30° and an azimuth of 324°. The current map corresponding to the E-W magnitude of this conical scan is shown in Figure 12.

VI. Conclusion

The relationship between the VLF magnetic field strength measured on the ground and the intensity of an overhead electrojet current has been treated in this paper. The currents that are being modulated in the D region map down from the E region where the electrojet source current flows. A finite difference scheme was implemented to find a numerical solution to the electrojet mapping boundary value problem. This numerical mapping model accommodates arbitrary conductivity profiles.

The VLF source was modeled as an incremental volume of current radiating in free space. This source model relates the magnetic field strength measured by a ground-based receiver to the strength of the modulated horizontal current density at the altitude of maximum heating. The associated ambient (DC) current was then determined. Finally, using this information, the strength of the polar electrojet could be estimated. The results of this analysis agreed favorably with values of electrojet current densities reported elsewhere in the literature.

The use of the HF beam steering VLF generation technique as a diagnostic tool was introduced. Results were presented from beam steering experiments performed during an electrojet event which occurred on July 21, 1988. Conical scanning data was used to infer ionospheric D region currents.

References

1. Ferraro, A. J., H. S. Lee, R. Allshouse, K. Carroll, A. A. Tomko, F. J. Kelly, and R. C. Joiner, VLF/ELF radiation from the ionospheric dynamo current system modulated by powerful HF signals, J. Atmos. Terr. Phys., 44, 12, 1982, 1113-1122.

2. Ferraro, A. J., H. S. Lee, R. Allshouse, K. Carroll, and R. Lunnen, Characteristics of ionospheric ELF radiation generated by HF heating, J. Atmos. Terr. Phys., 46, 10, 1984, 855-865.

3. Lunnen, R. J., H. S. Lee, A. J. Ferraro, R. F. Woodman, and T. Collins, Detection of radiation from a heated and modulated equatorial electrojet current system, Nature, 311, 5982, 1984, 134-135.

4. Stubbe, P., H. Kopka, H. Lauche, M. T. Rietveld, A. Brekke, O. Holt, T. B. Jones, T. Robinson, A. Hedberg, B. Thide, M. Crochet, and H. T. Lotz, Ionospheric modification experiments in Northern Scandinavia, J. Atmos. Terr. Phys., 44, 12, 1982, 1025-1041.

5. Rietveld, M. T., H. Kopka, and P. Stubbe, D-region characteristics deduced from pulsed ionospheric heating under auroral electrojet conditions, J. Atmos. Terr. Phys., 48, 4, 1986, 311-326.

6. Rietveld, M. T., H. P. Mauelshgen, P. Stubbe, H. Kopka, and E. Nielsen, The characteristics of ionospheric heating-produced ELF/VLF waves over 32 hours, J. Geophys. Res., 92, A8, 1987, 8707-8722.

7. Ferraro, A. J., H. S. Lee, T. W. Collins, M. Baker, D. Werner, F. M. Zain, and P. J. Li, Measurements of extremely low frequency signals from modulation of the polar electrojet above Fairbanks, Alaska, IEEE Trans. Antennas Propagat., AP36, 6, 1989, 802-805.

8. Baker, M. R., Development of a diagnostic system for ionospheric modification studies at high latitudes, M. S. Thesis, The Pennsylvania State University,

University Park, PA, 1988.

9. Werner, D. H., and A. J. Ferraro, Mapping of the polar electrojet current down to ionospheric D-region altitudes, Accepted for publication in a Special Issue of Radio Science on Ionospheric Modification in the Polar Region, 1990.

10. Werner, D.H., An investigation of the polar electrojet current system using radio wave heating of the lower ionosphere, Ph.D. Thesis, The Pennsylvania State University, University Park, PA, 1989.

11. Kamide, Y. R., and A. Brekke, Altitude of the eastward and westward auroral electrojets, J. Geophys. Res., 82, 19, 1977, 2851-2853.

12. Hughes, W. J., and D. J. Southwood, The screening of micropulsation signals by the atmosphere and ionosphere, J. Geophys. Res., 81, 19, 1976, 3234-3240.

13. Tomko, A. A., Nonlinear phenomena arising from radio wave heating of the lower ionosphere, Rep. PSU-IRL-SCI-470, Communications and Space Sciences Lab, The Pennsylvania State University, University Park, PA, 1981.

14. Papadopoulos, K., C. L. Chang, P. Vitello, and A. Drobat, On the efficiency of ionospheric ELF generation, Submitted for publication in a Special Issue of Radio Science on Ionospheric Modification in the Polar Region, 1990.

15. Olson, J. V., The University of Alaska at Fairbanks Geophysical Institute, Private Communication, 1988.

16. Wong, A. Y., and M. McCarrick, The University of California at Los Angeles Plasma Physics Laboratory, Private Communication, 1988.

Figure Captions

Figure 1. Normalized horizontal current density profiles for the altitude range between 100 km and 60 km.

Figure 2. Block-diagram of the model.

Figure 3. Magnetometer records for July 22, 1988. Alaska RGON magnetometer chain H-traces.

Figure 4. Magnetometer records for July 22, 1988. Alaska RGON magnetometer chain D-traces.

Figure 5. Magnetometer records for July 22, 1988. Alaska RGON magnetometer chain Z-traces.

Figure 6. Geometry for the conical scanning experiment.

Figure 7. Conical scan VLF magnitude data for the period 1358-1400 UT on July 21, 1988.

Figure 8. Conical scan VLF phase data for the period 1358-1400 UT July 21, 1988.

Figure 9. The relative intensity of the E-W component of the D region ionospheric currents associated with the E-W VLF magnitude data of Figure 7.

Figure 10. Conical scan VLF magnitude data for the period 1234-1236 UT on July 21, 1988.

Figure 11. Conical scan VLF phase data for the period 1234-1236 UT on July 21, 1988.

Figure 12. The relative intensity of the E-W component of the D region ionospheric currents associated with the E-W VLF magnitude data of Figure 10.

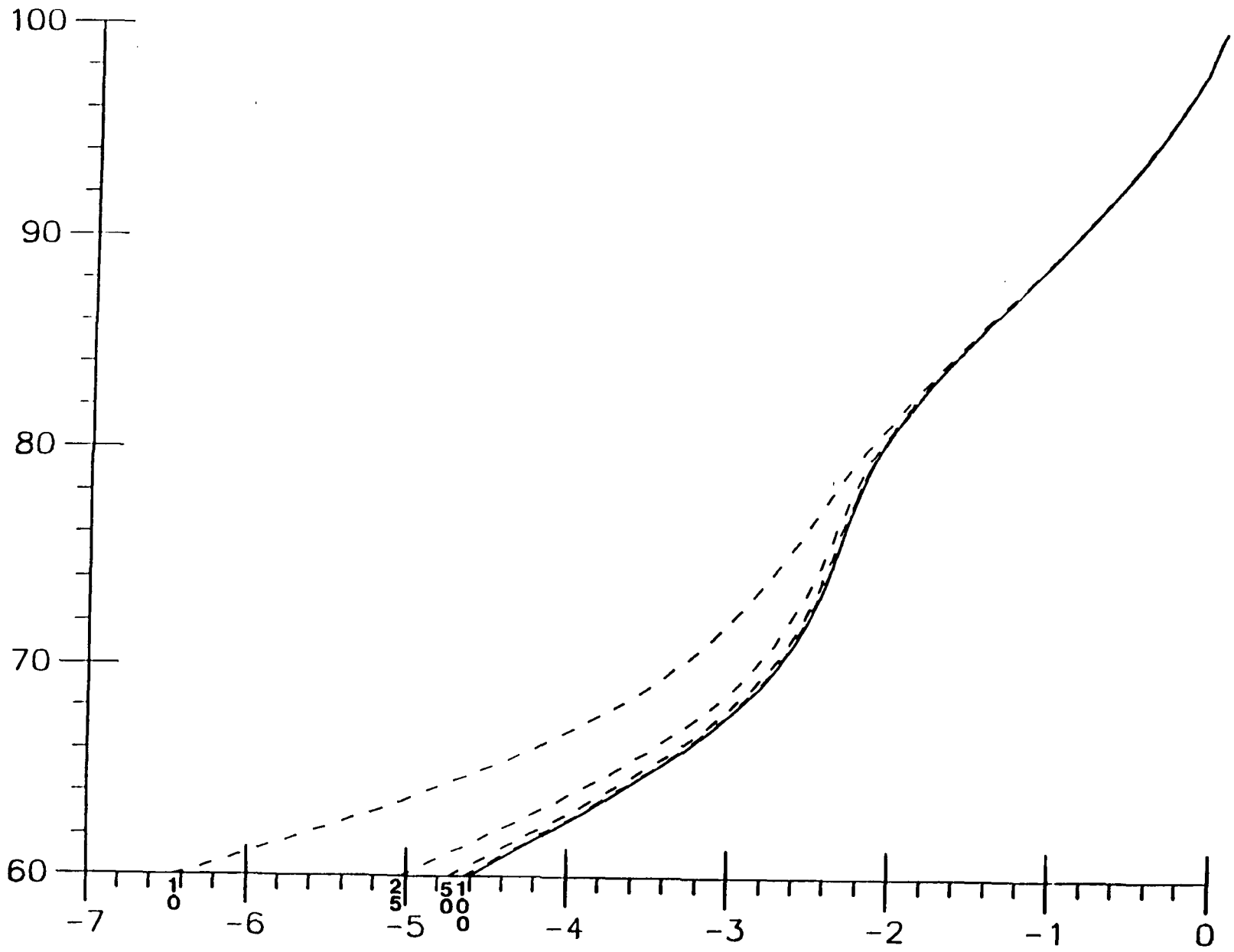

Figure 1

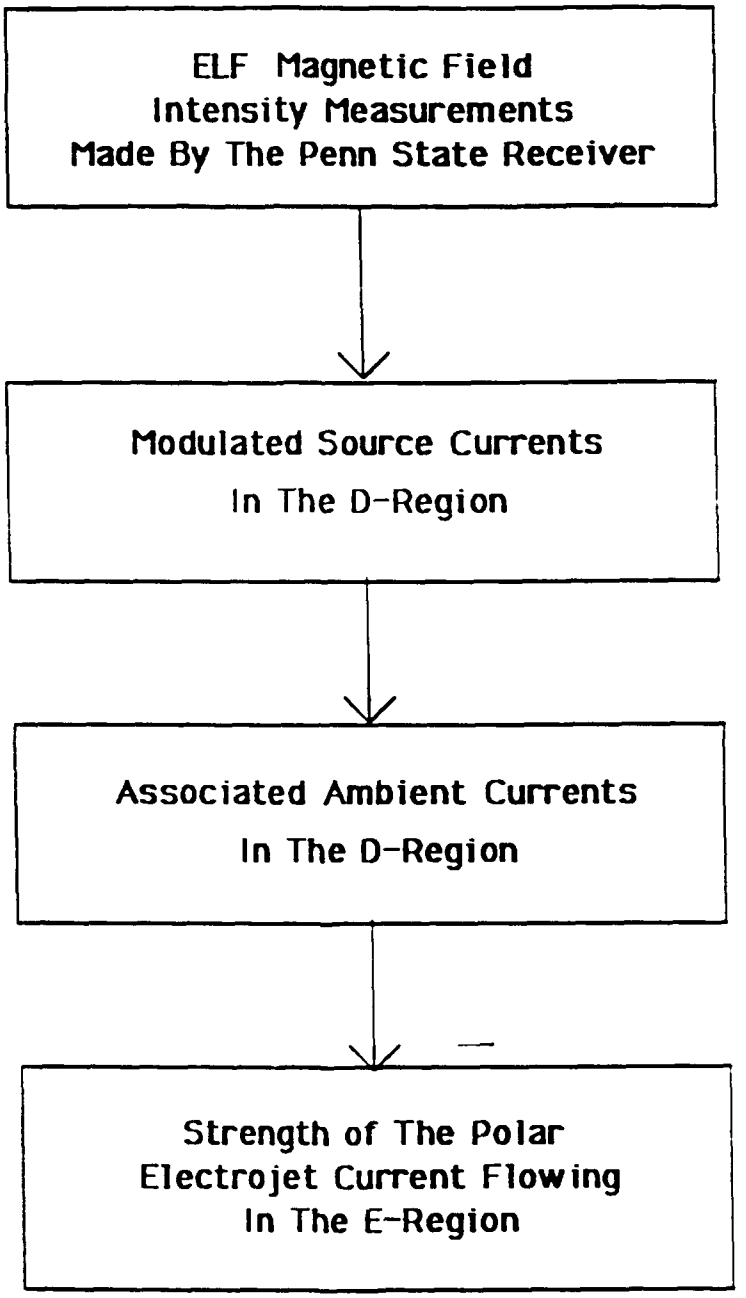
ELF Magnetic Field
Intensity Measurements
Made By The Penn State Receiver
Modulated Source Currents
In The D-Region
Associated Ambient Currents
In The D-Region
Strength of The Polar
Electrojet Current Flowing
In The E-Region

Figure 2

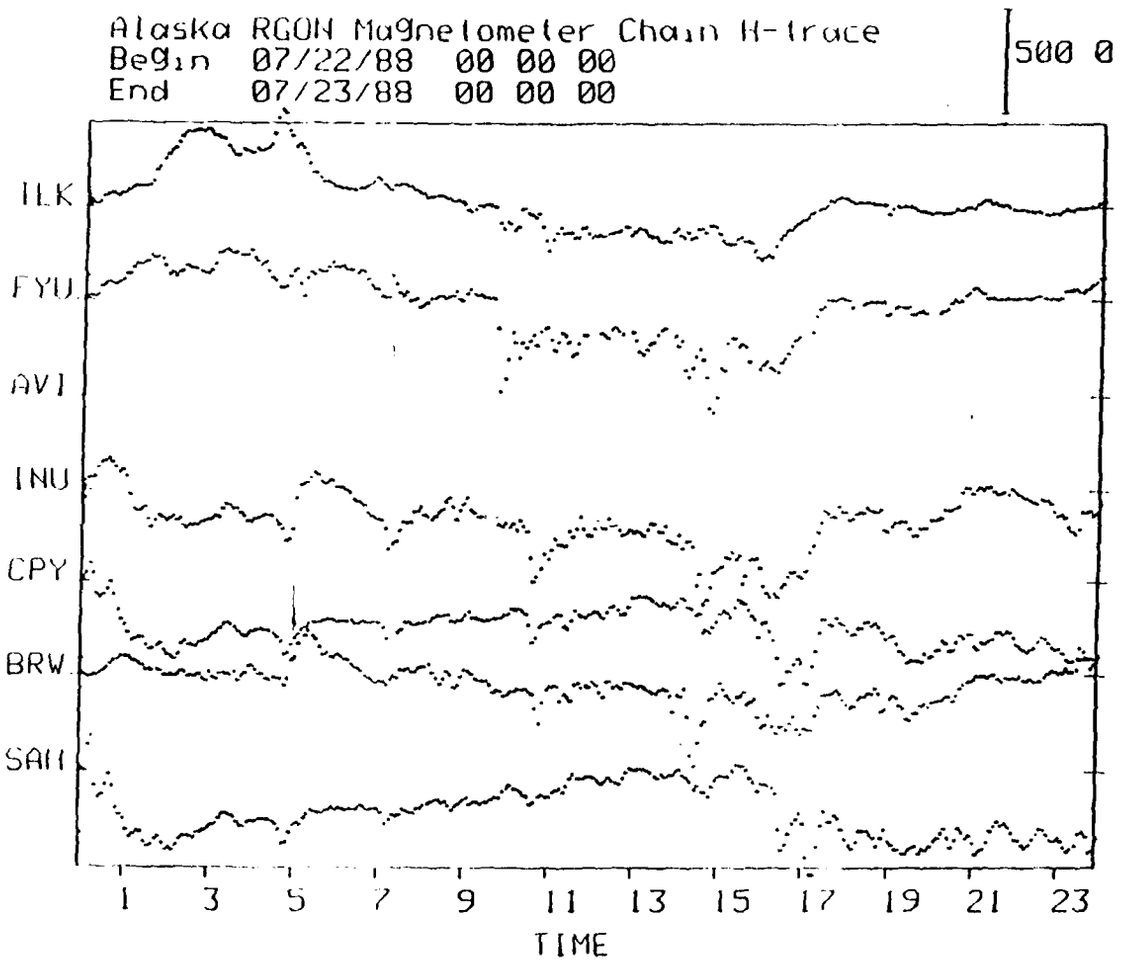
Alaska RGON Magnetometer Chain H-trace
Begin 07/22/88 00 00 00
End 07/23/88 00 00 00
500 0
ILK
FYU
AVI
INU
CPY
BRW
SAH
1 3 5 7 9 11 13 15 17 19 21 23
TIME

Figure 3

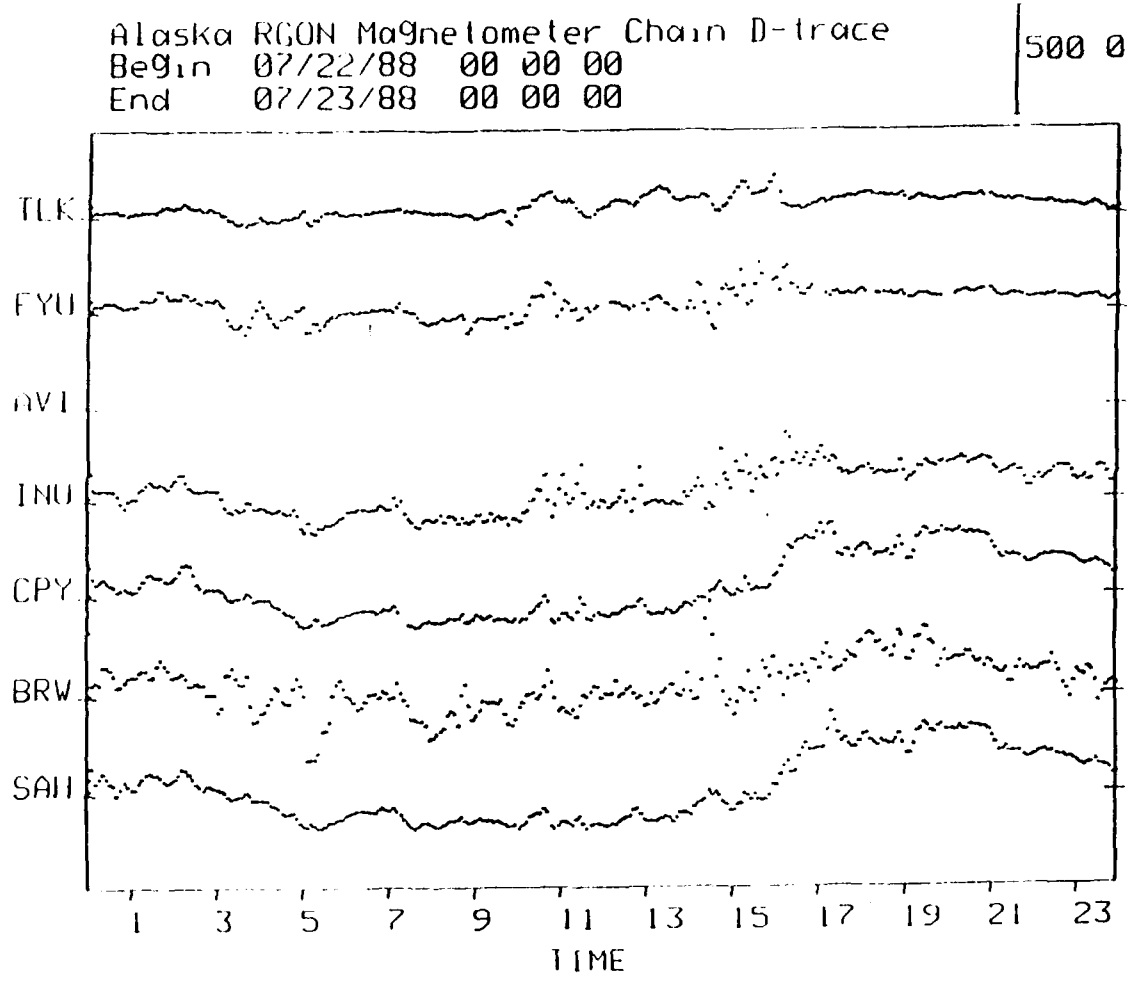
Alaska RGON Magnetometer Chain D-trace
Begin 07/22/88 00 00 00
End 07/23/88 00 00 00
500 0
TLK
FYU
AVI
INU
CPY
BRW
SAH
1 3 5 7 9 11 13 15 17 19 21 23
TIME

Figure 4

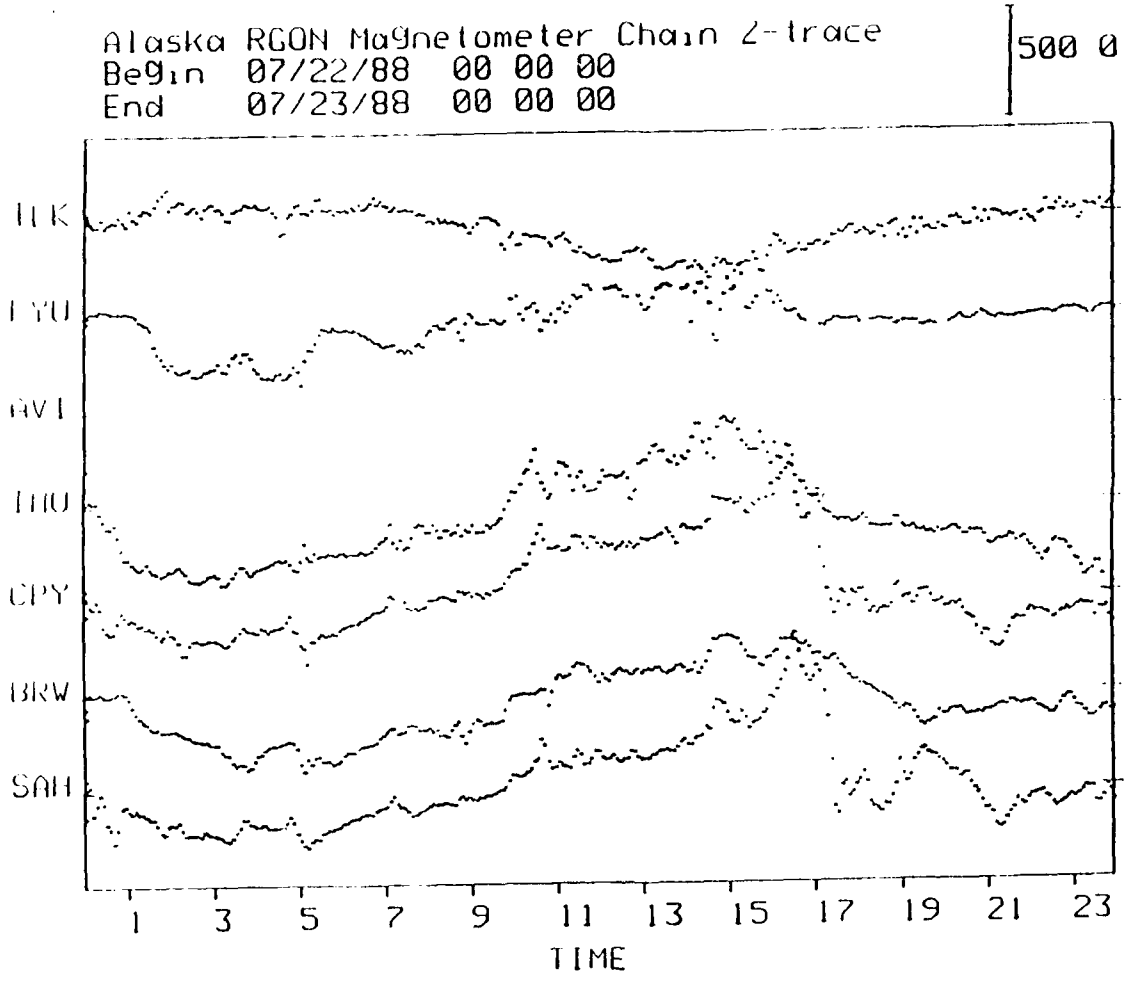
Alaska RGON Magnetometer Chain Z-trace
Begin 07/22/88 00 00 00
End 07/23/88 00 00 00
500 0
HLK
FYU
AVI
THU
CPY
BRW
SAH
1
3
5
7
9
11
13
15
17
19
21
23
TIME

Figure 5

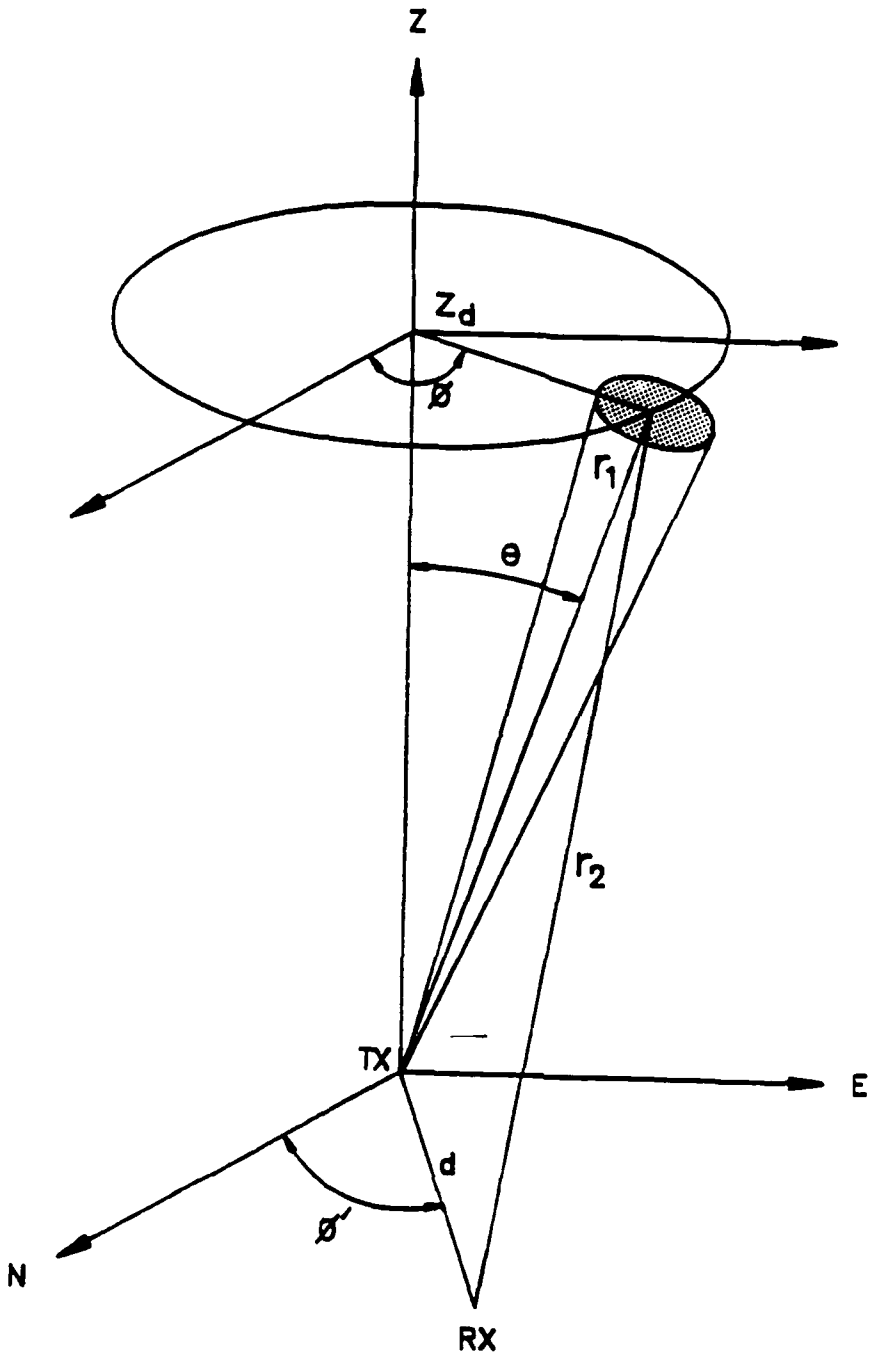

Figure 6

Figure 7

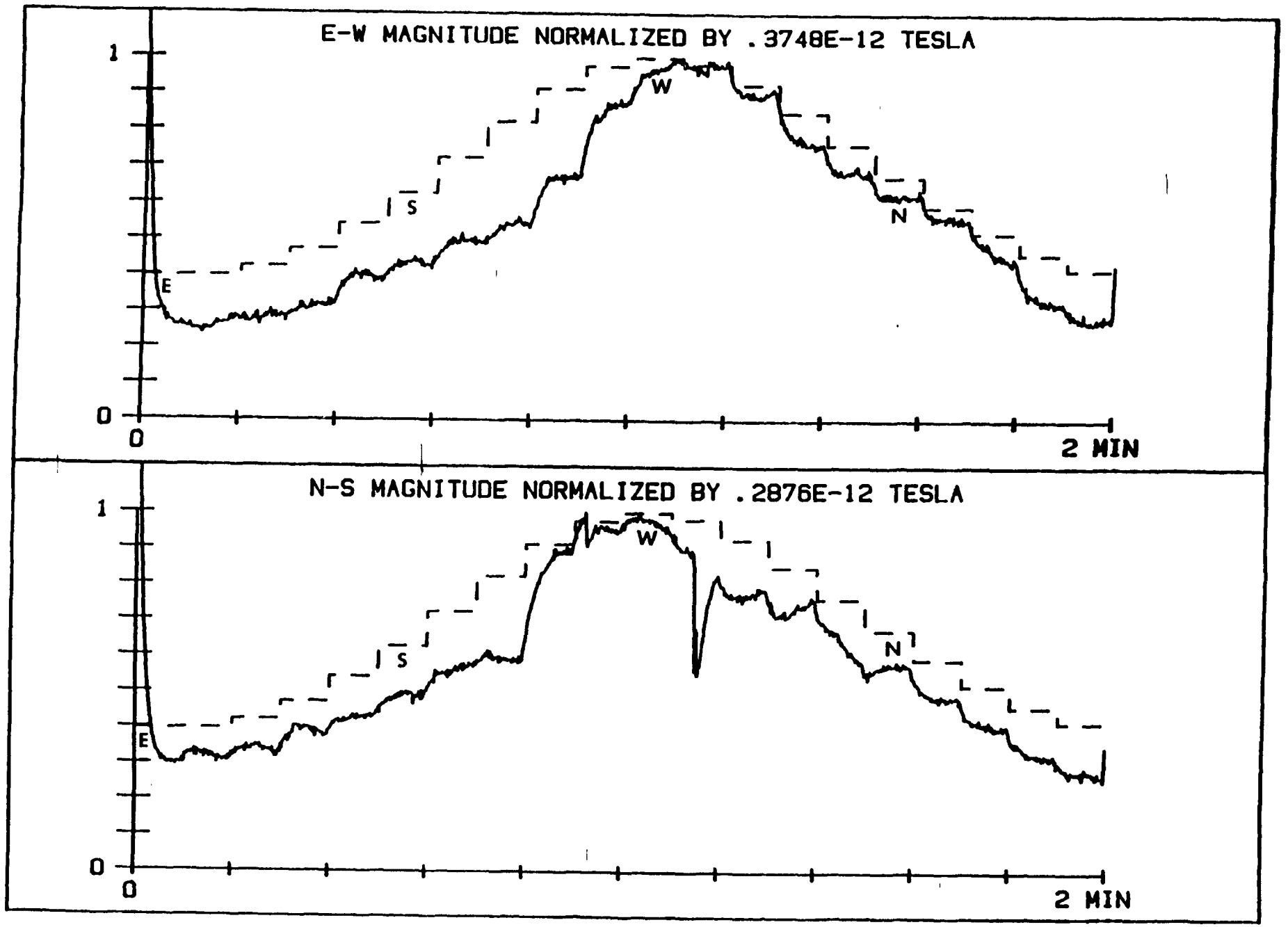
E-W MAGNITUDE NORMALIZED BY .3748E-12 TESLA
1
0
0
2 MIN
E
S
W
N
N-S MAGNITUDE NORMALIZED BY .2876E-12 TESLA
1
0
0
2 MIN
E
S
W
N

Figure 8

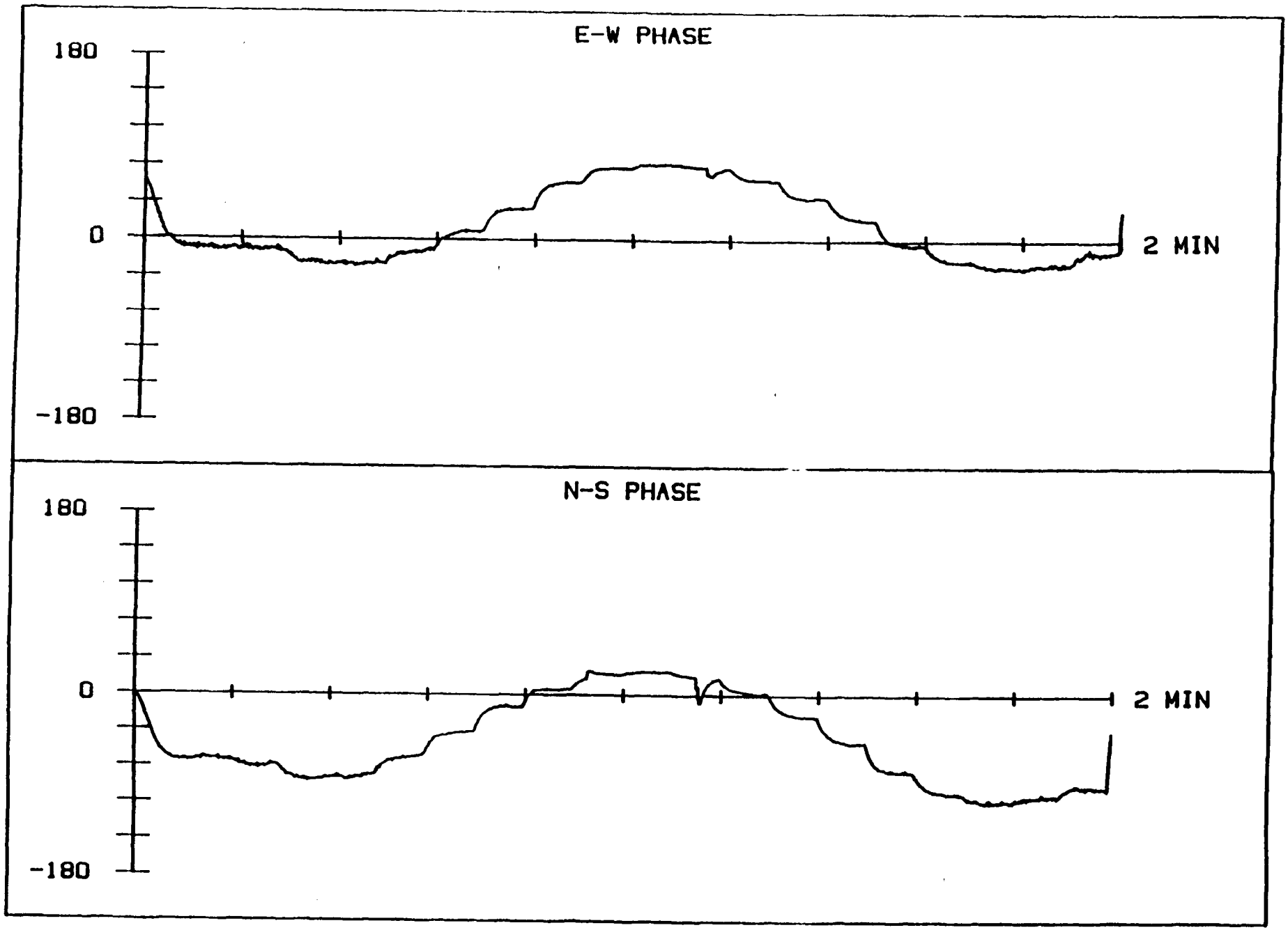

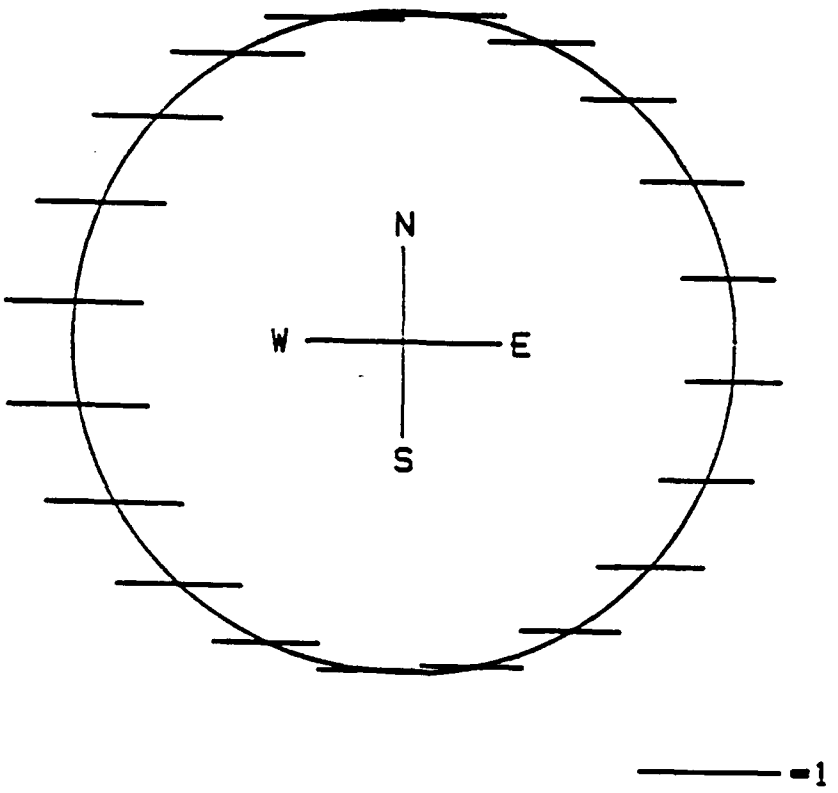

Figure 9

Figure 10

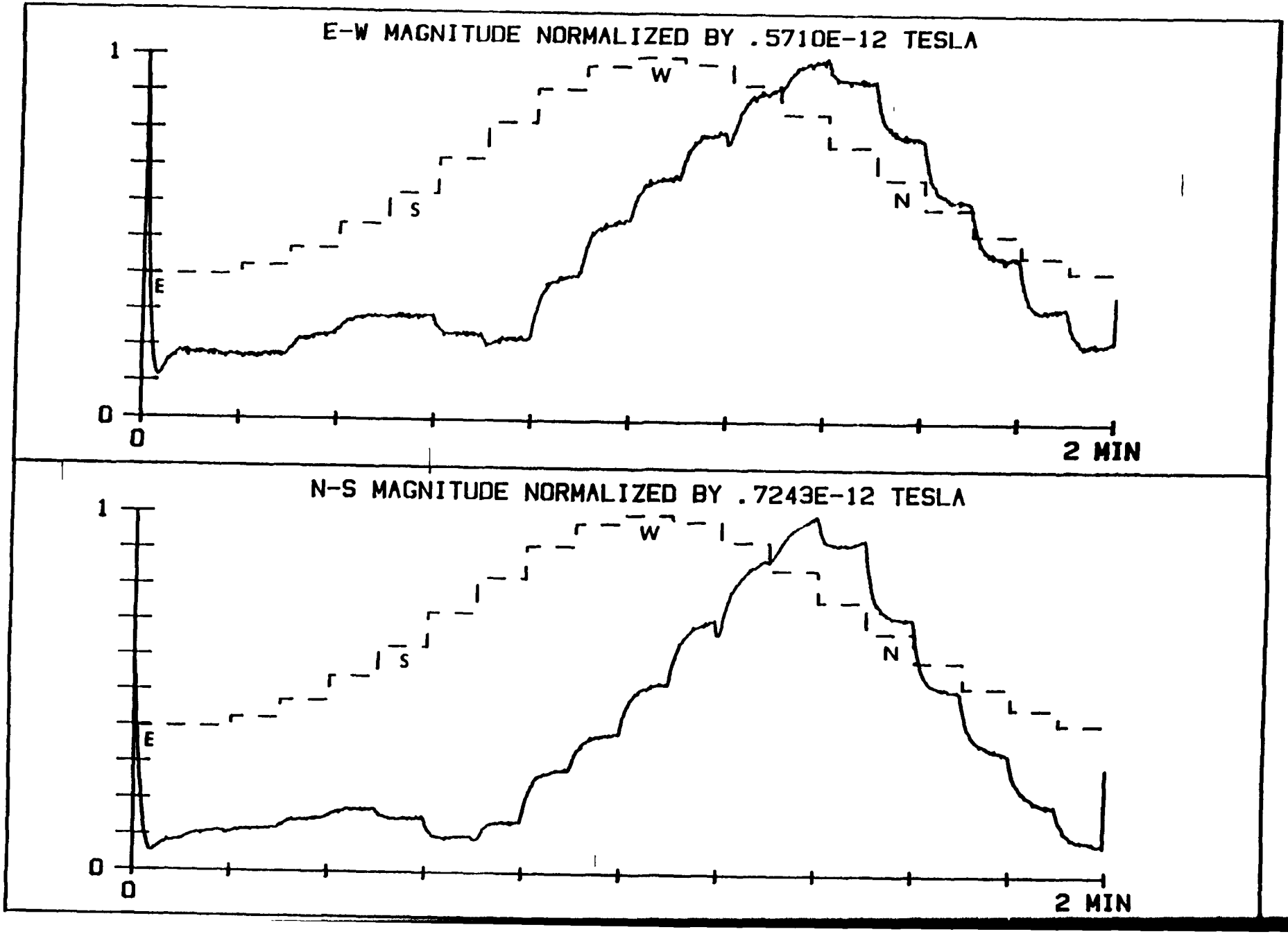
E-W MAGNITUDE NORMALIZED BY .5710E-12 TESLA
1
0
0
2 MIN
E
S
W
N
N-S MAGNITUDE NORMALIZED BY .7243E-12 TESLA
1
0
0
2 MIN
E
S
W
N

Figure 11

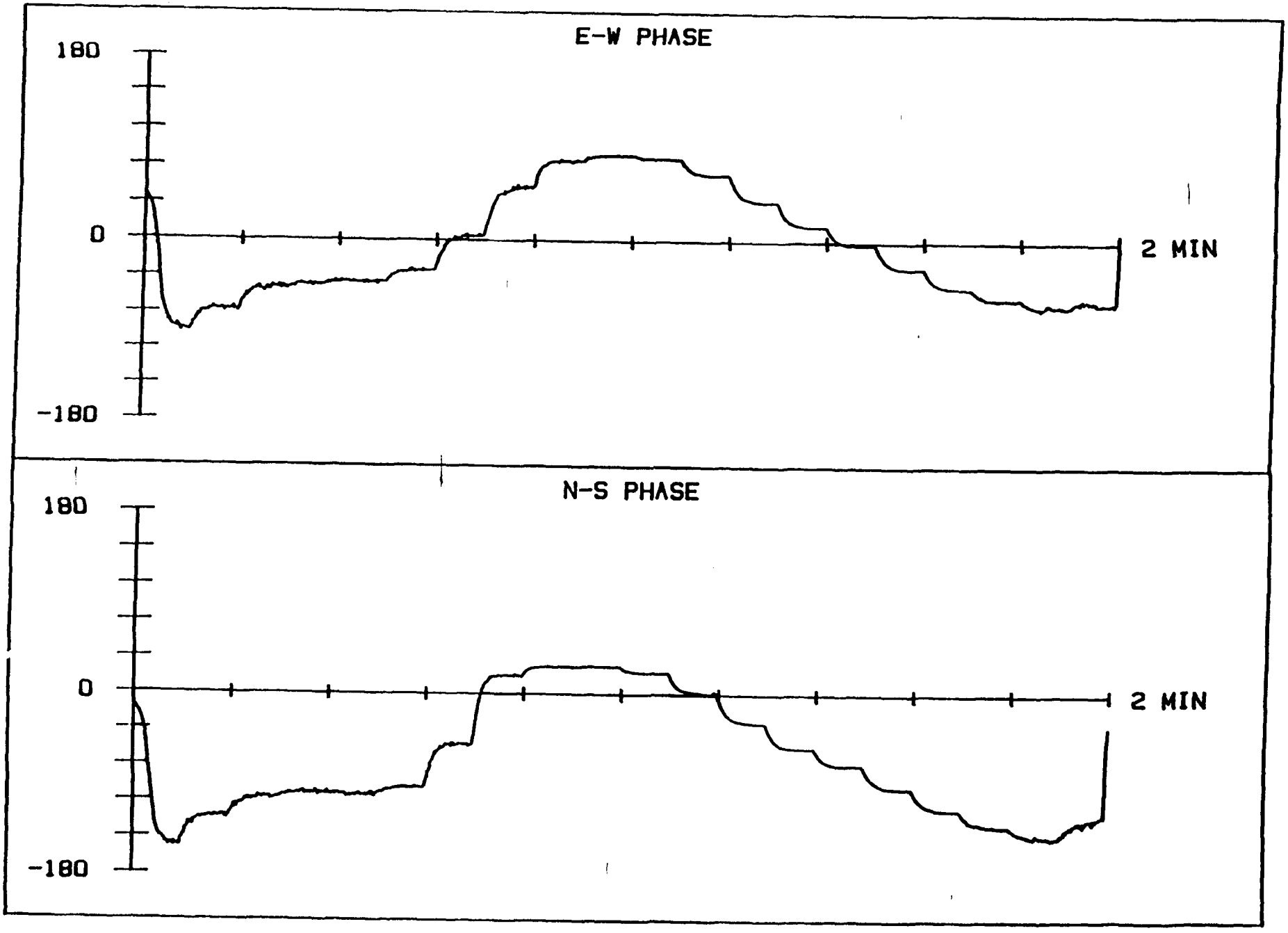

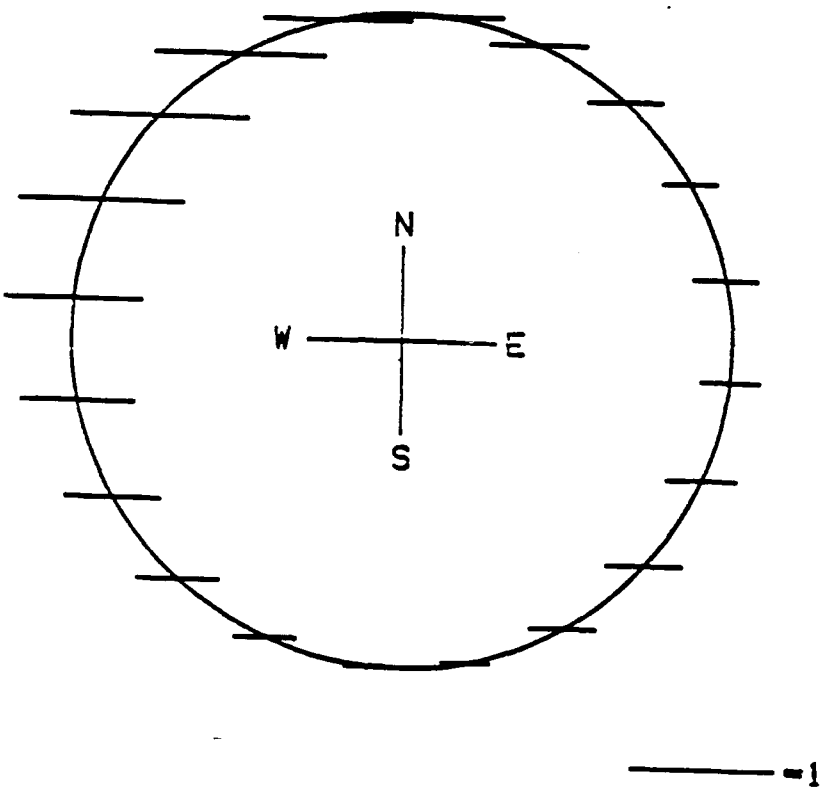

Figure 12

FINAL TECHNICAL REPORT

CONTRACT ONR-TPSU-UCLA-0677-387

OPERATION OF HIPAS FACILITY FOR COOPERATIVE EXPERIMENTS WITH PENNSYLVANIA STATE UNIVERSITY

SEPTEMBER 15, 1986 - SEPTEMBER 30, 1989

Submitted by

The Regents of the University of California
University of California, Los Angeles
Department of Physics
Los Angeles, CA 90024

Alfred Y. Wong
Professor of Physics
Principal Investigaztor

PROJECT REVIEW

During the period fom 9/15/86 to 9/30/90, UCLA's Plasma Physics Laboratory was under subcontract to The Pennsylvania State University, to collaborate with Professor A.J. Ferraro to conduct research on polar VLF excitation and generation. The whole program was under the sponsorship of the U.S. Congress Universities Research Initiative (URI), which was administered by the U.S.Navy's Office of Research, Washington D.C. UCLA's contributions to the URI initiative were its very high power radio frequency array 35 miles east of Fairbanks, Alaska; called HIPAS, which stands for HIgh Power Auroral Stimulation and UCLA's ionosonde diagnostics.

Four separate campaigns were conducted over the course of the URI/PennState subcontract; namely,

I June 15-25, 1987
II October 13-23, 1987
III July 11 -22, 1988

and

IV July 12- Aug 8, 1989

The four campaigns are summarized in Table I, which emphasizes the operation of the HIPAS radio frequency heater; namely, the campaign dates, the durations of uninterrupted operation, the total power radiated (ie 8x100KW means 8 transmitters at 100KW each or a total radiated power of 800KW), and comments on the over all operation during the specified period of operation.

Prior to the first campaign, the total radiated power was brought up to 800 KW at 3.345 MHz under the advice of John Carroll (the orginal Platteville chief engineer) who came and worked at the site. The sytem was next retuned to 2.85 MHz, which is close to the electron cyclotron frequency, and which should efficiently couple to the electrojet to generate VLF and ELF. This meant retuning both the transmitters, baluns, and antennas. The antennas were tuned by the addition of "end-straps" which were a pair of cables attached to the ends of each antenna and spread in angle and anchored to the ground to control both the impedance and frequency of a dipole. This method of antenna tuning was the contribution of Mr. William Harrison, a consultant to HIPAS. The baluns were tuned by replacing the coaxial cable that acted as capacitive ends loads by high voltage variable vacuum capacitors which could be continously tuned. The tops of the baluns were covered by large plastic boxes to protect the antenna connections from the elements, principally ice during the winter, but rain during the summer. The coaxial feed lines were also pressurized to a few inches gauge to thwart any intake of mosture laden air into the coaxial lines and baluns, with resultant build up of ice during the winter. Initially, this air was dried with commercial "Dri- Rite". Later a refrigeration type of drying sytem was added. The pressurization of the transmission lines and baluns with dry air soon showed that the system could be operated during the winter at temperatures as low as -40^{o}F.

TABLE I

TRANSMITTER PERFORMANCE SUMMARY

CAMPAIGN	DATES	TIMES	DURATIONS (hours)	POWERS	REMARKS
I	6/15/87	0600-0900	3	8x100KW	10°C ambient
	(Monday)	1530-1830	3	"	rain
	6/16/87	0700-1030	3.5	8x100KW	
		1800-2100	3		23°C
	6/17/87	0400-1600	12	8x100KW	Coolant problems
	6/18/87	0300-1100	8	8x100KW	
		1700-2300	6		22°C
	6/19/87	0600-1200	6	8x100KW	
	6/22/87	1000-1230	2.5	8x100KW	stopped due to arc in #0
	(Monday)				
		2030-2400	3.5		
	6/23/87	1230-1600	3.5		
		1900-2200	3		
	6/24/90	0800-1424	6.4	8x100KW	#6 out, insulator
		1424-1500	0.6	6x100KW	failure, #7 off for balance
		1500-1524	0.4	8x100KW	repaired
		1524-1600	1.0	4x100KW &	4x 70KW generator overheated
	6/25/90	0630-1100	4.5	8x100KW	
		2200-2400	2	8x100KW	trips due to air in water interlocks
		TOTAL hours	73.1		
II	10/13/87	1300-1900	5	8x100KW	
	10/14/87	1300-1500	2	"	
		1500-1600	1	8x 40KW	fly over
		1620-2000	3.3	8x100KW	
	10/15/87	0800-1400	6	8x100KW	1°C ambient
	10/16/87	0000- 600	6	8x100KW	
	10/19/87	1530-2200	6.5	8x100KW	
	10/20/87	0830-1200	-	-	interlock problems
		1330-1730	4	8x100KW	
	10/21/87	1530-1830	3	8x100KW	
		2000-2400	4	7x100KW	#6 off line
	10/22/87	1500-2300	8	8x100KW	
	10/23/87	1900-2300	4	8X100KW	
		TOTAL hours	50.3		

(continued)

TABLE I
(CONTINUED)

CAMPAIGN	DATE	TIMES	DURATION (hours)	POWERS	REMARKS
II	7/11/88	1100-1600	5	8x100KW	#5 off 15 minutes
	(Monday)	1900-2200	3	"	80°F ambient
	7/12/88	1800-2230	4.5	"	Power out at UA
	7/13/88	1100-1200	1	7x100KW	#6 off (meter shunt bad)
		1200-1400	2	8x100KW	
		2000-2400	4		77°F thunderstorm
	7/14/88	1800-2400	6	"	86°F thunderstorm lightening
	7/15/88	2040-	6.3	"	beautiful sunset
	7/16/88	0302			at 0019
	7/17/88	2100-	5.2	"	
	7/18/88	0220			
	7/18/88	2100-	6	"	
	7/19/88	0300			
	7/19/88 (Tuesday)	1800-2400	6	"	85°F ambient 2 frequency mod 2.85 &2.8525 MHz
	7/20/88	0900-1500	6	"	
	7/21/88	0300-0500	2	"	
		0545-9000	3.2	"	oil hose broke on diesel generator
	7/22/88	0000-0600	6	"	52°F ambient, rain at 0432
		TOTAL hours	65.2		

(continued)

TABLE I
(CONTINUED)

CAMPAIGN	DATES	TIMES	DURATIONS (hours)	POWERS	REMARKS
IV	7/12/89	0000-0600	6	8x100KW	rotating and
	7/13/89	0000-0345	3.75	"	scanning beams
		0345-0400	0.25	6x100KW	0 & 7 off due to
		0400-0630	2.5	8x100KW	interlock problem
	7/14/89	0000-0300	3	"	64°F ambient
	7/14/89	2100-	5	"	90°F ambient
	7/15/89	0200			
	7/15/89	2000-2230	2.5	"	74°F ambient
		2230-2300	0.5	6x100KW	0 & 7 off line
	7/16/89	2300-0100	2	8x100KW	
	7/17/89	2100-2400	3	"	63°F
		0000-0245	2.75	8x120KW	
	7/18/89	0245-0300	0.25	8x100KW	74°F
	7/18/89	2140-	4.75	"	delayed by #4
	7/19/88	0230			FCC Anchorage called
	7/19/89	2130-	4.5	"	#6 interlock
	7/20/89	0200			delay
	7/20/89	1900-2330	4.5	"	55°F
	7/21/89	2330-0300	3.5	8x120KW	78°F
	7/21/89	1900-0300	8	"	
	7/31/89	2100-	6	8x100KW	65°F ambient
	8/01/89	0300			
	8/01/89	2100-	6	"	"painting"
	8/02/89	0300			
	8/02/89	2100-	6	"	66°F ambient
	8/03/89	0300			
	8/03/89	2100-	7	"	
	8/04/89	0400			
	8/04/89	2100-	6	"	59°F ambient
	8/05/89	0300			
	8/06/89	2100-	6	"	78°F ambient
	8/07/89	0300			
	8/07/89	2100-	6	"	75°F ambient
	8/08/89	0300			
	8/08/89	2000-2130	1.5	7x100KW	#1 off line
		2130-0200	4.5	8x100KW	Finis
		TOTAL hours	104.5		

The second diesel generator was brought on-line and the two diesels were

actually run in parallel (ie synchronized). Although interesting as an exercise in power generation, parallel operation was abandoned in favor of the simpler arrangment in which one diesel drove four transmitters while the other drove the other four. This arrangment avoided the problem and dangers of loss of generator synchronization. With the two diesels operational, all eight transmitters could be run at 100KW each for long durations.

The original Henry Radio radio frequency amplifiers that drove the Platteville transmitters were replaced by ENI (Model 240L, 50 Watt) broadband units, which were much more reliable.

During the first campaign, 73 hours of operation were delivered. On one day, (6/17/87) the system suported the Penn State experiments continously for 12 hours. Occationally, transmitters would stop when interlocks over reacted, but generally the transmitters could put were back on-line within minutes.

The HIPAS heater is described in a paper that has been accepted for publication in Radio Science in 1990. It is attached as Appendix I, and is a very complete description of the HIPAS heater during all of the campaigns. Noteworthy of the array is the fact that each antenna is driven from a single Platteville transmitter and each can be individually controlled in phase, permitting the RF beam pattern to be scanned or pointed or defocused. Another feature of the array are the crossed radiating dipoles which produce either right or left circular polarized patterns depending on how the antennas are connected to their balun terminals. The circular polarization of the radiating beam is described in considerable detail the Appendix I paper.

At the onset of the first campaign, any polarization change had to be made by climbing the antenna towers and changing the antenna connections by hand, which meant that half a day was typically needed to change the polarization of the the array. By the time of the third campaign switches had been installed on the tops of each antenna, so that the change could be made from the ground. The polarization can now be changed in less than five minutes. The polarization switches were of HIPAS design and were fabricated both at the site and with the aid of the UCLA Physics Department machine shop.

During the first two campaigns the array was phased or pointed manually, via delay boxes with switches that set the delays on the inputs to the individual Platteville amplifiers and associated antennas. The beam was pointed by pre calculation of the array pattern. Two operators, working furiously, could reset the direction of the beam in about 2 minutes. By the time of the third campaign, voltage variable phase shifters had been installed and the pointing or dephasing was controlled by a personel computer (PC). A beam forming time of 10 milliseconds was achieved with this first PC controlled system. The system was as shown in Figure 4 of the Appendix I paper. At the onset of the last campaign an even faster system had been installed with 15 microscond beamforming times. The new sytem permitted "painting" experiments.

To phase the array properly each antenna has to be sampled and compared

with the others. The base of each antenna (see also Figure 4, Appendix I) has a sampling loop which is now connected to a 1000 foot long piece of RG-9U coaxial cable. The cables ends are all brought to a distribution panel at the control console; there the phases are compared with either an oscilloscope or vector voltmeter. The excess cable on each run are left wound on the cable spools to serve as chokes to keep RF induced on the outerbraid from interfering with the phase measurments (on the center conductors). The longer cables to the most distant antennas (ie, #'s 1, 2, 6, & 7)are finished by by winding ends on magnetic cores. The phasing cables were orginally RG-58U coax which was too light weight. Many were broken, RF burned, and poorly spliced. They were all replaced with the forementioned RG-9U cables with end chokes.

During the first campaign, harmonics of the radiating HF were found to interfere with television reception of channel 2 within the local community of Two Rivers, Alaska. The problem was solved by series resonant "traps" across the main tank circuit of the Platteville transmitters. The traps were tuned while monitoring televison reception at the bunk house, one half mile away. There was no problem in subsequent campaigns

We also procured a broadband isotropic RF radiation safety monitor (ie NARDA Model 8616 with 8662B Efield (0.3-1000MHz) and 8652 H field (0.3-30 MHz) probes). The monitor was used to carefully survey the site for unsafe levels of radio freuqency radiation, especially when the array was radiating a the megawatt level. At 3 MHz the US standard for whole body radiation, averaged over 0.1 hours, is 100 mW/cm^2. This corresponds to approximately 500 volts/meter amplitude. This standard was not exceeded beyond 100 feet of any antenna when the array was radiating at a megawatt. During operation, access roads into the antenna field are barricaded, a flashing light on the top of the generator building is activated, and the antenna field surveyed from control room for inadvertent intrusion.

Between the third and fourth campaign, Dr. Michael McCarrick of this laboratory moved with his family to the HIPAS site, for the purposes of better cooordinating the scientific work at the facility. It was during his tenure at HIPAS that diagnostics were set up at the NOAA, Gilmore Creek, approximately 35 kilometers North West of HIPAS, the fast beam switching system was installed, and the array was completely controlled by computers. With an ionosonde at NOAA, ionograms could be recorded while the heater was operating. During this same period special ELF detectors, developed by Dr. Dave Sentman of UCLA Space Sciences Group under a contract with the US Air Force, were installed at the NOAA site. With these special detectors, we were able to detect heater induced ULF excitation at 11 Hz, between the first two (7 & 14 Hz) Schuman earth E&M resonances.

Data links were also set up between the PSU receiver site at the University of Alaska and the HIPAS transmitter control , which allowed instantaneous monitoring of the VLF resonance at the transmitter control center, and allowed an experimenter to see cause and effect in an on-line fashion. This was very important during the beam steering experiments. The same data line via IBM PC was also established between NOAA Gilmore Creek and the HIPAS control room allowing us to monitor the ionospheric conditions while the heater was running continuously.

The electric starting motors on the diesel generators were replaced by air starters, which are much more reliable; particularly since replacement electric motors are no longer available.

The reliablity of HIPAS depends on regular maintenance, especially during severe winter periods. The diesel generators are checked on a weekly basis and all the heating and cooling systems now have back ups. HIPAS weathered two severe winters (one where site temperatures dropped to -70°F) and was able to run campaigns after each. We attributed this performance to the excellant on-site staff mebers, who were able to foresee potential problems and take action.

Reference to Table I, Campaign IV includes long-duration runs at total radiated power of one megawatt. The transmitters ran for a total of 104.5 hours with less than 1-2% down times.

Appendix II contains a copy of a paper written by R.G.Brandt for presentation at a special conference (May 1990) in Tromso, Norway on ionosphereic modification. It is an apt summary of the HIPAS's contribution to the four Penn State URI campaigns. Dr. R.G.Brandt is the Program Manager of the Office of Naval Research's which supported the entire project.

SUMMARY

In summary, the PSU and HIPAS staffs worked very well together during the four URI campaigns. HIPAS scientists would have liked to have had greater access to the data gathered during the campaigns, as well as participated in more post campaign discussions, as was orginally agreed upon the onset of the program. In reptrospect, the "opportunity" mode (in which experiments are conducted when conditions are favorable) would have been more preferable to the "campaign" mode (in which experiments are conducted during a block of time regardless of conditions), particularly due to the fact that the ionosphere is so variable.

During the URI program the HIPAS facility has been brought to a high degree of operational reliablity. It can now be operated any time of the year. In addition the facility has been instrumented to a stage that it can be controlled locally or remotely by computers. The invention of the "phase-modulation" technique by HIPAS sceintists made it possible to modulate the HF radiation at any low frequency without affecting the diesel power sources.

APPENDIX I

Paper submitted for publication in Radio Science which descrobes the HIPAS radio frquency heater essentually as it was during the four PennState URI campaigns:

A.Y.Wong,et all, High Power Radiating Facility at the HIPAS observatory, Radio Science, accepted for publication.

High Power Radiating Facility at the HIPAS Observatory

A. Y. Wong, J. Carroll*, R. Dickman, W. Harrison**, W. Huhn,
B. Lum, M. McCarrick, J. Santoru***, C. Schock, G. Wong****, and R. F. Wuerker

Department of Physics
University of California
Los Angeles, CA 90024-1547

and

HIPAS Observatory
7795 Chena Hot Springs Rd.
Fairbanks, AK 99712

ABSTRACT

UCLA's radio frequency ionospheric heater, 25 miles east of Fairbanks, Alaska, is described. The heater consists of eight crossed dipole antennas arranged in a circular pattern to give a gain of 18.4 db over isotropic at 2.85 MHz (~ 2nd electron cyclotron harmonic). At 1.2 MW total radiated power the array has a calculated ERP of 84 MW. Each antenna is driven by a 150 KW transmitter, originally from the Platteville heater. The eight transmitter-antennas are managed by a personal computer which controls power, modulation and beam steering. Methods of tuning the antennas, to achieve either right (O-mode) or left (X-mode) circular polarized radiated beams, are described. The heater is powered by two 1500 HP diesel electric generators. It can be operated throughout the year over -30°C to 40°C ambient temperature extremes. Future improvements include the construction of an even larger 840 x 840 meter (24 x 24 antenna) array with a gain of 37.5 dbi.

* P.O. Box 44, Glenn Haven, CO, 80532
** Wavecom, 9036 Winnetka, Northridge, CA, 91324.
*** Hughes Research Laboratories, 3011 Malibu Canyon Rd, Malibu, CA, 90265
**** Institute for Bosan Studies, 525 S. San Gabriel Blvd, Pasadena, CA, 91107

I. INTRODUCTION

The HIPAS Observatory was developed as an outdoor laboratory for research on nonlinear space plasma physics using high power radio frequency (RF) electromagnetic waves to actively stimulate the auroral ionosphere, hence the acronym HIPAS (HIgh Power Auroral Stimulation).

The Observatory was begun in 1981, [A. Wong, 1981]. The site has the feature that (like the one in Tromso, Norway) the RF beam can be launched along the earth's magnetic field [Stubbe, 1982]. It also passes under the auroral oval, resulting in spectacular auroral displays throughout the late fall to early spring months [Elvey, 1957]. It is accessable, over good roads, to Fairbanks (25 miles to the west), the University of Alaska (UA), the UA's Geophysical Institute, UA's Poker Flat rocket launching site, the NOAA Gilmore Creek Satellite Tracking Station, Eielson AFB, and Fort Wainwright.

The heart of the system is a circular eight antenna radio frequency array of 84 MW Equivalent Radiating Power (ERP), when the transmitter outputs are 1.2 MW total (i.e. 8 x 150 KW). The array is summarized in Table I.

The first column of Table I lists the frequencies at which the system has been operated. The system is not frequency agile. The antennas have to be retuned whenever the operating frequency is changed more than 10 KHz. The present operating frequency is 2.85 MHz which is close to the second harmonic of the electron cyclotron frequency about the earth's (~ 1/2 Gauss) magnetic field, and also one of our licensed frequencies.

A top view schematic of the array is given in Figure 1. The array consists of seven antennas equally spaced around a circle of 208 meters diameter with the eighth at the center. Each antenna is connected to its own

150 KW (max) amplifier through seven inch outside diameter (2-1/2 inch center conductor), dry air pressurised (1-2 psi gauge) coax made from agricultural irrigation pipe. The individual final amplifiers and coaxial lines are all modifications from the now legendary Platteville heater, which ceased operation in the late 1970's [Carroll, 1974]. This equipment was loaned to UCLA, which reconfigured each transmitter with new individual power supplies. The eight transmitters are now housed in a building on the edge of the antenna field, as indicated in Figure 1. Close by is a transformer yard and a large barn-like building that houses the two 1500 horsepower (or 1.2 MW each) diesel electric generators which power the system.

As shown in Table I, at 2.85 Hz, the array has a calculated gain of 18.4 dbi. At a total radiated power of 1.2 MW, this corresponds to an ERP of 84 MW, which means that at a range (R) of 100 Km, a RF flux ($F = ERP/4\pi R^2$) of 0.67 mW/m^2, or a peak vacuum RF electric field amplitude of 0.7 V/m [calculated from the flux and the chacteristic impedance of free space (Z_o = 377 ohms); namely, $E_{peakRF} = \sqrt{2Z_oF}$].

A recent (1988) photograph of one of the antennas (i.e., #4 in Figure 1) is shown in Figure 2. The crossed dipoles are 46 feet above the ground. Seen also in this picture are the balun, the coaxial feed line, and the "end-loading-straps" that are used to retune the antenna(s) to frequencies in the range of 2.8 - 4.9 MHz. A second antenna is in the background. The picture also gives a sense of the environment at the HIPAS site in the spring (April). During the winter, the antenna field is completely snow-covered, but usually not more than a few feet deep.

By phasing the north-south dipole currents 90 degrees with respect to the east-west dipole currents, the array can be made to radiate either right (O mode) or left (X mode) circularly polarized patterns, depending on the

connection of the east-west dipoles to the balun, as shown schematically in Figure 3. When the antennas are connected to radiate a left hand circularly polarized beam, the radiated electric field rotates in the same direction as free electrons in the ionosphere about the earth's magnetic field. This is called the X-mode. The other, right hand circular, polarization is called the O-mode. It propagates through the ionosphere with less loss.

The whole system now (1988-89) operates rather routinely at a total radiated power of one megawatt CW throughout the year, over -30°C (winter) to +40°C (summer) ambient temperature extremes. The transmitters can be amplitude modulated from 0.15 - 10 KHz. The antennas can also be rephased for the purpose of modulating the far field pattern at ULF frequencies, or for steering the beam 30° off the vertical at rates up to 100 Hz.

Details about the contruction of the present RF ionospheric heater system with its eight Platteville transmitters, new antennas, diesel power sources, arctic water cooling system, and original pulsed transmitter are included below.

II. RADIO FREQUENCY SYSTEM

A. CW TRANSMITTERS

Figure 4 shows the whole HIPAS RF system schematically. One can start at the triaxial balun at the right side of the page. The antennas, as seen earlier in Figure 3, are connected to the inner and mid balun conductors. The 7 inch agricultural coaxial lines connect to the bottom of the balun through a coaxial right angle reducer. The coaxial lines (see Figure 1) run to the transmitter building where they connect to coaxial power meters (Bird Company) and then to the Platteville cabinets, containing the 4CV100,000 (class C) final and 3-1000Z (class B) intermediate amplifiers. The Platteville intermediate amplifier is driven by a linear ENI 240L driver, a

linear Mini Circuit ZFL 500 preamplifer, a variable attenuator, a manual phase shifter, an electronic phase shifter (Merrimac PSE-4, 0-360 degree voltage variable phase shifter), and finally the output port of a 10 way RF power splitter, the input of which is connected to a frequency synthesizer which drives the system at low level. The other seven antennas are identically connected to the other output ports of the 10 way power splitter.

The array can be amplitude modulated at audio frequencies through a TTL circuit, driven by another audio frequency synthesizer. The lowest AM frequency is presently 156 Hz, due to one Henry chokes in each 4CV100,000 plate power supply. For even lower frequency modulations, half of the antennas are shifted in phase by 180^{o} at the modulation frequency. This change in the phasing of the array destroys the central lobe of the radio beam. Such a method of antenna phase modulation has been used to modulate the array at very low frequencies (0.1-160 Hz) without stressing the final plate power supplies or harming the diesel generators through any sympathetic mechanical resonances.

The most recent improvement in the whole RF system has been the introduction of a Personal Computer (PC) to contol and manage the operation of the eight transmitters. The PC now controls the second frequency synthesizer which amplitude modulates the transmitters at audio frequencies. It also controls the phasing of the antennas for the purposes of modulating the antenna's far field pattern at very low (ULF) frequencies and for pointing the RF beam as much as 30^{o} off the vertical. Its description will be the subject of a subsequent paper.

A Platteville amplifier is shown schematically in Figure 5. The final Eimac 4CV100,000 power tetrode has its screen grid grounded, and as a result requires two power supplies. The plate supply is 16 KV. The screen supply

is continously variable (0-1200 V) and is used to control the output RF power. It is connected between the ground and the tube's cathode. At low cathode voltage the tube is cut off and the RF output is zero. With increasing cathode voltage the tube conducts periodically in the class C mode.

The Eimac 3-1000Z drives the control grid of the final amplifier through its own resonant plate circuit. It operates as a Class B grounded control grid triode. Its cathode is connected to ground by a 50 ohm resistor that also terminates the cable from the remote ENI 240L amplifier. Both amplifiers have to be retuned whenever the operating frequency is changed. They are described in more detail in the original Platteville paper [Ibid]. The ENI and Minicircuit amplifiers are linear types which require no tuning.

The Bird power meters at the output of the Platteville amplifers monitor the forward and reflected powers in the coaxial lines to the individual antennas. Whenever high standing waves are present in a line, the Bird meter circuitry trips off the final amplifier's high voltage supply. Additional trips are included in the plate and screen current meters on each 4CV100,000 tube. The (UCLA constructed) 4CV100,1000 power supplies are only shown symbolically in Figure 5. In reality, both are unregulated three phase rectified units, with 1 H filter chokes and 10 uF output filter capacitors.

The Platteville transmitters,along with their individual power supplies, were mounted in pairs within surplus highway trailers. This reassembly was all done at UCLA. On completion, the trailers were shipped to the site and attached to the side of a specially constructed building on the edge of the antenna field, as seen in Figure 1. The central building now functions as the transmitter operation center. Figure 6 is a photograph of the resulting transmitter complex. The southwest corner of the generator building is seen

in the lower left edge of the picture. The transformer yard is between the generator building and transmitter complex. The antenna field is in the background. The picture was taken on the same day as Figure 2.

B. TRANSMITTER COOLING SYSTEM

The 4CV100,000 tubes were designed to be cooled by the evaporation of water. Each (massive copper) anode fits "upside-down" in a EIMAC boiler, filled with distilled water, as shown schematically in Figure 7. A side arm connects the boiler to an overhead heat exchanger (also of EIMAC manufacture) via an electrically insulating 4 inch diameter pyrex glass tube. Condensed water is brought back to a make up reservoir on the side of the amplifier cabinet. Water is then returned to the boiler via a 12 foot long (electrically insulating) piece of 1 inch ID silicone rubber hose. Since the boiler and tube anode are both at a combined RF and DC voltage of 32 KV peak, the pyrex vapor line and long rubber return have to be carefully maintained. The boiler and tube are supported (off ground) by 6 inch long ceramic insulators.

In addition, the 4CV100,000's tank circuit inductor (made from 2 inch diameter copper tubing) and RFC choke are both cooled with distilled water from the make up reservoir. These cooling schemes were all part of the original Platteville design [Ibid].

To run the Platteville amplifiers in Alaska, four separate secondary (glycol) cooling loops were built. Each has its own radiator and fan, which can be seen in Figure 6, on the ends of the trailer roofs. Each glycol loop circulates water through two 4CV100,000 steam heat exchangers, which are mounted in the small sheds on the roof of each trailer (seen also in Figure 6). In addition, one of each pair of glycol loops is used to cool (through another heat exchanger) the distilled water system for four transmitters.

This secondary loop can be completely bypassed, to avoid freezing of the distilled water during the winter by glycol cooled to sub zero temperatures by the ambient air.

Air is also used to cool the interior of the Platteville cabinets. It is drawn through a floor duct. During winter, the duct is closed to prevent freezing of components by the cold air.

To further prevent freezing of distilled water and harm to the electrical components, the whole transmitter complex is heated by forced air and backup electrical heating systems. Winter temperatures in Alaska can even exceed the low temperature ratings on many oil filled capacitors. An alarm system has also been installed to monitor both the coolant and air temperatures throughout the transmitter complex.

The water cooling system is completely interlocked. The transmitters cannot operate without proper water flow. Failure of any loop shuts down its 4CV100,000 plate supply. For a transmitter to operate, water flows have to be correct, plate and screen currents below maximum rated values of 12 and 1 amperes respectively, and reflected power from the antennas below 5 KW. The complete water cooling system is shown schematically in Figure 7.

C. DIESEL ELECTRIC GENERATORS

The HIPAS site is at the very end of the Golden Valley Electric Company's line from Fairbanks. At the site, the commercial line has only 50 KW capacity.

The problem of powering the eight Platteville transmitters was solved by shipping three 1500 horsepower (1.2 MVA each) 4800 volt-3 phase diesel electric generators from surplus sites in California. Two of the generators are now used to operate (4 each) transmitters, via the transformer yard, which also powers the water cooling systems. The third generator is a source of spare parts.

The transmitter and generator control circuity, building lighting, and building heating are all run off the Golden Valley line.

After the generators had been installed on concrete foundations, the generator building was erected. The third generator bay now functions as a combined meeting and recreation hall. The second floor portion of the building also functions as the site office, a library, a conference room, and storage space. The location of this building was shown in Figure 1; an edge of it was seen in Figure 6.

Figure 8 is a photograph of one of the diesel-electric generators, which had recently been upgraded with pneumatic starters, one of which can even be seen in the picture.

When the system is radiating 1 MW RF, the two diesels together consume 120 gallons of fuel per hour.

D. PULSED TRANSMITTER

Prior to the installation of the Platteville transmitters at the HIPAS site, a 1.8 MW pulsed sytem was built and used. It was lost (March 1984) in a building fire. Though this pulsed system is no longer available, it is reviewed because it may be the key to achieving very high (100 GW ERP) peak powers with a new array. It is a resource since all the drawings are still avialable, the engineering is completed, and the system successfully operated at the site.

The original pulsed system was a master oscillator-amplifier chain, not unlike the present (Figure 4) CW system. It started with commercial ENI 403LA (37 db) and ENI 240L (50 db) linear preamplifiers, an Intermediate Power Amplifier (IPA; with 21 db gain and EIMAC 4CX250BC tetrode), a Power Amplifier (PA, with 17 db gain and EIMAC 4CX5000A tetrode), and finished with a Final Power Amplifier [FPA, with 17 db gain and a Machlett ML 7560 triode].

The FPA had a 26 KV supply with a 166 microfarad (45 KJ) capacitor bank. Pulsed RF output of the system was 1.8 MW for one millisecond. The whole amplifier is described in more detail in other publications [Wong, 1983; Santoru, 1984].

We have recently considered reproducing 12 of these pulsed high power amplifiers for the purpose of achieving an ERP of 100 GW with a new array.

III. ANTENNA SYSTEM

The present antenna array was shown earlier in Figures 1, 2, and 6. When all the antennas are driven in phase, the radiated beam is concentrated vertically overhead. The calculated radiation pattern for this case is included in Figure 9. The center of this pattern (see Table I) has a theoretical gain at 2.85 MHz of 18.4 dbi and a half power width of 21.5 degrees, which corresponds to a diameter of 30 Km at 100 KM range. The sun and moon, in comparison, are only one-half of a degree wide (10^{-2} radians).

By adjusting the phases of the antennas relative to one another the beam pattern can be changed. An example is shown in Figure 9, which corresponds to the case where the beam is tipped 30^{o} off the vertical. At this angle, the peak intensity is a factor of two lower than the vertical case (Figure 6), while the side lobe power has increased.

The two dipoles of each antenna are physically supported 46 feet above the ground by a central (original) steel tower and by four wooden telephone poles topped with G-10 fiber glass standoffs, as seen in Figure 2. The central tower also supports the single "bazooka balun" which converts the unbalanced coax cable input to a balanced drive.

Figure 3 showed that there are two ways of connecting the two antennas on each tower together. One connection produces a right circularly polarized radiation pattern (called the O or ordinary mode). The other connection

produces a left circular pattern (called the X or extraordinary mode). For circularly polarized emission, the currents in the two orthogonal dipoles have to be 90^{o} out of phase with respect to one another. For this to happen, both antennas have to be specially tuned; first, the east-west dipoles are disconnected from the (already tuned) triaxial balun. The north-south dipoles are then tuned to have an impedance,

$$Z_{ns} = 50 + j50 \text{ ohms} \qquad (1)$$

at the transmitter operating frequency. Next, the tuned north-south dipole is disconnected from the balun and the east-west dipole reconnected. This dipole is then tuned to an impedance of

$$Z_{ew} = 50 - j50 \text{ ohms.} \qquad (2)$$

When the two antennas are reconnected together in parallel (on the balun) the resulting impedance Z_r of the combination is,

$$1/Z_r = (1/Z_{ns}) + (1/Z_{ew}) = (50+j50)^{-1} + (50-j50)^{-1} = 1/50, \qquad (3)$$

or 50 ohms of real resistive impedance, which properly terminates the 50 Ohm coaxial cable that drives the antenna. When the parallel combination is driven by an RF voltage of V, the currents to the dipoles are the applied RF voltage divided by the individual dipole impedances; namely,

$$I_{ns} = V/Z_{ns} = V(1 - j)/100 \text{ ohms} \qquad (4)$$

and

$$I_{ew} = V/Z_{ew} = V(1 + j)/100 \text{ ohms}$$

As can be seen, the two current are phased 90° with respect to one another. The current into the common connection is the sum of the two; namely,

$$I_{in} = I_{ns} + I_{ew} = V/50 \text{ ohms} \qquad (5)$$

When the antenna currents are in quadrature, the radiation from the antenna is circularly polarized. Right or left circular polarization is now only determined by the parallel connection of the east-west dipole to the north-south dipole; namely, whether the east half dipole is connected to the south half dipole or to the north half dipole, as diagrammed earlier in Figure 3. This rather elegant scheme for producing a right or left circularly polarized radio beam was suggested to us by the Platteville design.

Originally, the HIPAS array was changed between X and O modes by climbing the antenna towers and manually interchanging the east-west dipole connections. We recently (1989) developed an antenna switch, which now let us quickly change the antenna polarizations manually from the ground. Soon , electric motors will be added and the polarization changed from the control room.

Each balun also has to be tuned to the transmitter's operating frequency before the antennas can be tuned. The balun is basically a quarter wave resonator, orginally resonant at 4.9 MHz. A 0-1800 pF vacuum variable capacitor was placed between the outer coaxial balun sleeve and the outer conductor of the coxial feed line, so that the balun circuit could also be resonated at lower operating frequencies. To tune a balun, the antennas are disconnected. Next, the center balun conductor is connected to the outer

most (triax) conductor by a low inductance copper shorting strap. The variable vacuum capacitor is then tuned until the transmission line appears to have an open circuit at the transmitter's operating frequency. Afterwards, the short is removed and the dipoles individually tuned as described above. The tuning of a balun and its antennas is expedited by the use of a commercial network analyzer such as the Hewlett Packard 8753A.

For frequencies below 4.9 MHz, the antennas have to be lengthened and retuned. This is now done by adding a pair of conductors to the ends of each dipole. The ends of these conductors are each terminated with a 20 centimeter diameter stainless steel kitchen bowl, which functions as a corona shield. Polypropolene rope is attached to a "hook eye" within the bowl. By pulling the ropes from the ground, the added conductors or "end-straps" are extended in a straight line away from the ends of the dipoles. A dipole is then retuned by spreading the end-straps away from one another and by adjusting their angle with respect to the ground. The spread between the two straps primarily changes the reactance of the antenna, while the angle of approach to the ground principally varies the antenna's resistance. The end-straps on either end of a dipole are manipulated symmetrically until the dipole fulfills either equation 1 or 2 at the new operating frequency. Tuning a dipole is a five man operation, with one person on each end-strap rope, and the fifth manning the network analyzer, connected at the output of the power amplifier (in the transmitter building). Once the end-straps are properly positioned, stakes are driven in the ground and the ropes "tied off." Each new operating freqeuncy requires a new set of end-straps and stake locations. The antenna end-straps and corona bowls are seen clearly in

Figure 2. The end-straps are actually lengths of RG-9U coaxial cables which use the outer braid as the RF conductor. By this technique we have achieved VSW's of 1.1.

The "dog house" on the top of the antenna, and seen in Figure 2, protects the balun and antenna connections from rain, snow, and ice. With these recent protective houses, the system can be operated during rain storms, as well as in the winter. In the past, the open antenna connections became encased in ice and the system could not be operated.

As noted earlier, the irrigation coax lines and baluns are pressurized to about 1 psi gauge with dry air to prevent the accumulation of water or ice inside. This pressurization scheme is another reason that the system can be operated in the winter (-30^{o}). A commercial refrigeration system is now used to dry the air.

The present 125 KW power capability of each antenna is due to a three inch diameter right angle coax bend between the Platteville coax and the vertical balun. At Platteville, the individual transmitters could all be run at 160 KW outputs. To operate again safely at this power, the baluns and right angle bends would all have to be enlarged in diameter. The transmitters have however been tested at 160 KW for short durations.

Loop couplers (shown in Figure 4) have been installed in each antenna coax, close to the transition to its balun, for the purpose of phasing the antennas. The individual monitoring loops are connected to a 1000 foot long piece of RG-8 cable, which ends in the transmitter control room. With equal length cables on each monitoring loop, the system can easily be phased with either a high frequency X-Y oscilloscope or a Vector voltmeter. Excess cable is left on the individual shipping spools so that the remaining cable functions as chokes to surpress RF, induced on the outer conductor, from

getting into the control room and effecting the phase measurements. The monitoring cables to the more distant antennas are, for the same reason, wrapped around large ferrite cores before entering the control room.

IV. PERFORMANCE REVIEW

The HIPAS system, as described above, operates regularly at 1 MW total output. It has produced some remarkable ionospheric effects, particularly when the ionosphere critical frequencies match the transmitter frequency and the array operates in the O-mode. This usually means waiting for the ionosphere's plasma frequency to either fall in the evening through the transmitter frequency or rise during the morning. Unlike at Platteville, the antennas are not broadband. Also the frequency agility of the amplifiers (originally possible at Platteville) has not yet been implemented.

The heater has also excited ELF waves by modulating the ionospheric currents, with the array radiating mainly in the X-mode continuously for up to 24 hours. These effects are the subjects of companion papers.

V. FUTURE

The HIPAS site now represents one MW of installed RF power at auroral lattitudes. The total radiated power could be increased to 1.3 MW by operating each of the Platteville amplifiers again at 160 KW. Such an improvement will require new baluns, and would increase the ERP to 88 MW. We could even increase the radiated power to 200 KW. the limit of the 4CV100,000 tubes. This improvement would double the ERP of the present array to 140 MW and would require higher voltage plate supplies, as well as the new baluns.

We are now considering other ways of increasing the system ERP by dramatically increasing both the size of the array and also increasing the

operating frequency. One idea envisions a new 24 x 24 or 576 dipole array, 830 x 830 meters on a side (i.e., 2700 x 2700 ft), operating at 7.5 MHZ (40 meter wavelength). Such an array would have a gain of 37 dbi and a beam width of only 2.5°. With twelve (12) new pulsed 1.8 MW peak transmitters, identical to the one originally built for HIPAS (see II.D), a peak ERP of 110 GW would be realized. At 100 Km range, this system would achieve a flux of 0.9 W/m^2 or a peak RF (vacuum) amplitude of 26 volts/meter. Flux values for other ranges are given in Table II.

With twelve of the present Platteville transmitters, operating continuously at 160 KW each, an ERP of 10 GW would be realized. These upgrade studies are on going and will be the subject of future papers.

VI. SUMMARY

A "new" 1 MW (70 MW ERP) continous wave radio frequency ionospheric heater is now operational in Alaska. The radiated beam can be either O or X mode of circular polarization. The heater uses eight RF power amplifiers from the Platteville heater. It has been operated at frequencies of 2.85, 3.349, 4.53, and 4.905 MHz. It presently (April 1988- December 1989) operates at 2.85 MHz, which corresponds to the second harmonic of the electron cyclotron frequency. The heater can be amplitude modulated 160 Hz - 20 KHz, and effectively amplitude modulated at lower (ULF) frequencies by dephasing half of the antennas in the array. Beam pointing ($\pm$ 30°) is now controlled by a personal computer. The transmitters are powered by two 1500 HP diesel electric generators. The system is capable of almost year round operation and has been operated without any interruption for as long as 12 hours.

Future improvements include the construction of a larger array operating at higher frequencies to minimize the array size. Arrays with 37 dbi gains

are being considered, along with pulsed amplifiers to raise the ERP to ~100 GW.

ACKNOWLEDGEMENTS

The author's wish to acknowledge the support of Eldon Thompson, and the recent help of Edward Sonafrank and Arlin Hogenson, all of Fairbanks, Alaska, for the maintenance of the transmitters and operation of the system during recent winter and summer campaigns; Roger McElmell in the preparation of this paper and his help at the site; David C. Johnson for help in formalizing the PC beam steering and control program, as well as help at the site; Drs. Andras Kuthi and Lothar Schmitz for perfecting the antenna tuning scheme.

We also acknowledge Professor A. Ferraro of the Pennsylvania State University for discussion and use of the site for ELF and ULF experiments.

Finally, and most important, we acknowledge the support of the Office of Naval Research, and in particular Dr. Richard Brandt, who has supported the project literally through rain, snow, ice, and fire.

REFERENCES

Wong, A. Y. and J. Santoru, Active Stimulation of the Auroral Plasma, J. Geophys. Res., 86, 7718-7731, 1981.

Stubbe, P., H. Kopka, H. Lauche, M. T. Rieveld, A. Biekke, O. Holt, T. B. Jones, T. Robinson, A. Hedberg, B. Thide, M. Crocketr, and H. J. Lotz, Ionospheric Modification Experiments in Northern Scandinavia, J. Atmos. Terr. Phys., 44, 1025-1041, 1982.

Elvey, C. T., Aurora Borealis, in L. Marton Editor, "Advances in Electronics and Electron Physics," 9, 1-49, 1957.

Carroll, J. C., E. J. Violette, W. F. Utlaut, The Platteville High Power Facility, Radio Science, 9, 889-894, November 1974.

Wong, A. Y., J. Santoru, C. Darrow, L. Wang, and J. G. Roederer, Ionospheric Cavitons and Related Nonlinear Phenomena, Radio Science, 18, 815-830, November-December 1983.

Santoru, J., Low and High Altitude Ionospheric Modification Experiments, Ph. D. Thesis, University of California at Los Angeles, 1984.

FIGURE CAPTIONS

Figure 1: Schematic of the present HIPAS ionospheric radio frequency heater showing the generator building, transformer yard, transmitter complex, and antenna field.

Figure 2: Photograph of one of the HIPAS antennas taken April 1988. The antennas were orginally constructed for 4.9MHz operation. Their operating frequencies were lowered by the addition of the end-straps visible in the picture. When the picture was taken the antenna was tuned for 2.85 MHz. Also seen in the picture is the balun and rigid coax to the antenna's nominal 125 KW amplifier. The dipoles are 46 feet above ground.

Figure 3: Schematic view, from above, of a HIPAS antenna, showing the connections to the balun to produce either right (O-mode) or left (X-mode) circularly polarized radiation patterns. Also included in this picture is the direction of the earth's magnetic field (into page) and direction of rotation of a free electron in the field.

Figure 4: Schematic of the HIPAS radio frequency system.

Figure 5: Schematic of one of the Platteville transmitters.

Figure 6: Photograph (April 1988) of the transmitter building, with the array and transmission lines in the background. The edge of the generator building is seen in the lower left corner of the picture. The transformer yard is also in part visible. The four radiators for the glychol cooling loops are on the far ends of the building.

Figure 7: Schematic of the cooling system

Figure 8: Photograph of one of the (two) 1500 HP diesel electric generators, used to drive the RF system.

Figure 9: Top: Calculated HIPAS beam pattern at 2.85MHz when all eight antennas are in phase; namely, 18.5 dbi gain over isotropic, with a divergence 21.5 degrees (FWHM); bottom: Calculated HIPAS beam pattern for 2.85 MHz, when the antennas are phased to tip the RF beam 30^{o} off the vertical.

TABLE I

HIPAS OPERATING PARAMETERS

Frequencies	Calculated Antenna	ERP (@1.2MW)	FLUX (@100km)	Peak Amplitude (Vacuum @ 100km)
MHZ	Gain (dbi)	(MW)	mW/m^2	Volts/m
4.905	17.7	71	0.56	0.64
4.530				
3.349				
2.85*	18.4	84	0.67	0.71

*1987, 1988, and 1989 operating frequency
Number of crossed half wave dipole antennas: 8
Array diameter: 207 meters (680 feet)
Polarization: Left (X mode) or Right (O mode) Circular
AM Modulation: 160 Hz - 20 KHz
Antenna Phase Modulation: > 0.1 Hz - 156 Hz
Beam Direction: <30° off Zenith, at >0.01 seconds
Geographic Location: 62° 52' 22" N, 146° 50' 06" W.
Magnetic Location: 28° 02' E declination, 76° 30' dip angle

TABLE II

PERFORMANCE OF THE PROPOSED 110 GW ERP ARRAY

RANGE (Kilometers)	FLUX (W/m^2)	RF AMPLITUDE (E_{peakRF}, volts/m)
25	14.4	104
50	3.6	52
100	0.9	26

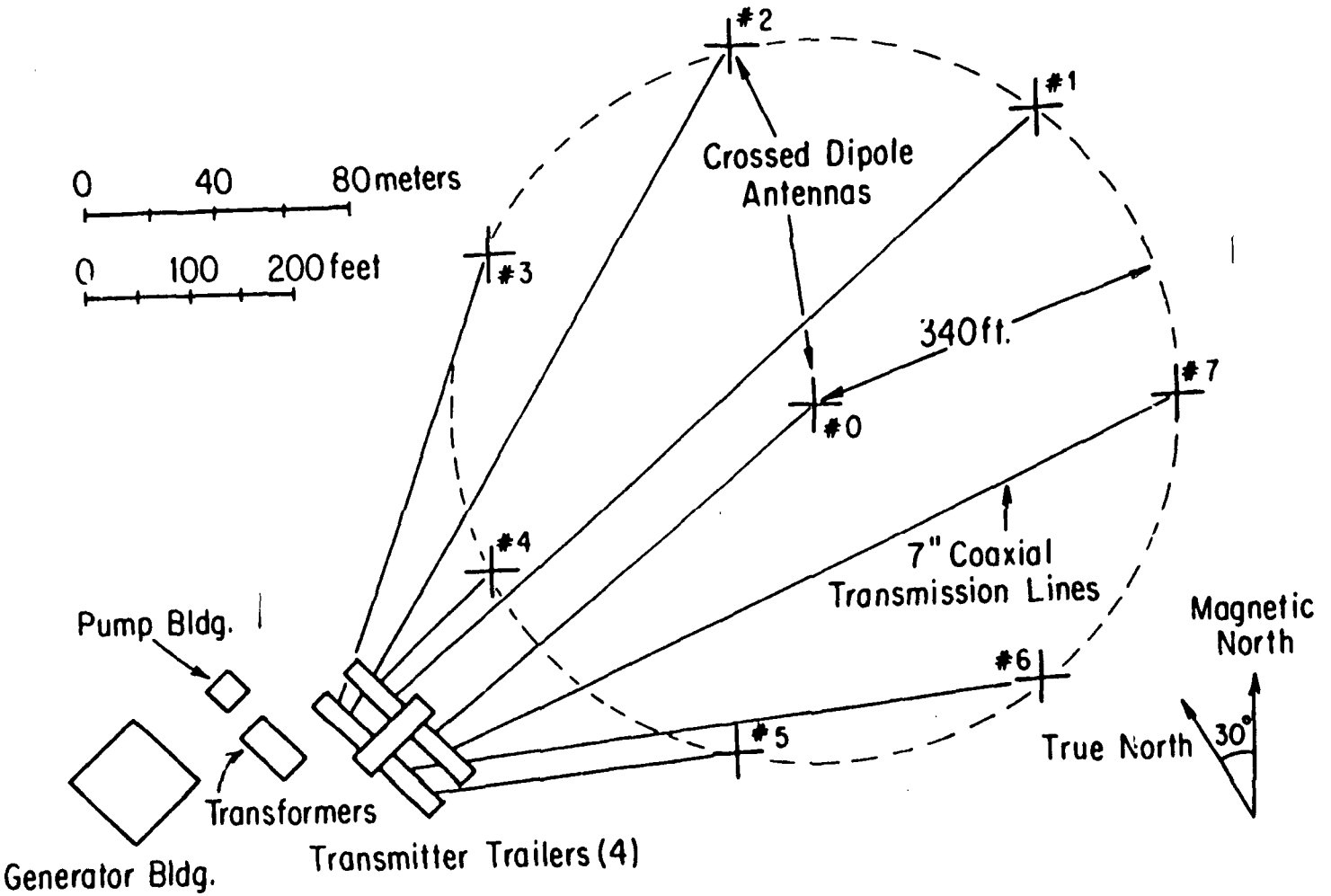
#2
#1
Crossed Dipole
Antennas
0 40 80 meters
0 100 200 feet
#3
340ft.
#7
#0
#4
7" Coaxial
Transmission Lines
Pump Bldg.
Magnetic
North
#6
#5
True North
30°
Transformers
Transmitter Trailers (4)
Generator Bldg.

Figure 1

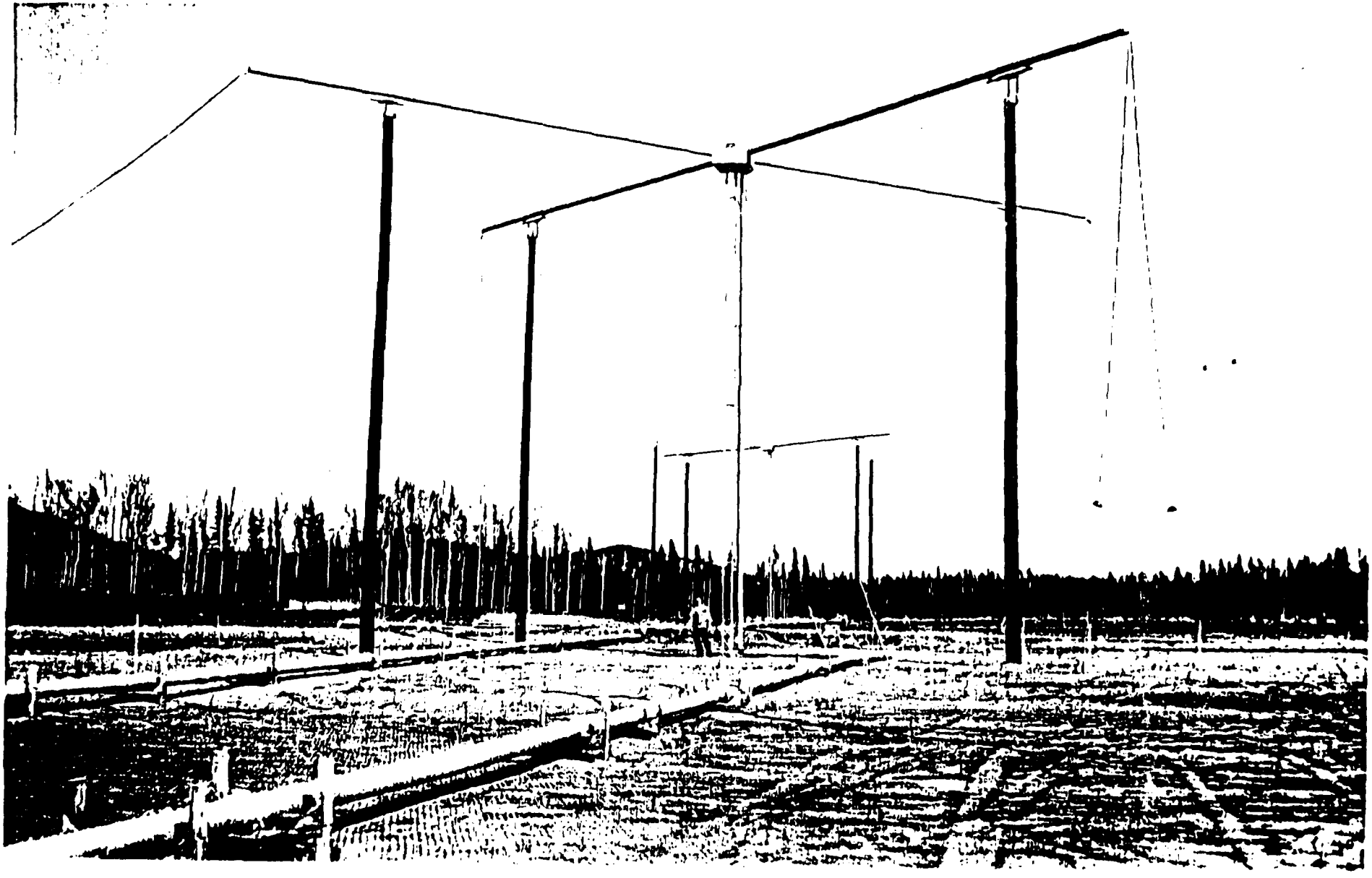

Figure 2

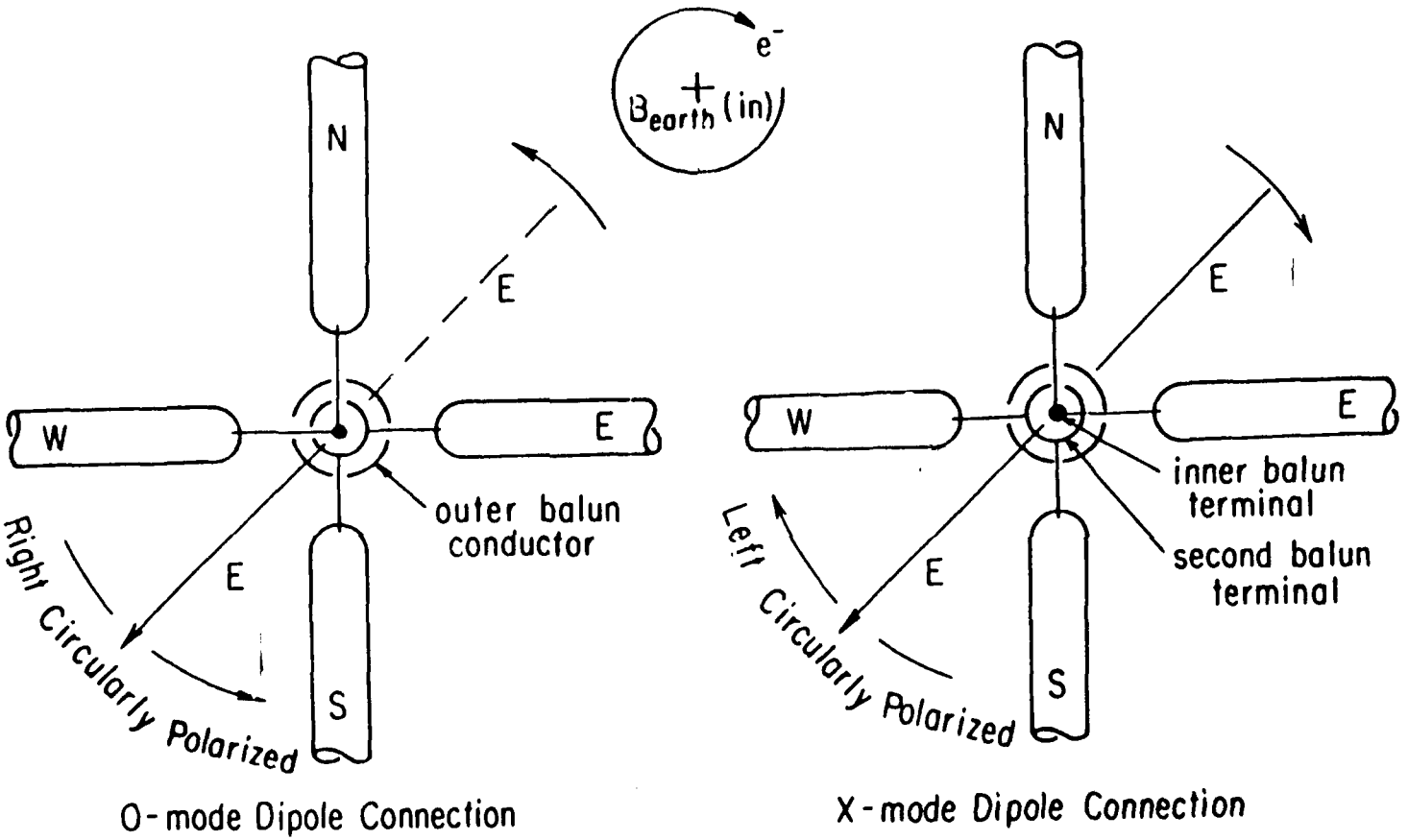
e⁻
B earth (in)
N
E
W
E
outer balun conductor
E
Right Circularly Polarized
S
O-mode Dipole Connection
N
E
W
E
inner balun terminal
second balun terminal
E
Left Circularly Polarized
S
X-mode Dipole Connection

Figure 3

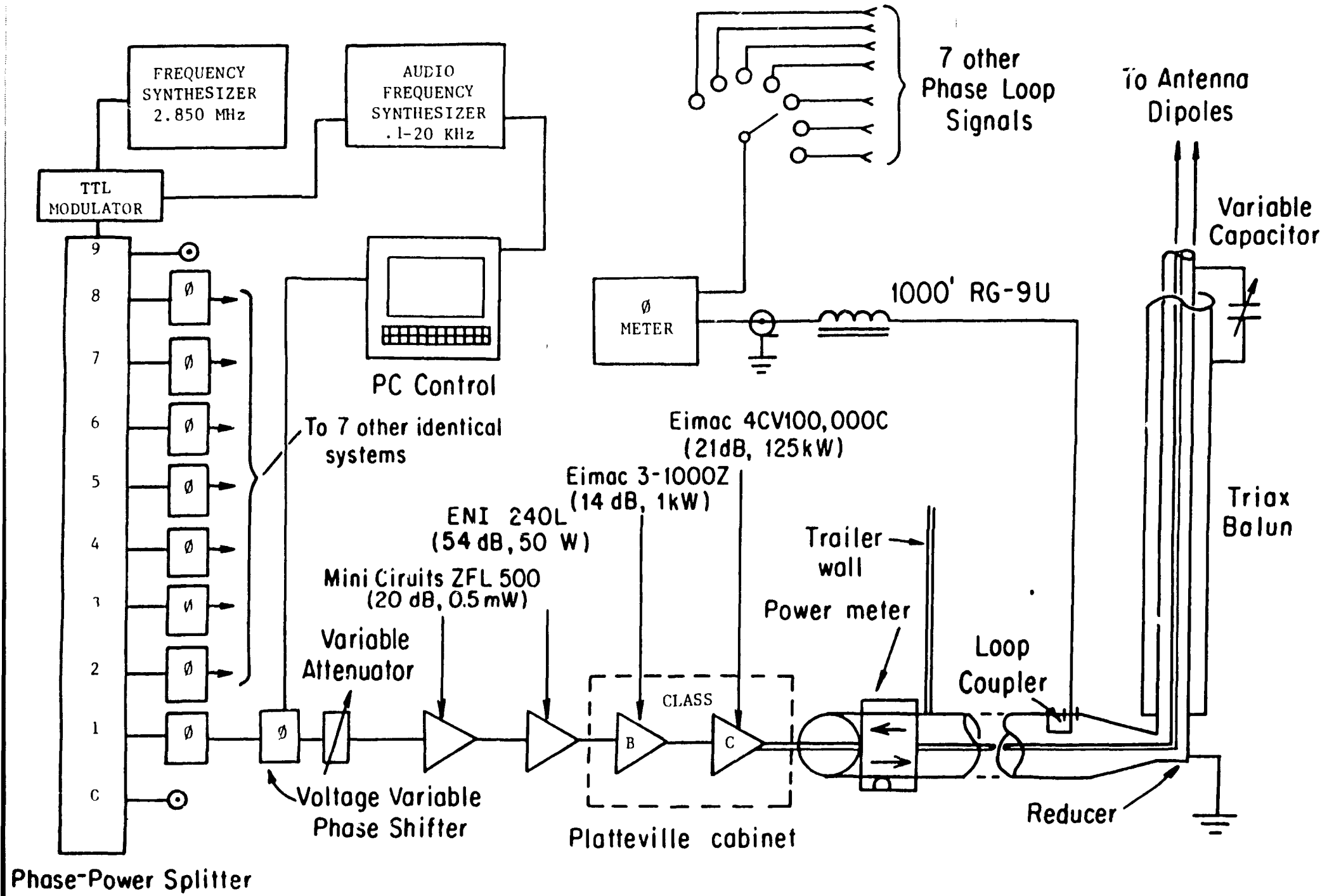
FREQUENCY SYNTHESIZER 2.850 MHz
AUDIO FREQUENCY SYNTHESIZER .1-20 KHz
TTL MODULATOR
7 other Phase Loop Signals
To Antenna Dipoles
Variable Capacitor
PC Control
Ø METER
1000' RG-9U
To 7 other identical systems
Eimac 4CV100,000C (21dB, 125kW)
Eimac 3-1000Z (14 dB, 1kW)
ENI 240L (54 dB, 50 W)
Mini Ciruits ZFL 500 (20 dB, 0.5mW)
Trailer wall
Power meter
Triax Balun
Variable Attenuator
Loop Coupler
CLASS
B
C
Voltage Variable Phase Shifter
Platteville cabinet
Reducer
Phase-Power Splitter

Figure 4

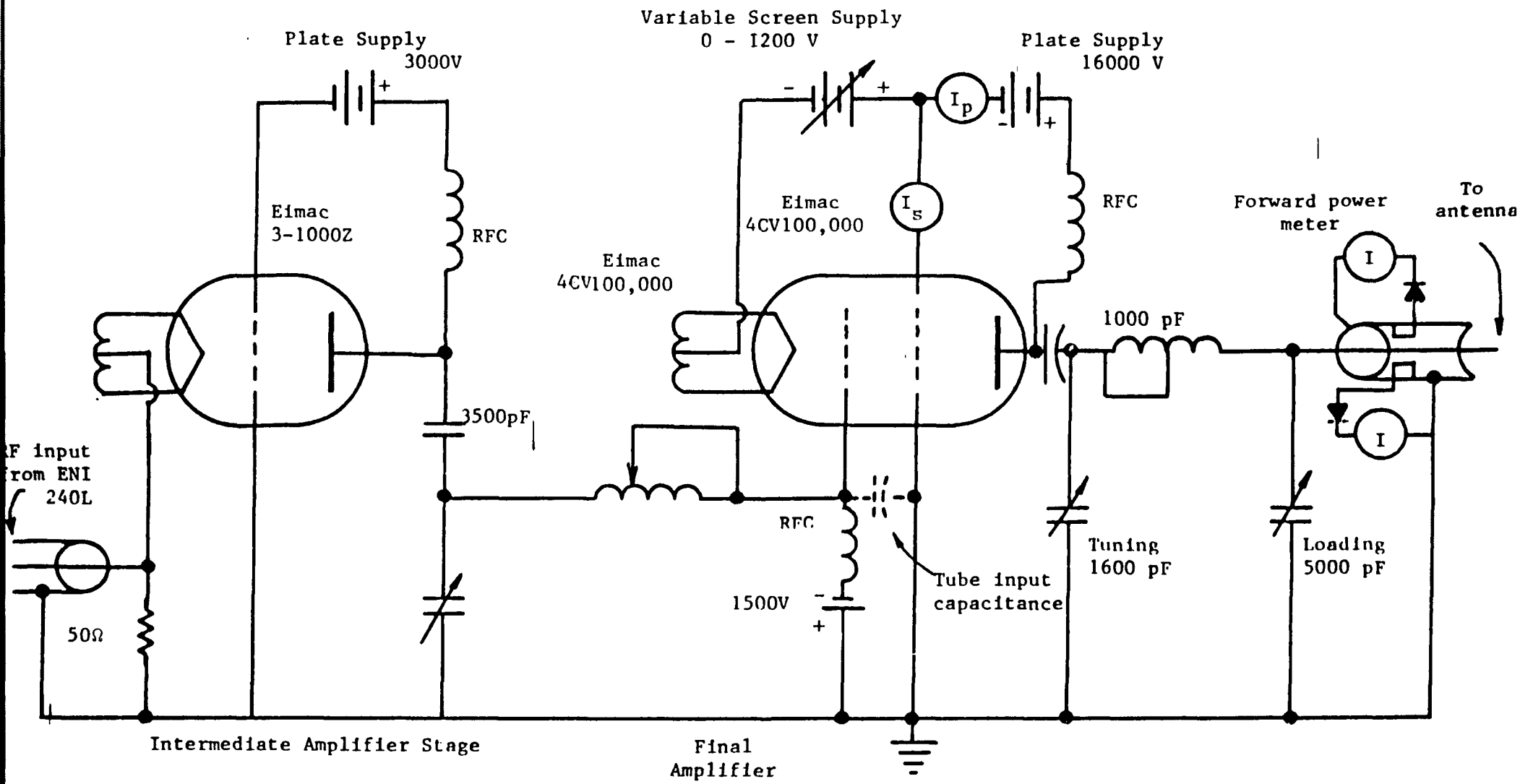
Plate Supply
3000V
Variable Screen Supply
0 - 1200 V
Plate Supply
16000 V
Eimac
3-1000Z
RFC
Eimac
4CV100,000
I_s
I_p
RFC
Forward power
meter
To
antenna
Eimac
4CV100,000
1000 pF
3500pF
RF input
from ENI
240L
RFC
1500V
Tube input
capacitance
Tuning
1600 pF
Loading
5000 pF
50Ω
Intermediate Amplifier Stage
Final
Amplifier

Figure 5

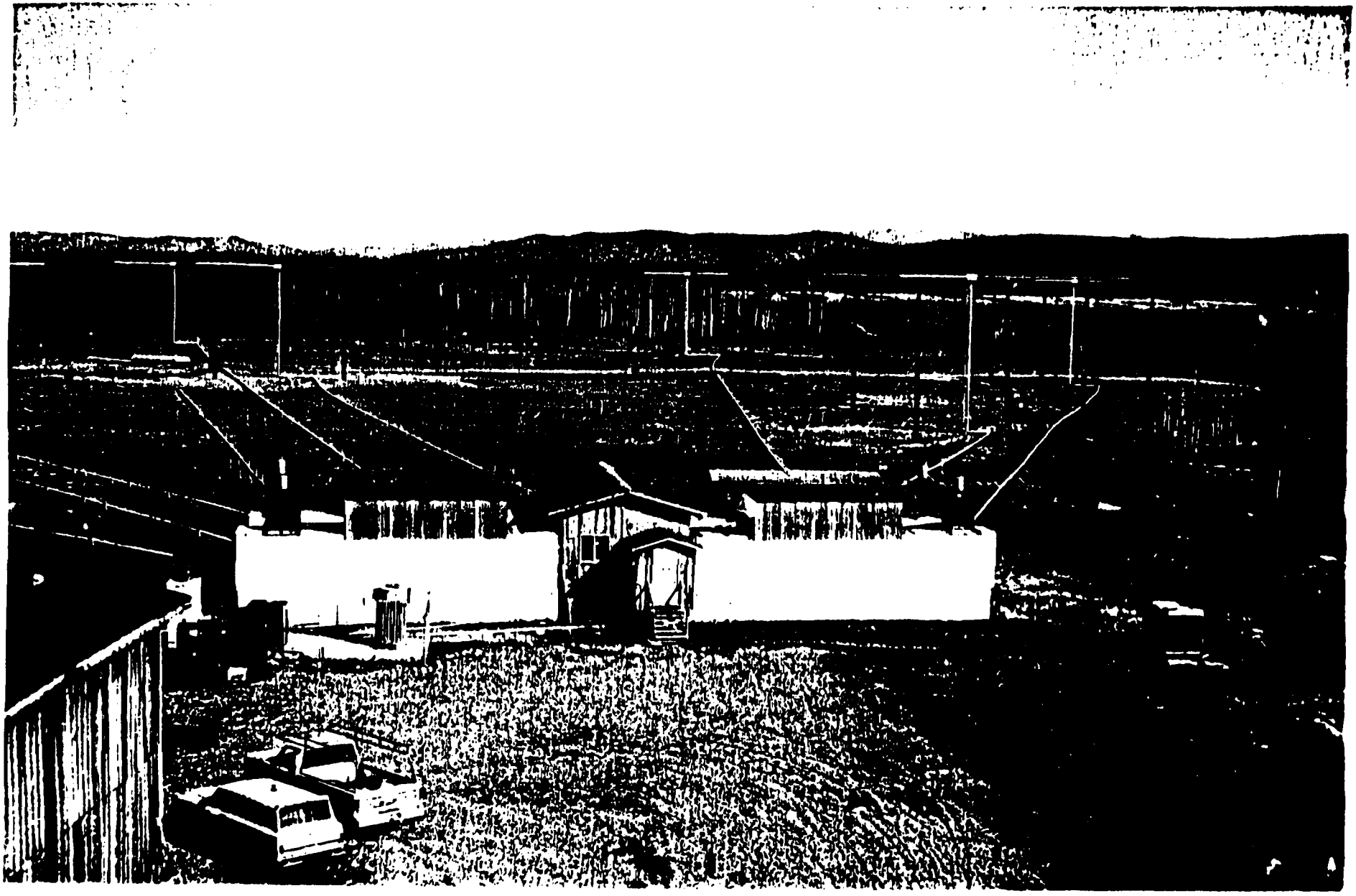

Figure 6

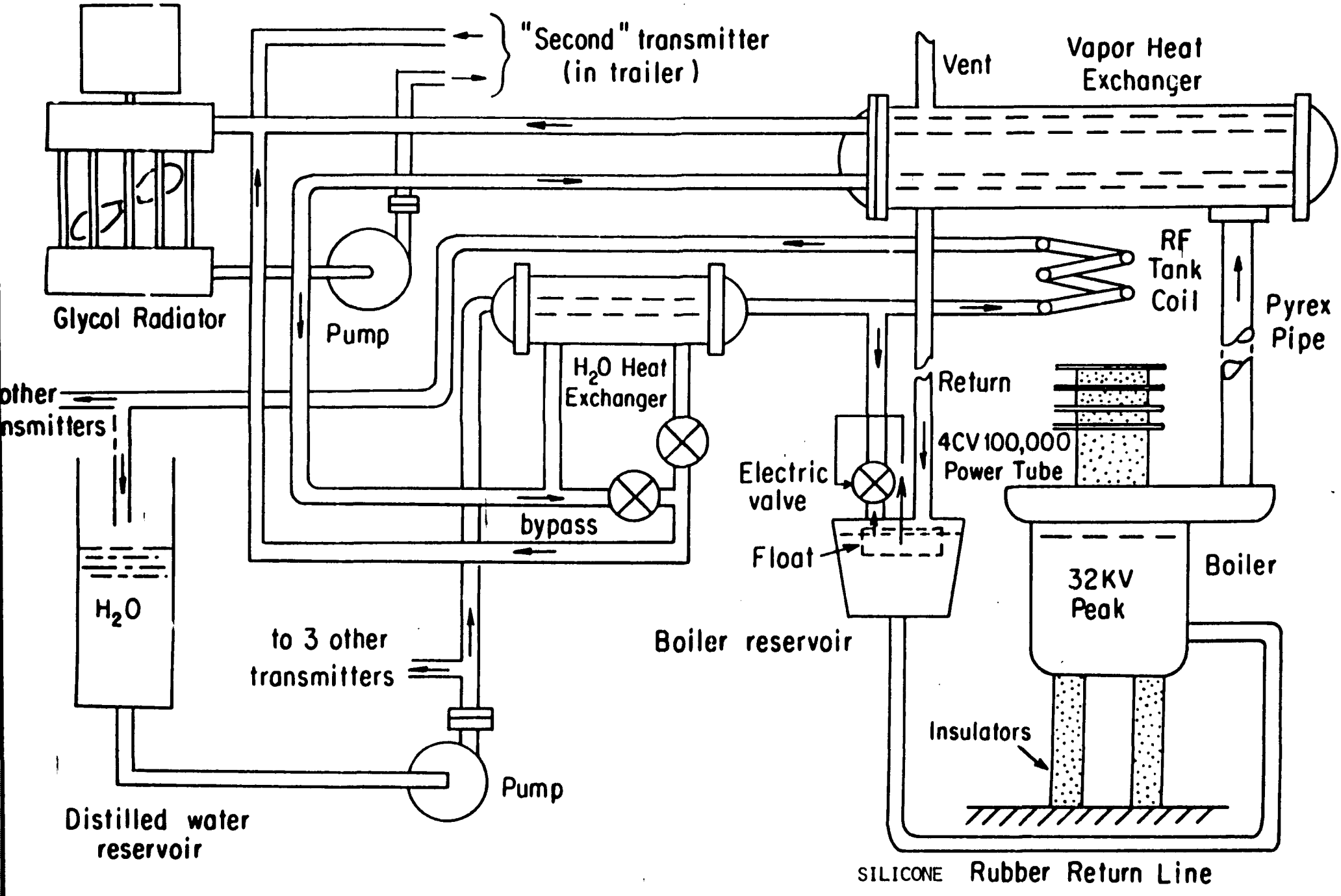
"Second" transmitter
(in trailer)
Vent
Vapor Heat
Exchanger
Glycol Radiator
Pump
RF
Tank
Coil
Pyrex
Pipe
H_2O Heat
Exchanger
Return
4CV100,000
Power Tube
Electric
valve
bypass
Float
Boiler
32KV
Peak
H_2O
to 3 other
transmitters
Boiler reservoir
Insulators
Pump
Distilled water
reservoir
SILICONE Rubber Return Line

Figure 7

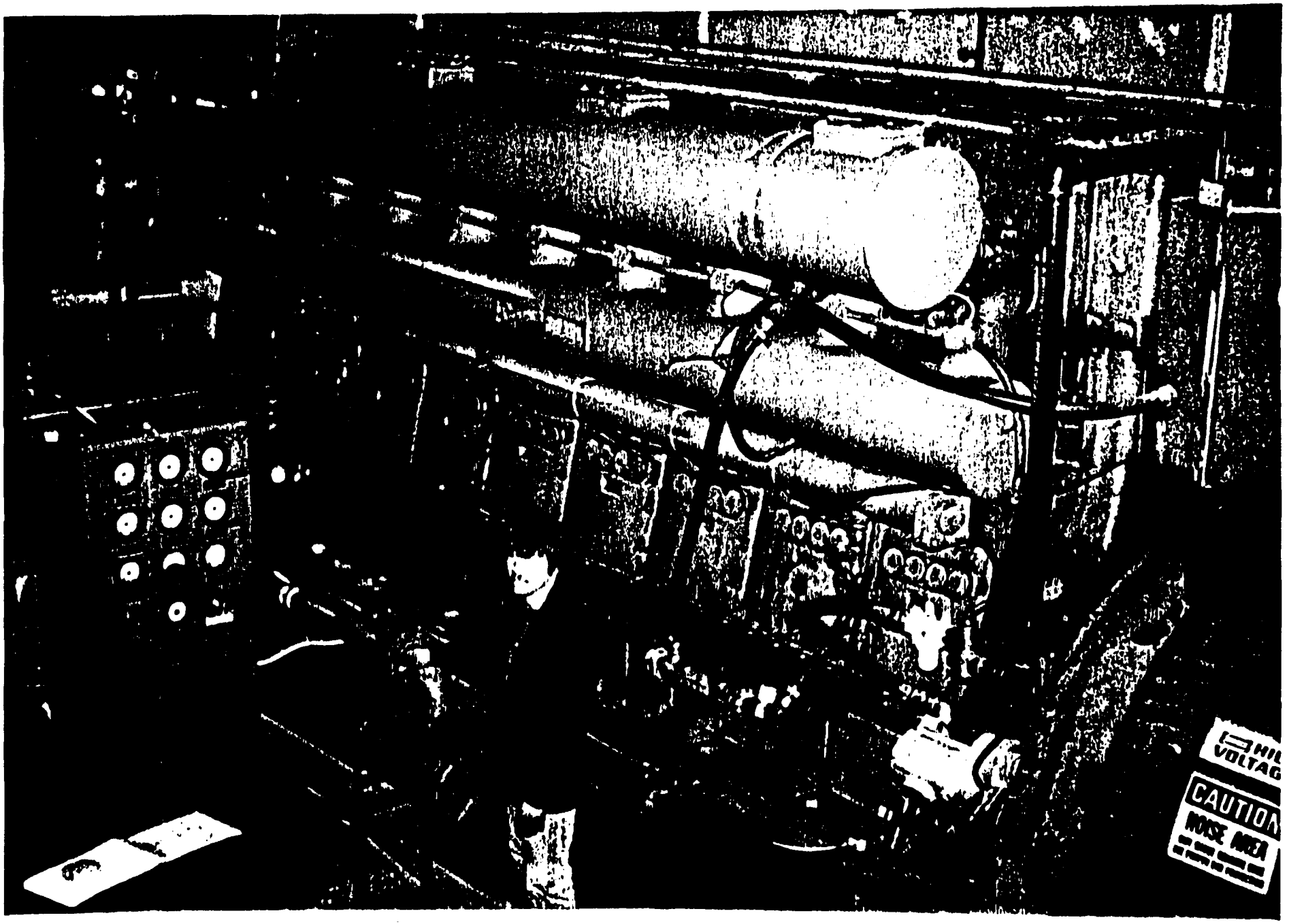

Figure 8

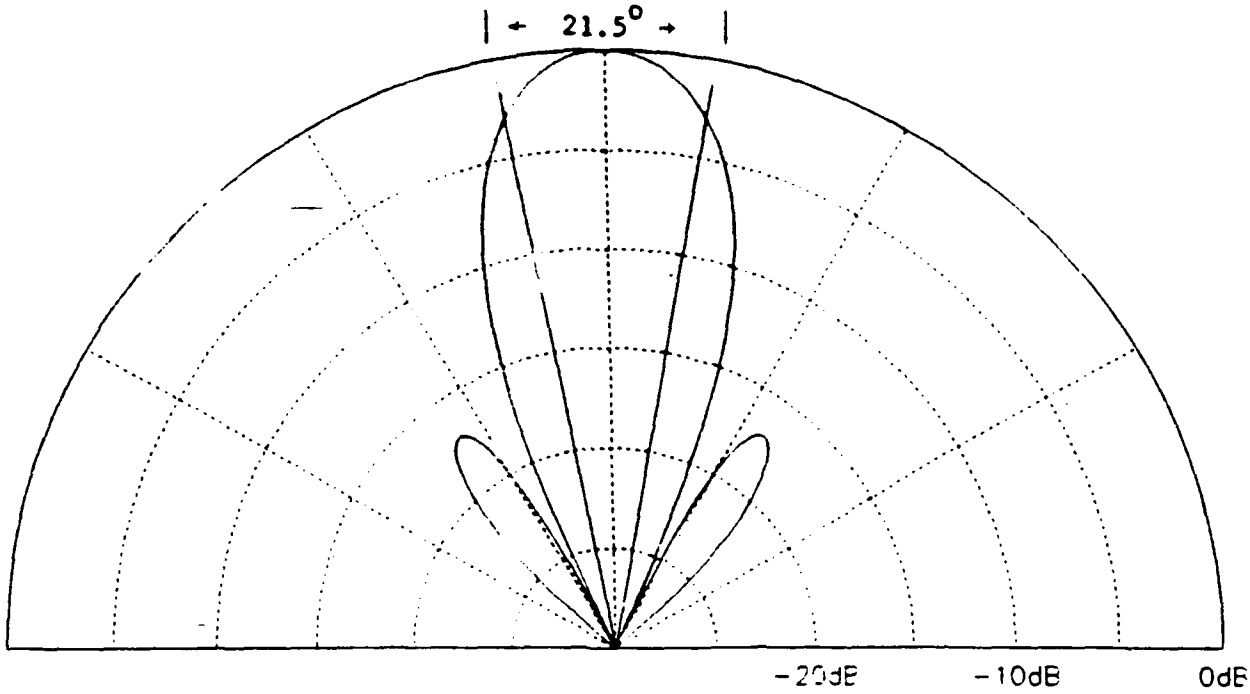

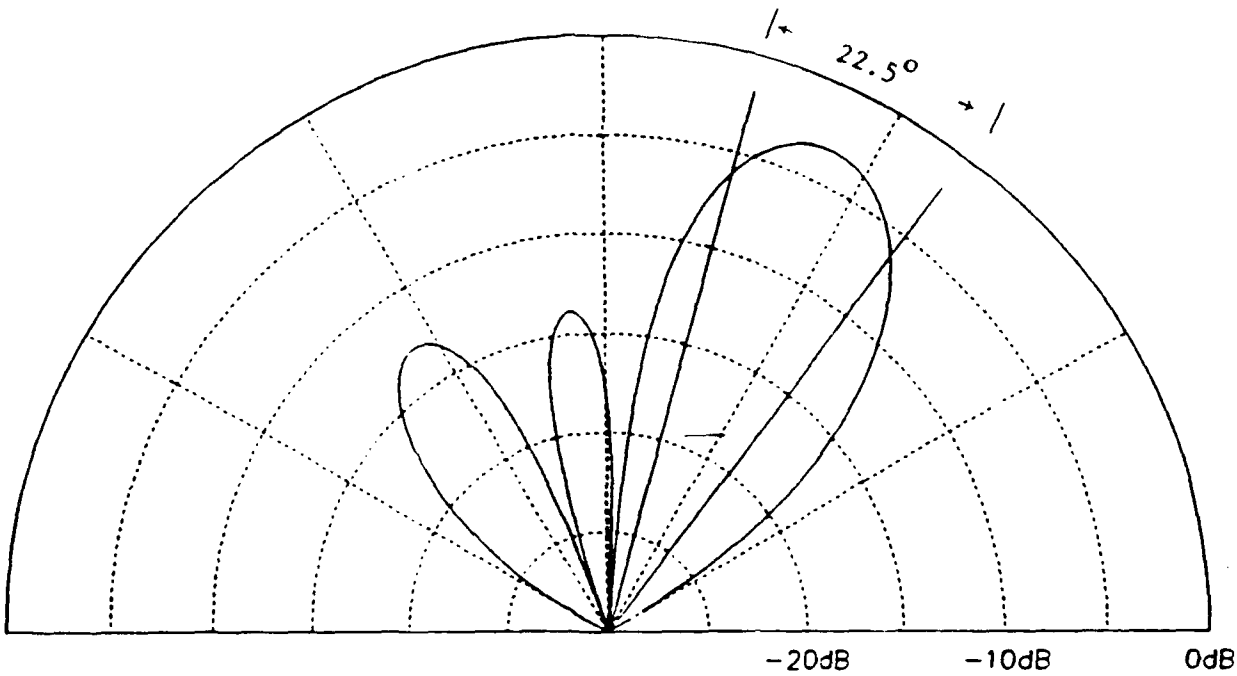

Figure 9

APPENDIX II

Paper prepared by R.G.Brandt, ONR Program Manager, for presentation at the May 1990 AGARD meeting in Tromso, Norway. This paper summarises both the URI results as well as later experiments on ULF generation with the HIPAS facility;

R.G.Brandt, Ionospheric Modification Research at HIPAS,

IONOSPHERIC MODIFICATION RESEARCH AT HIPAS

by
Richard G. Brandt
Office of Naval Research
800 N. Quincy Street
Arlington, VA 22217
U.S.A.

SUMMARY

The HIPAS ionospheric heating facility radiates a total power of 1.2 MW with an ERP of 84 MW. It presently operates at an HF frequency of 2.85 MHz but is tunable to about 5 MHz. Electrojet modulation experiments have been conducted at frequencies from 5 Hz to 5 kHz. The magnetic field amplitudes, measured close to the heater, can be 1 pT or larger under very strong electrojet conditions. Even under much weaker conditions when the amplitudes are highly variable, the phase of the ELF signal is relatively stable. The efficiency of converting HF to ELF is presently too low for a practical communication system. Beam painting has been proposed as a method for improving the conversion efficiency in D region heating by causing a much larger area of the ionosphere to radiate coherently; this concept will be tested using microsecond beam steering. Use of shorter heating pulses (lower duty cycle) already seems promising. Even larger gains are expected for E region heating as compared to D region heating.

PREFACE

This review of ionospheric modification research at HIPAS starts with a brief description of the facility which began operating at the megawatt average power level in 1986. The research conducted at HIPAS since that time is described. This research has focused on the generation of ELF radiation. The review concludes with an indication of future research directions.

1. THE HIPAS FACILITY

The HIPAS ionospheric heater is located in the auroral zone 40 km east of Fairbanks, Alaska. The acronym HIPAS stands for HIgh Power Auroral Stimulation. It was originally conceived as a high pulse power heater, rather than high average power, because of the recognition that many plasma nonlinearities are excited by large instantaneous electric fields [Wong and Santoru, 1981]. When HIPAS became operational in October 1981, it delivered 1 ms HF pulses with a peak power of 2 MW at a pulse repetition rate of 1 Hz. The average power, therefore, was only 2 kW, and the antenna gain was

17.7 dB at a radiating frequency of 4.905 MHz. This facility was initially used for probing short-term nonlinear plasma phenomena, especially enhancement of the incident electric fields at the resonant altitude and creation of electromagnetic cavitons via ponderomotive forces. These cavitons are localized depletions in electron density with scale sizes from 1 to 100 m.

In 1982 several events occurred which altered the original research plan. First, in March 1982 the incoherent scatter radar at Chatanika was moved to Greenland. Much of the detailed work on caviton structure and dynamics was subsequently carried out at the Arecibo facility with its excellent incoherent scatter radar. Second, in late 1982 the HF transmitters from the Platteville heater became available, and a decision was made to incorporate these transmitters in the HIPAS facility, transforming it into a high average power heating facility.

Eight of the Platteville transmitters are now operating at HIPAS, each connected to an individual element in the transmitting antenna array [Wong et al, 1990]. This modular design allows the phase of the high power radiation emitted by each element in the array to be controlled at the low-level input to each transmitter and thus permits rapid beam steering and related modulation techniques. Each transmitter is normally operated continuously at 100 to 150 kW, although the maximum rating is 200 kW. Instead of relying on commercial prime power, two megawatt diesel electric generators were installed at HIPAS so that operational costs would be minimized.

The antenna consists of a circular (208 m diameter) array of seven crossed half-wave dipoles approximately one quarter of a wavelength above the ground plus one similar crossed dipole in the center. Although the antenna elements were designed to be resonant at 4.905 MHz, a novel scheme was developed [2] for retuning the antenna to lower frequencies by making use of a pair of wires attached to the end of each dipole element; the angle between these two wires and the angle these wires make with the ground determine the new resonant frequency. Using this technique, the array has been successfully retuned and operated at the additional frequencies of 4.503, 3.349 and 2.805 MHz. The antenna gain remains essentially constant at about 18 dB. At 2.85 MHz the calculated effective radiated power (ERP) is 84 MW at a total radiated power of 1.2 MW.

With the upgrade of HIPAS to the megawatt average power level, the research directions changed. These new research activities capitalized on the existing diagnostic capabilities which included ionosondes, an HF imaging radar, magnetometer chain data, riometer data, and ELF receivers. More recently, a 50 MHz coherent radar has become operational. In addition, satellite receivers and beacons have been utilized at various times. The initial scientific studies were concerned with optimal approaches for

coupling energy into the ionospheric plasma [Wong et al, 1989]. Beginning in 1987 the research has focused on the subject of generation of ELF radiation in the ionosphere by modulation of the powerful electrojet current flowing in the auroral region.

2. ELF/VLF GENERATION

The ELF generation experiments at HIPAS began in 1987. This team effort involved A. Ferraro (Pennsylvania State University), A. Wong (University of California, Los Angeles), D. Papadopoulos (Science Applications International Corporation), J. Olson (University of Alaska) and coworkers. In these experiments the ELF receivers were located about 50 km west of HIPAS. The receivers [Baker et al, 1990] used standard coherent detection techniques, and the heater and the receivers were synchronized using separate frequency standards. Most of the measurements were made at modulation frequencies between 1 and 5 kHz where the detection sensitivity was best. The heater was almost always amplitude modulated with 100 percent modulation depth.

These experiments continued through 1989 during which time progressively more sophisticated beam steering capability was implemented. Initially, the heater beam could be steered by manually adjusting the eight phaseshifters in the lines leading to the individual antenna elements. In 1988 electronic phaseshifters were introduced and placed under computer control, and a beamforming time of 10 ms was achieved. In 1989 this capability was upgraded to provide 15 μs beamforming time.

The initial experiments [Ferraro et al, 1989] served to demonstrate the ability to generate ELF and confirm earlier results obtained at Tromso. As an illustration, Figure 1 shows data obtained at a modulation rate of 2.5 kHz during a strong electrojet event which occurred overhead of the HIPAS facility as indicated by magnetometer data. We see that the amplitude and phase of the ELF signal remain constant during the 2-minute period of modulation, after which the amplitude falls to zero and the phase becomes random. The magnetic signal strength is 0.6 pT. Even when the electrojet is very weak and the amplitude of the ELF signal is small and highly variable, the phase remains remarkably constant as illustrated in Figure 2.

This phase stability of the ELF signal suggests that phaseshift keying might be a viable signal modulation technique for an ELF communication system based on ionospheric generation. To explore this hypothesis, several phase shifting experiments were performed. The tests performed in 1987 were relatively simple, consisting of periodically changing the phase of the ELF signal by 180 degrees. Some of these data [5] are illustrated in Figure 3 and indicate a very stable phase for periods of 0.5 minute. Following these initial biphase stability tests, various quadphase tests were conducted in 1989 in which the phase was periodically

switched from 180 to 90 to 0 to -90 to -180 degrees. Representative data [5] are shown in Figure 4 and again indicate phase stability for periods of 0.5 minute. All these measurements were made at the receiving site 50 km from HIPAS and at a frequency of 2.5 kHz. In 1989 several attempts were made to receive data using a mobile receiving station located at more remote sites in Alaska. Data obtained from Cantwell, Alaska, about 210 km from HIPAS [5] are shown in Figure 5. Switching between the various phase states is clearly evident, although the transitions between these states are less sharp.

Other experiments were performed to determine whether these ELF signals could be generated at less than full power levels. Some of these data [5] are shown in Figure 6. The curious spikes in the data were caused by a local thunderstorm. In this experiment the modulation frequency was 2.5 kHz, and the total radiated power was varied from a maximum of 800 kW to a minimum of 80 kW. At maximum power the measured magnetic field amplitude was less than 0.1 pT which indicates that there was no strong overhead electrojet. Nonetheless, ELF signals were generated at all HF transmitter power levels including at 80 kW when the measured magnetic field amplitude was less than 0.02 pT. There is some indication that the effect is beginning to saturate at the higher power levels, suggesting that there would be little advantage in using a heater with an even higher ERP.

3. BEAM PAINTING/LOW DUTY CYCLE HEATING

The experimental results described above clearly demonstrate the ability to generate ELF signals under a variety of ionospheric conditions. Although the amplitude of these signals may be variable, the phase is reasonably stable. The efficiency of the generation process, however, is quite low. The total radiated HF power is approximately 1 MW. Except under strong electrojet conditions, the ELF power is very modest. When there is no strong electrojet directly overhead, the ELF power is no more than 10 mW, corresponding to a conversion efficiency of 10^{-8}. This ELF power is calculated from the measured near-field amplitudes using a far-field formula for dipole radiation in free space.

Papadopoulos and coworkers [Papadopoulos et el, 1990] have developed a theory which suggests an approach for achieving dramatic improvements in HF-to-ELF conversion efficiency, namely, beam painting. For low altitude heating they calculate that the ERP of the current HIPAS heater is sufficient to achieve the full saturated value of Hall conductivity modulation. Any further increase in power density would be wasted. Papadopoulos et al [6] conclude that the only way to achieve an increase in conversion efficiency in low altitude heating is to cause a much larger area of the ionosphere to radiate coherently. The predicted ELF power is then proportional to the square of the radiating area. In principle, this can be accomplished by beam painting, that is,

using the present beam spot size but rapidly steering the beam such that many different spots are heated and not allowed to cool off before they radiate. At 75 km altitude the time required to increase the electron temperature by a factor of 2 (a sufficient increase to produce most of the conductivity change) is typically about 10 μs; this heating time decreases somewhat at higher power densities. At the same altitude the cooling time is of the order of 100 μs, at least for temperatures below 2000 K. The concept of beam painting, therefore, requires that many spots be visited and that the temperature rise produced during each visit is not dissipated before that same spot is revisited. The total time available for heating is a half cycle of the ELF modulation or about 5 ms. During that time the temperature of each spot must be increased, in cummulative fashion, by at least a factor of 2.

Papadopoulos and coworkers [6] have also analyzed the case of heating at 100 km, the altitude at which the electrojet flows. Here the situation is more complex. At these altitudes the Pederson conductivity modulation dominates over the Hall conductivity modulation and does not saturate until power densities of at least 10 mW/m^2 are reached, a factor of 10 higher than that available at HIPAS. When saturation occurs, the predicted increase in conductivity modulation is by a factor of 100 which leads to an increase in the efficiency of ELF generation by a factor of 10^4. This increase would be obtained without beam painting. The practical difficulty in realizing the high altitude scheme, especially under day time conditions, is the fact that self absorption at lower heights could deplete the power density before reaching the higher altitudes. Another potential disadvantage of high altitude heating is that the coupling of the ELF fields into the earth-ionosphere waveguide may be more inefficient. Nonetheless, the potential gain in generation efficiency by a factor of 10^4 is a significant prize worth pursuing, and several schemes for defeating the self absorption problem have been suggested. However, none of these ideas for increasing the efficiency of high altitude generation of ELF has yet been tested experimentally.

The recent experiments at HIPAS were designed to maximize heating in the low altitude regime because of the choice of operating frequency (2.85 MHz which is near the second harmonic of the electron cyclotron frequency) and the use of X mode polarization (same sense of rotation as the electron cyclotron motion). An initial effort was made to demonstrate that beam painting could produce an efficiency enhancement in generation of ELF at low altitudes. At present the beam forming time at HIPAS is 15 μs. Each spot must be heated almost 10 μs during each visit. Therefore, in order to heat 10 spots, for example, about 250 μs is required which is longer than the cooling time of each spot. This simple arithmetic clearly illustrates that a significantly faster beam forming time is required before an efficiency enhancement can be demonstrated. The initial tests at HIPAS, therefore, did not

yield an efficiency enhancement, but the dependence of generated signal strength on beam painting parameters was in accordance with theory.

Other experiments were performed [Papadopoulos and Ferraro, 1989] which directly relate to the beam painting concept. A series of measurements were made in which the duty cycle of the ELF modulation of the HF waves was varied. The ELF modulation frequency was 833 Hz, and the duty cycles selected were 50 percent (600 μs on, 600 μs off), 37.5 percent (450 μs on, 750 μs off), 25 percent (300 μs on, 900 μs off), 12.5 percent (150 μs on, 1050 μs off), 6.25 percent (75 μs on, 1125 μs off), 2.5 percent (30 μs on, 1170 μs off), and 1.25 percent (15 μs on, 1185 μs off). The amplitudes of the generated ELF signals were measured for all duty cycles, and the data are shown in Figure 7. The error bars represent the scatter in the results for repeated measurements. The results clearly show that the same ELF signal strengths are generated at 25 percent duty cycle as at 50 percent duty cycle. Below 25 percent duty cycle the amplitudes fall off approximately linearly. The conclusion is that the efficiency of generating magnetic field signals can be increased by a factor of 2 and thus the efficiency of generating ELF power can be increased by a factor of 4 merely by decreasing the duty cycle from 50 percent to 25 percent, that is, by reducing the average HF power by a factor of 2. For single spot heating only about the first 300 μs of the heating pulse is effective; the rest is wasted. Pulses shorter than 300 μs do not saturate the conductivity modulation although they do produce a measurable effect. The time between heating pulses is longer than the cooling time, and thus energy cannot be accumulated.

4. ULF/ELF GENERATION

ELF generation was also investigated in the frequency range below 100 Hz [McCarrick et al, 1990]. In these experiments it was initially not possible to use full amplitude modulation as in the higher frequency experiments because of various transmitter system resonances. Instead, an alternate procedure was developed known as beam-dephasing modulation. In this procedure all eight transmitters were operated continuously, while the phase of four of these transmitters was switched in a square-wave fashion between 0 and 180 degrees with respect to the phase of the other transmitters. In this way the beam was alternately focused and defocused at the desired modulation rate. When the beam is defocused, there still is some residual heating of the ionosphere, both overhead and in the sidelobes, and thus the effective modulation depth is less than in 100-percent amplitude modulation. It was calculated that the power density in the main lobe is reduced by more than 75 percent during the out-of-phase half-period.

The receiver used in these experiments is located at the NOAA

Gilmore Creek Facility, 35 km from HIPAS. The system was developed by D. Sentman for the purpose of studying the natural Schumann resonances of the earth-ionosphere waveguide. The receiver consists of a pair of orthogonal magnetic coils, a vertical electric field sensor, associated amplifiers and signal conditioning electronics, and a dedicated data acquisition and storage system. To reduce the sensitivity to 60 Hz background radiation, a low-pass filter is placed between the coils and the amplifiers. The attenuation is 4.4 dB at 76 Hz and becomes very large above 100 Hz. The data obtained at this site are transmitted in real time to the HIPAS control room where they are displayed together with environmental data from the ionosondes, the magnetometer chain, and, more recently, from the coherent radars.

Using the dephasing modulation technique and the receiving system just described, experiments were performed at the frequencies of 5, 11, 21, 23, 41, and 76 Hz. In Figure 8 is shown a typical background noise spectrum obtained from a 4-minute incoherent average of the east-west coil output [8]. The first three Schumann resonance peaks at 7.5, 14 and 21 Hz are well defined. In order to observe the generated ELF signals which are often weaker than the natural atmospheric noise background, coherent detection techniques were used, including conventional lock-in amplifiers and digital signal processing routines. A typical coherent ELF spectrum from the east-west coil [8] is shown in Figure 9. Here we see the 11 Hz signal generated by HIPAS as well as the third harmonic of this signal at 33 Hz. A 4-minute averaging period was used. Similar quality data were obtained from the north-south magnetic sensor as well as the vertical electric field sensor. Note that the measured magnetic field strength at 11 Hz is in excess of 1 pT.

These experiments were performed under a variety of ionospheric conditions in order to correlate the strength of the observed signals with measures of geomagnetic activity. Basically, whenever the magnetic activity is high enough, as determined by the Kp index or by magnetometer chain data, large ELF signals can be generated. In terms of Kp index, which is an indication of how far south in geomagnetic latitude the auroral oval has expanded, it was found that signals in excess of 1 pT could be generated whenever the Kp index exceeded 3. Similarly, ELF signal strength correlates strongly with strength of the electrojet as determined from magnetometer chain data. Figure 10 shows data for the north-south magnetometer at College, Alaska during a time period corresponding to an ELF generation experiment [8]. Data from a single ground-based magnetometer are somewhat difficult to interpret since the ionospheric currents move in geographic location as well as increase and decrease in amplitude throughout the day. However, in Figure 11 we see the measured ELF amplitudes during the same time period. Both signals begin at high levels and then fall to minimum values at 0700 UT, followed by a significant rise. Finally, as the magnetometer output decreases and then changes sign corresponding

to a reversal of electrojet current direction, there is a decrease and then a very rapid increase in ELF amplitude. At the same time as this current reversal is occurring, the otherwise steady phase of the ELF signal experiences a discontinuous phase shift.

Other favorable situations for ELF generation include the occurrence of visible aurora and the existence of a sporadic E layer as determined by ionosondes. An unfavorable time for ELF generation is under high absorption conditions, as indicated by riometer readings. Such high absorption conditions are caused by high-energy proton and electron precipitation during major solar events. Under these conditions most of the HF power appears to be absorbed at a very low altitude and cannot effectively modulate the conductivity where ionospheric currents are flowing.

These measurements prove that the beam-dephasing modulation technique works successfully, but with an effective modulation depth of less than 100 percent. Very recently [Wong et al, 1990] it has been demonstrated that the transmitters can be amplitude modulated at frequencies down to 50 Hz by increasing the filter capacitance in the high voltage power supplies. At the present time four of the eight transmitters have been so modified. Initial tests have been performed to compare the performance of amplitude modulation with dephasing modulation at 76 Hz. The resultant electric field signal amplitudes are shown in Figure 12. In all cases the total radiated power was kept constant at 400 kW. The data labeled 8DM indicates that all eight transmitters were operated at the 50 kW level and modulated by dephasing. The label 4DM denotes that four transmitters were modulated by dephasing, each operated at the 100 kW level. When four transmitters were full amplitude modulated and operated at the 100 kW level, the resultant signal amplitudes are labeled 4AM. Comparing the 4AM results with the 4DM results, we see that the 4AM amplitudes are larger than the 4DM amplitudes by a factor of more than 3, corresponding to an increase in ELF power by at least a factor of 10. This increase is achieved at the same total radiated power and the same ERP. The only change is an improvement in effective modulation depth. In the 8DM case the ERP is much higher and even larger amplitudes are obtained, indicating that the conductivity modulation effect is not saturated at the lower power density. It is anticipated that similar gains can be realized when all eight transmitters are converted to full amplitude modulation.

5. FUTURE RESEARCH DIRECTIONS

Additional ELF generation experiments will be performed at HIPAS later in 1990 in order to investigate more fully various approaches for enhancing the HF-to-ELF conversion efficiency. The beam steering capability will be upgraded to a 2 μs beam forming time, allowing more definitive tests of the beam painting concept. Other experiments will evaluate the use of short pulses (low duty cycle heating) to improve efficiency. All transmitters will be

modified to allow full amplitude modulation down to 50 Hz. The receivers will be optimized for detection in the 75 to 150 Hz range, and measurements will be made at distances of hundreds of kilometers from the heater using a mobile receiving station. It is anticipated that a single HF heating frequency will be used, chosen to maximize absorption in the D region, although dual frequency operation would permit exploration of some of the concepts for improved efficiency via E region heating. The measured ELF amplitudes will be correlated with real-time environmental data from ionosondes, the riometer and the magnetometer chain plus data from 50-MHz coherent radars operating near Anchorage and at HIPAS. The understanding gained from these new measurements and their interpretation will be valuable in future research planning and in the design of new facilities.

REFERENCES

1. Wong, A. Y., and J. Santoru, Active Stimulation of the Auroral Plasma, J. Geophys, Res., vol. 86, no. A9, pp. 7718-7732, 1981.

2. Wong, A. Y., J. Carroll, R. Dickman, W. Harrison, W. Huhn, B. Lum, M. McCarrick, J. Santoru, C. Schock, G. Wang and R.F. Wuerker, High Power Radiating Facility at the HIPAS Observatory, to be published in a special issues of Radio Sci., 1990.

3. Wong, A. Y., P. Y. Cheung, M. J. McCarrick, J. Stanley, R. F. Wuerker, R. Close, B. Baker, E. Fremouw, W. Kruer and B. Langdon, Large-Scale Modification in the Polar Ionosphere by Electromagnetic Waves, Phys. Rev. Lett., vol. 63, pp. 271-274, 1989.

4. Baker, M. R., T. W. Collins, H. S. Lee and A. J. Ferraro, A Diagnostic System for the Study of Extremely Long Wavelength Emission Produced by Ionospheric Modification, to be published in a special issue of Radio Sci., 1990.

5. Ferraro, A. J., H. S. Lee, T. W. Collins, M. Baker, D. Werner, F. M. Zain and P. J. Li, Measurements of Extremely Low Frequency Signals from Modulation of the Polar Electrojet Above Fairbanks, Alaska, IEEE Trans. Antennas Propagat., vol. 37, pp. 802-805, 1989; other data provided prior to publication by A. J. Ferraro, 1989.

6. Papadopoulos, K., A. S. Sharma and C. L. Chang, On the Efficient Operation of a Plasma ELF Antenna Driven by Modulation of Ionospheric Currents, Comments Plasma Phys. Controlled Fusion, vol. 13, no. 1, pp. 1-17, 1989; Papadopoulos, K., C. L. Chang, P. Vitello and A. Drobot, On the Efficiency of Ionospheric ELF Generation, to be published in a special issue of Radio Sci., 1990.

7. Papadopoulos, K., and A. J. Ferraro, Summary of July-August 1989 HIPAS Campaign, preliminary report provided by the authors, 1989.

8. McCarrick, M. J., A. Y. Wong, R. F. Wuerker, B. Chouinard and D. D. Sentman, Excitation of ELF Waves in the Schumann Resonance Range by Modulated HF Heating of the Polar Electrojet, to be published in a special issue of Radio Sci., 1990.

9. Wong, A. Y., et al, data provided prior to publication, 1990.

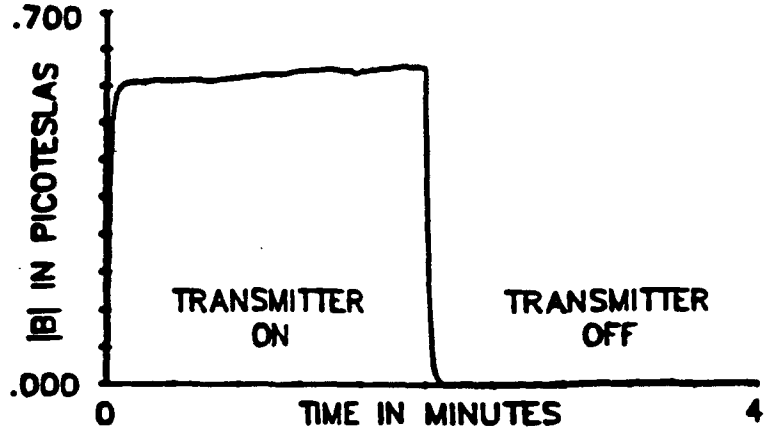

Figure 1: Magnitude and phase of strong 2.5 kHz signal.

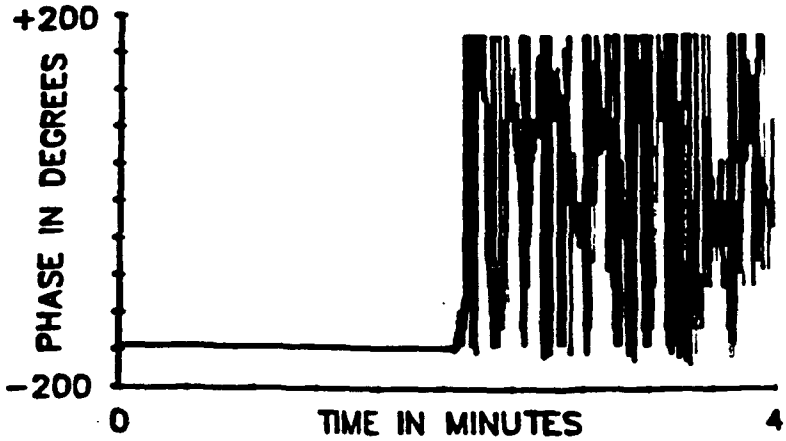

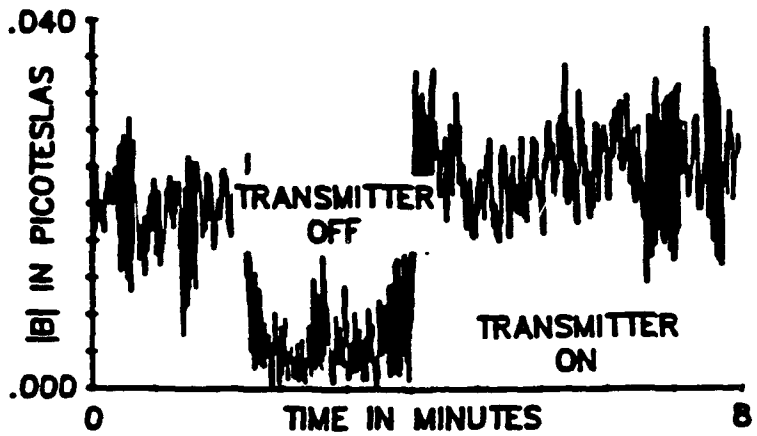

Figure 2: Magnitude and phase of weak 2.5 kHz signal.

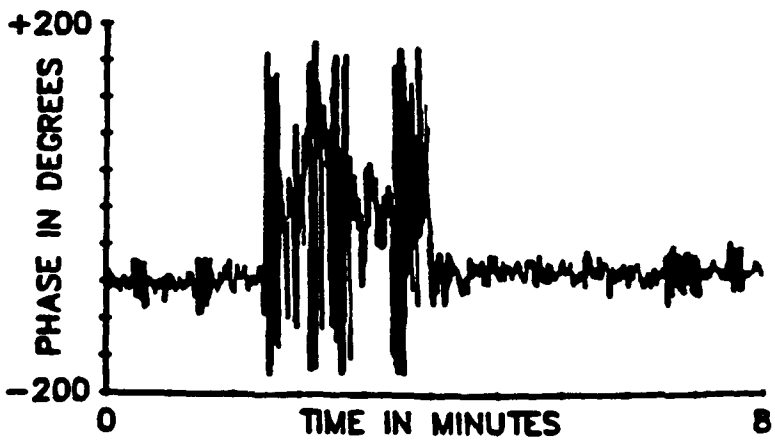

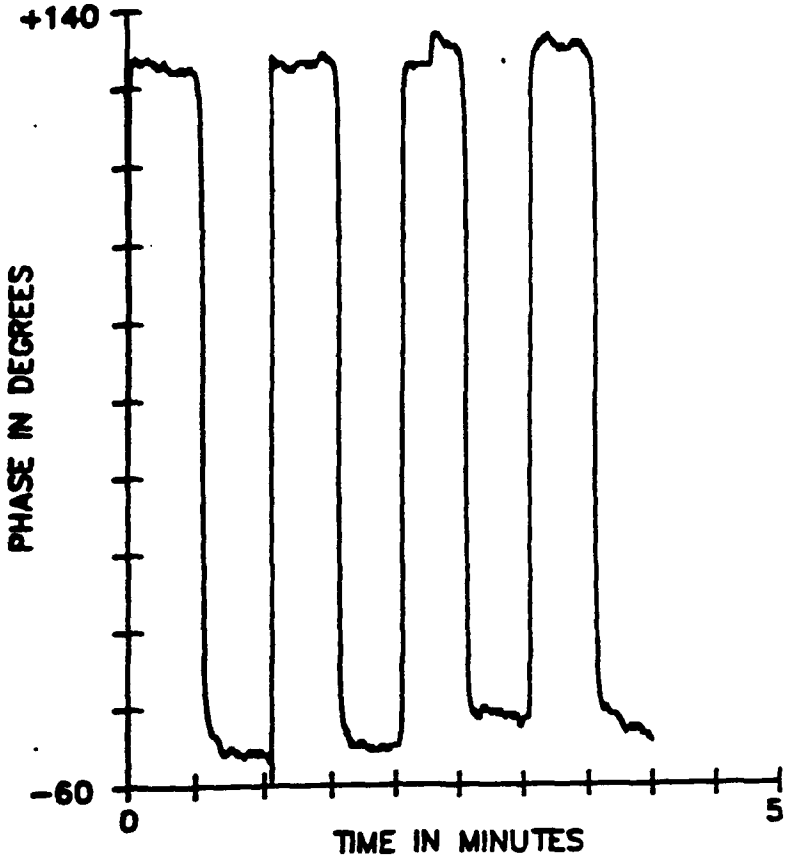

Figure 3: Detected phase of 2.5 kHz signal in phase keying test. Phase inverted by 180 degrees at 30 second intervals.

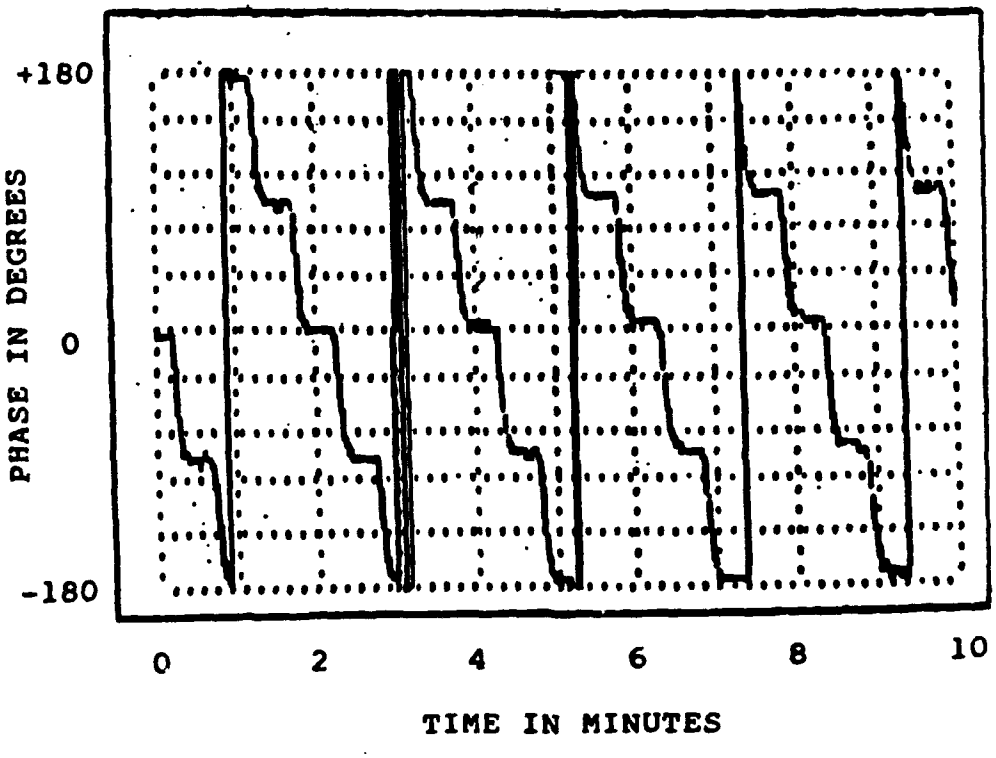

Figure 4: Detected phase of 2.5 kHz signal in phase shift keying test. The phase is shifted from 180 to 90 to 0 to -90 to -180 degrees.

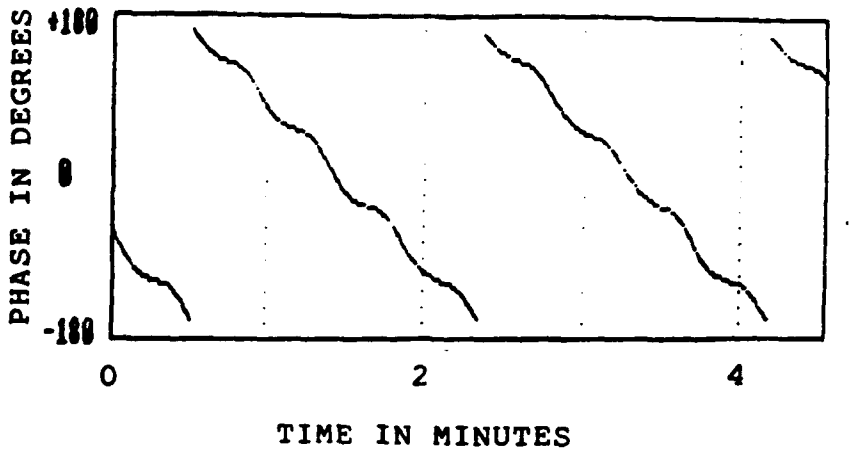

Figure 5: Detected phase of 2 kHz signal in phase shift keying test. The phase is shifted from 180 to 90 to 0 to -90 to -180 degrees. The receiver is located 210 km from the heater.

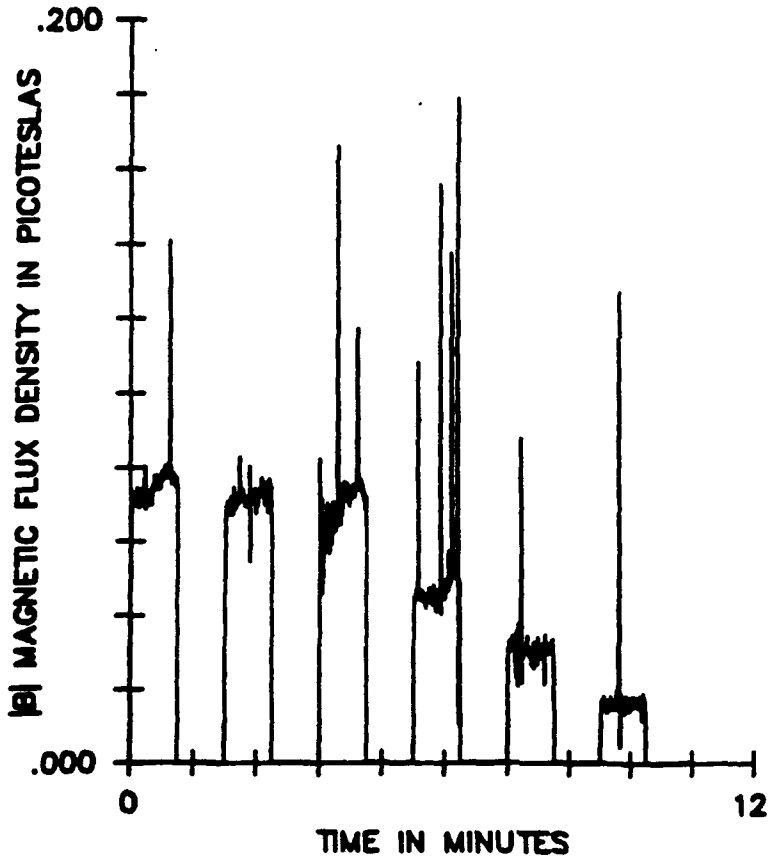

Figure 6: Magnitude of received 2.5 kHz signals in power reduction test. Total HF power is reduced from 800 to 640 to 480 to 320 to 160 to 80 kW.

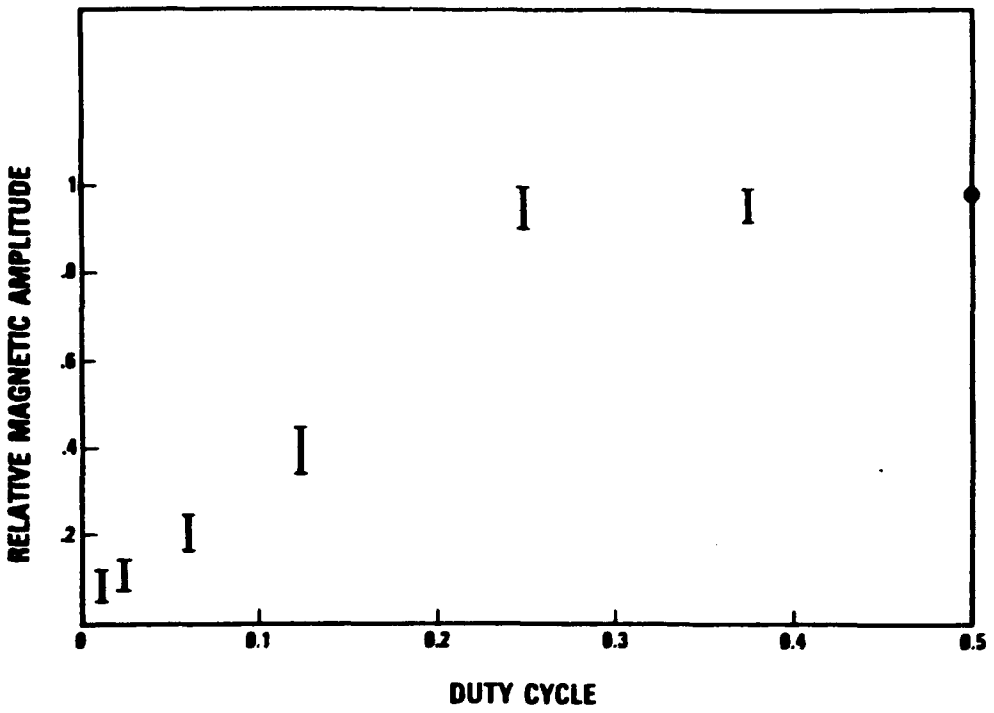

Figure 7: Relative signal amplitudes at various heater duty cycles

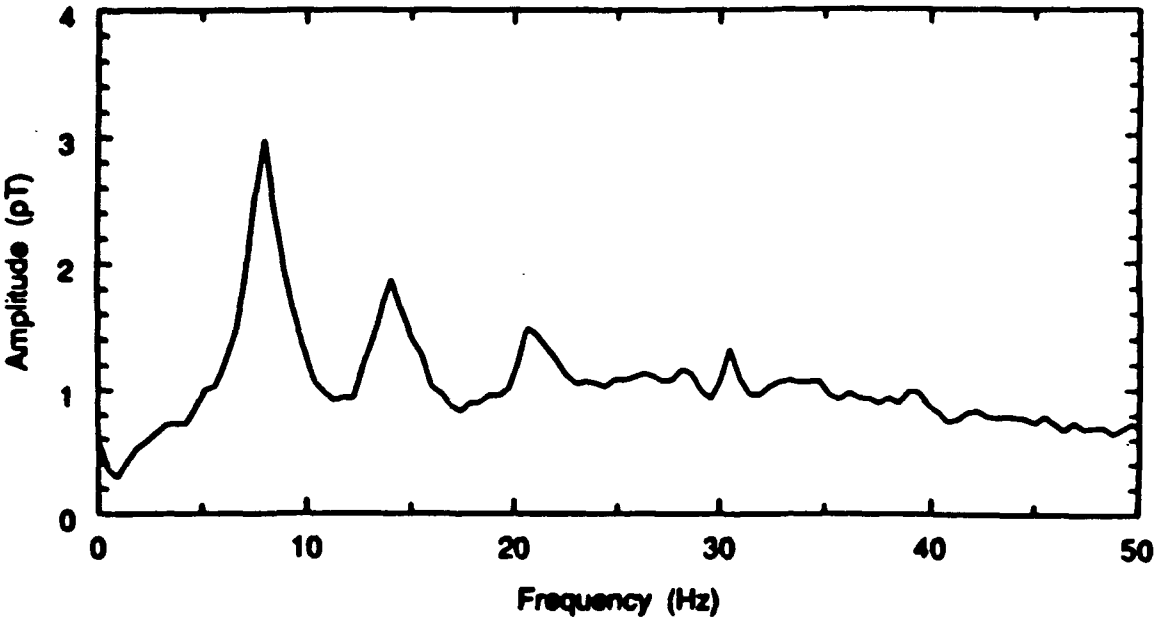

Figure 8: Background noise spectrum

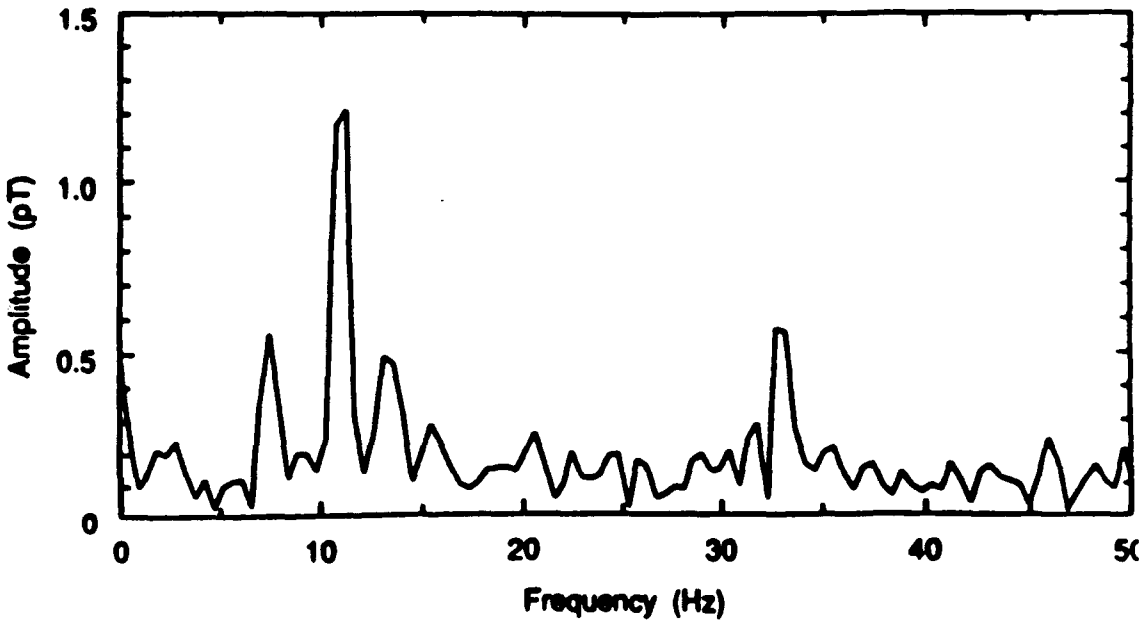

Figure 9: Signal spectrum resulting from modulation at 11 Hz.

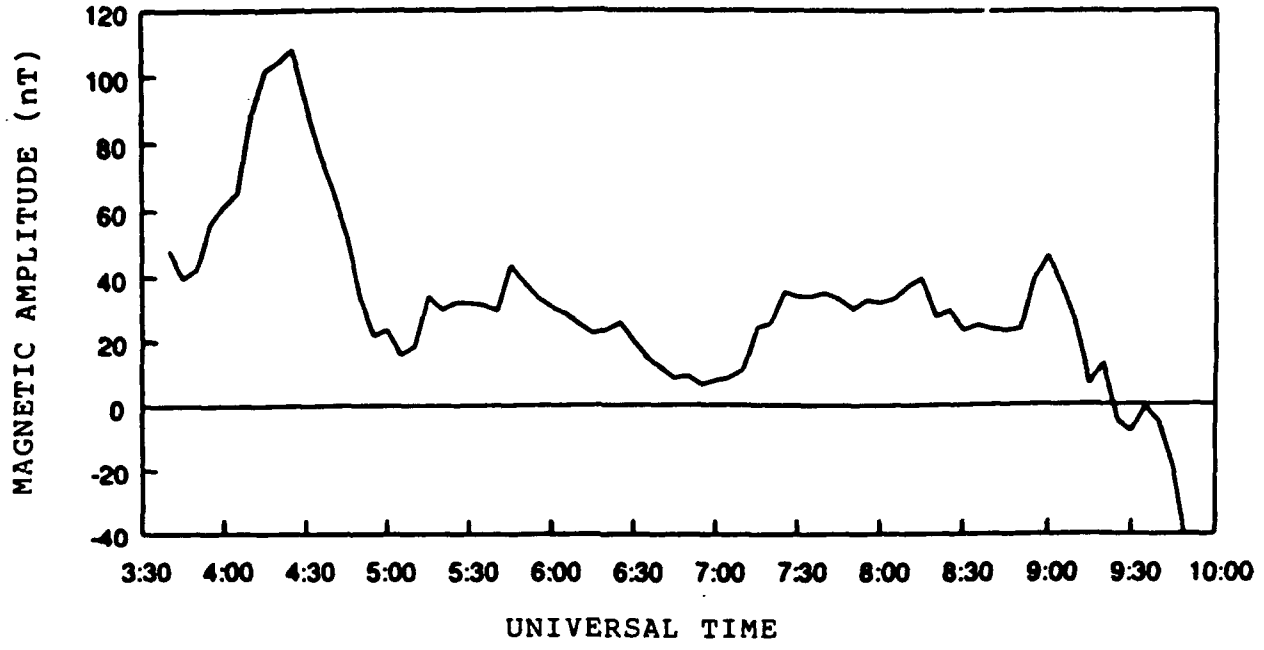

Figure 10: H-axis output of magnetometer at College, Alaska

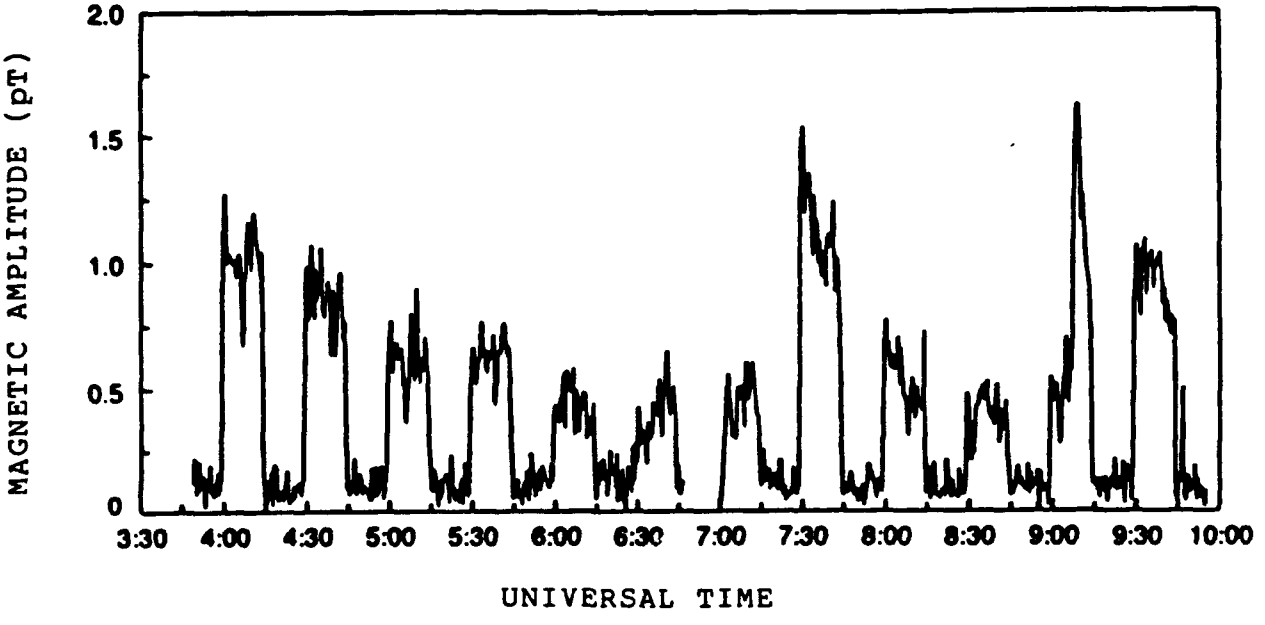

Figure 11: Signal strength at 11 Hz for same time period as in Figure 10.

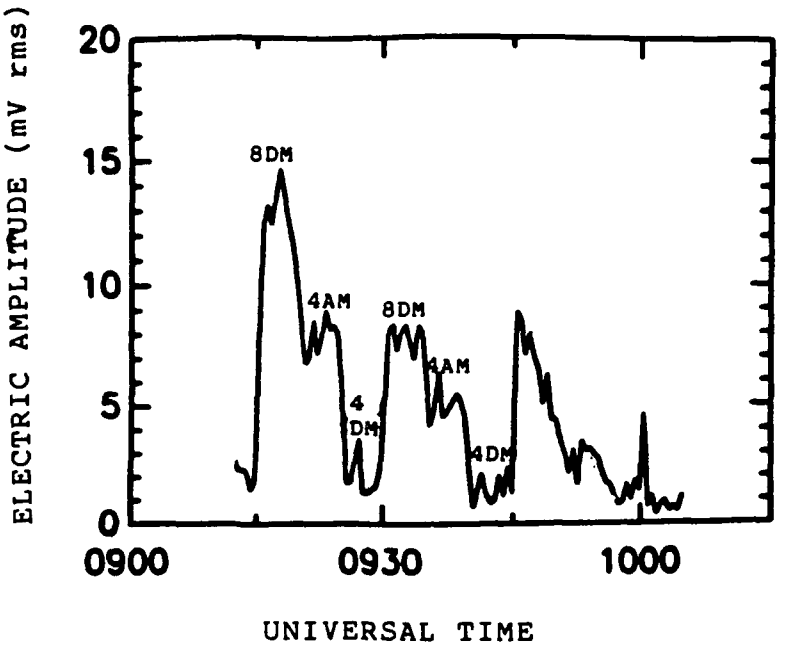

Figure 12: Signal amplitude at 76 Hz for various modulation schemes. AM denotes amplitude modulation; DM denotes dephasing modulation; 4 and 8 indicate number of transmitters being modulated. The total radiated power in all cases is 400 kW.

The following preprints which summarize the main research activities of Dr. K. Papadopoulos, Science Applications International Corporation, under Subcontract No. ONR-TPSU-SAIC-0677-388.

ON THE EFFICIENCY OF IONOSPHERIC ELF GENERATION

K. Papadopoulos, C.L. Chang, P. Vitello and A. Drobot

Science Applications International Corporation
1710 Goodridge Drive
McLean, Virginia 22102

June 1988

ABSTRACT

The scaling laws that control the efficiency of converting ground based HF power to ELF power by using modulation of the polar electrojet current is discussed. The analysis is based on kinetic calculations of the modification of the ionospheric conductivity by HF waves in conjunction with the experimental results reported from the Tromso Max Planck and the Alaska HIPAS facilities. It is shown that the efficiency can be increased by more than a factor of 10^4 by

(i) Using phasing to sweep the antenna beam over an area spanned by a maximum tilt of 35°, on a timescale faster than the cooling rate at the heating altitude (< 100 μsec).

(ii) Localization of the heating at the E-region (90-100km) where electron runaway can be induced resulting in substantial modification of the Pederson conductivity.

1. INTRODUCTION

Generating ULF/VLF/ELF waves by utilizing the ionosphere as an active medium is an exciting prospect. The technique provides frequency agility and avoids many of the geopolitical and economic difficulties associated with large and inefficient ground based facilities. By adjusting the HF beam geometry, the low frequency waves can be made to propagate upwards in the magnetosphere for use in active magnetospheric stimulation experiments or downwards into the earth ionosphere waveguide for communication and geological probing purposes. One of the mechanisms discussed for downconverting HF power to ULF/ELF/VLF power by interactioning with the ionosphere requires the presence of ambient ionospheric currents, such as the auroral or equatorial electrojets (Germantsev et al. 1974, Kotik and Trakhtengerts 1975, Stubbe and Kopka 1977, Chang et al. 1981, Ferraro et al. 1982), while another relies on pure plasma non-linearities and does not require the presence of ionospheric currents (Papadopoulos et al. 1982, 1983. Papadopoulos and Chang 1985, Ko et al 1986, Ganguli et al. 1986). Although both mechanisms have been verified experimentally, the predominance of the experiments dealt with the modulation of ionospheric currents because this technique demands lower HF transmitter power and antenna directionality.

Generation of ULF/ELF/VLF waves by modulating ionospheric currents has been confirmed for both the equatorial and the auroral electrojet in experiments conducted in the USSR (Migulin and Gurevich 1985, Belyaev et al. 1987), the Max-Planck Tromso facility (Stubbe et al. 1982, Barr and Stubbe 1984a, b, James et al. 1984, Barr et al. 1985) and the U.S. (Ferraro et al. 1982, Ferraro 1988, Ferraro et al. 1988). Most of the experiments were performed using HF frequencies in the range of 2-5 MHz, while the power density at the interaction region varied between 10^{-4} - 10^{-3} W/m^2. The most exhaustive studies were performed at the Tromso Max Planck facility and the typical results are summarized in Fig. 1. These results are in general terms consistent with results produced at other facilities, (Ferraro et al. 1988, Belyaev et al. 1987) although the precise values of the detected field amplitudes depend on local conditions, characteristics of the HF facility and other specific factors. The purpose of this paper is to explore the potential and the limitations of the ionospheric generation of ULF/ELF/VLF waves using as a guide the current experimental results in conjunction with theoretical extrapolations. Namely, starting from the current experimental and theoretical status, we develop scaling laws and use them to explore the efficiency with which HF power can be converted to the desired low frequency range. It is expected that the conclusions will be useful in guiding future facilities and experiments. For specificity we selected for our study the ELF frequency range (i.e. 50 Hz - 500 Hz), since in this range the interpretation of the results is not complicated by waveguide

resonances, high order modes and skin layer thickness. The plan of the paper is as follows. The next section summarizes the status of understanding of ELF generation by current modulation and the resulting scaling laws. Section 3 discusses the level of conductivity modification as a function of the incident power density and altitude. Contrary to previous studies which used fluid analysis to calculate the electron heating, a completely kinetic treatment is used here. Such a treatment is required for power densities exceeding 10^{-3} W/m^2. Based on the analysis of Sections 2 and 3, Section 4 discusses techniques for increasing the HF to ELF conversion efficiency. The final section summarizes the results and pinpoints high leverage research issues.

2. IONOSPHERIC ELF GENERATION-SCALING CONSIDERATIONS

Relating the amplitude of the ELF waves on the ground, to the extent and characteristics of the modified region in the ionosphere and to the design characteristics of the HF transmitter is a complex problem. Aspects of the problem have been examined by many authors (Kotik and Trakhtengerts 1975, Belustin et al. 1977, Tripathi et al 1982, Fejer and Krenzien 1982, Barr and Stubbe 1984a,b). It involves a series of sequential steps. First, based on the transmitter characteristics (power, gain, H.F. frequency and modulation frequency) and the applicable model of the ambient ionosphere the conductivity modulation is computed as a function of altitude. This allows for the calculation of the modulated current altitude profile, for a specified ambient ionospheric electric field (assumed or measured). This calculation involves computation of the primary current, the polarization currents required to set up quasineutrality, and the induction currents caused by the time dependence of the magnetic field. Third, from the modulated current profile the excitation and propagation of the ULF/ELF/VLF waves in the earth's ionospheric waveguide can be computed by using either the extended source technique (Tripathi et al. 1982) or with an equivalent ULF/ELF/VLF moment in the ionosphere the reciprocity principle (Galejs 1968, 1971; Barr and Stubbe 1984a,b). A comprehensive analysis of these factors lies beyond the scope of this paper. Within the experimental and theoretical uncertainties our purpose can be accomplished by starting from the current experimental results in the frequency range of 50-500 Hz and analyzing them under the assumption that the power generated is proportional to the square of the dipole moment

$$M \equiv IL \tag{1}$$

where I is the total modulated current contributing to the ELF field on the ground and L is the linear size of the modulated region. All other factors entering the efficiency calculation will be taken from the current experimental data basis. For concreteness we use as a

baseline the measurements and analysis of the Tromso results (Barr and Stubbe 1984a). These results are similar to the ones reported from HIPAS (Ferraro et al 1988). The range of 50-500 Hz has been selected in order to avoid effects associated with waveguide resonances which arise for frequencies above 1 kHz.

The experimental results indicate that when the heating transmitter operated at a power level of 150 MW ERP the amplitudes of the ELF field measured on the ground are ~100 mV/m or 1 pT. These correspond to about 10-100 mW of radiated ELF power in the 200-500 Hz range (Barr and Stubbe 1984a) The equivalent radiating horizontal dipole at 75-80 km altitude in the ionosphere is IL ≈ $3-5\times10^4$ A-m which corresponds to an equivalent ground based electric vertical dipole with IL = $2-4\times10^3$ A-m. The polarization is consistent with predominance of Hall current modulation. For the frequency range, computations based on a fluid model indicate that for an assumed electric field E_0 = 25 mV/m the peak values of the modulated current density are in the range of 10^{-8} A/m^2 and are located between 75-80km in altitude. The effective horizontal radiated current moment M can be estimated by height integration as

$$M = IL = \Delta j \Delta z L^2 = \Delta\sigma \Delta z E_0 L^2 \qquad (2)$$

where Δj is the modulated current density, Δz is the extent of the effective radiating layer, in altitude and $\Delta\sigma$ is the modulated conductivity. For the typical experimental conditions L ≈ 20km (i.e. at a heater beam width of 7.5°), $\Delta z \approx$ 10km, $E_0 \approx$ 25 mV/m . the value of IL ≈ $3-5\times10^4$ A-m corresponds to a peak value of $\Delta\sigma \approx 3-4 \times 10^3$ sec^{-1} This is achieved with an incident HF power density of 2 mW/m^2 at 75-80 km height. Finally it should be noted that the value of IL is independent of frequency and the frequency dependence in the ELF power is attributed to the scaling of the excitation efficiency (Galejs 1971).

Since the quantities that can be controlled from the ground are the value (and possibly the altitude location) of the conductivity modulation $\Delta\sigma$ and the size L, it is instructive to cast the experimental data as interpreted by Barr and Stubbe (1984a) in the form of Fig. 2. Notice the important scaling valid for each ELF frequency, i.e.

$$P_{ELF} \sim M^2 \sim (\Delta\sigma)^2 L^4 \qquad (3)$$

For instance, if we increased the peak conductivity modulation by a factor of 10 while keeping L≈ 20km, the radiated power at 500 Hz would increase from 100 mW to about 10W. Similarly, if we increased the size L by a factor of 5 while keeping $\Delta\sigma \approx 3-4 \times 10^3$ sec^{-1}, the radiated power would increase by a factor of $(5)^4 \sim 6 \times 10^2$.

A critical scaling needed for the determination of the factors that optimize P_{ELF} is the dependence of the conductivity modification $\Delta\sigma$ on the HF power density S at the modified height.

$$S \equiv \frac{P_{HF}}{L^2} \tag{4}$$

where P_{HF} is the ground HF power and L is the spot size at the appropriate height. Of course this neglects absorption at lower heights, a point that we will return later on. Assuming that

$$\Delta\sigma \sim \left[\frac{P_{HF}}{L^2}\right]^{\alpha} \tag{5}$$

we find from (3) - (5) that

$$P_{ELF} \sim P_{HF}^{2\alpha} L^{4(1-\alpha)} \tag{6}$$

For $\alpha = 1$, we find that P_{ELF} is independent of the antenna gain and scales as

$$P_{ELF} \sim P_{HF}^2 \tag{7}$$

Namely the HF to ELF conversion increases as the square of the HF power. The conversion efficiency depend predominately on P_{HF} for $\alpha >> 1$, while for $\alpha << 1$ more efficient conversion requires large spot sizes. A computation of the value of α for various altitudes and HF power densities is performed in the next section.

3. DEPENDENCE OF CONDUCTIVITY MODIFICATION ON ALTITUDE AND POWER DENSITY

In this section we evaluate the level of conductivity modulation at various ionospheric heights as a function of the incident HF power density S. The calculation is "local" and neglects transport. From the modulated conductivity we can easily evaluate the modulated current for a given ionospheric electric field. As opposed to previous studies (Stubbe and Kopka 1977, Tomko 1981, Chang et al 1981, James 1985) which used fluid equations to compute the variation of the electron temperature T_e as a linear approximation, the present study uses the complete time dependent kinetic equation for the electron energy distribution function $f(\varepsilon)$. For a HF electric field of amplitude E_0 and frequency ω_0 at the chosen height $f(\varepsilon)$ is given by (Gurevich 1978)

$$\frac{\partial}{\partial \varepsilon} f(\varepsilon) = \frac{1}{\sqrt{\varepsilon}} \frac{\partial}{\partial \varepsilon} (\varepsilon^{3/2} D \frac{\partial f}{\partial \varepsilon}) - L(\varepsilon) \tag{8}$$

$$D(\varepsilon) = \frac{1}{6} \frac{e^2 E_o^2}{m} \frac{\nu(\varepsilon)}{(\omega_o \pm \Omega)^2 + \nu^2(\varepsilon)} \tag{9}$$

where $\nu(\varepsilon)$ is the energy dependent electron-neutral collision frequency at the chosen height and Ω is the electron cyclotron frequency. The $\pm$ signs correspond to o (+) and x (-) mode heating correspondingly. $L(\varepsilon)$ is an operator that represents the energy loss due to various inelastic processes. It's form is discussed in the Appendix which includes excitation of rotational, vibrational and optical levels as well as ionization and attachment for N_2 and O_2. Note that the latter process is not important for the power densities analyzed here. Equation (8) was solved numerically for $f(\varepsilon,t)$ at various altitudes, HF power density values S and modulation frequencies ω. The time dependence of the conductivity is found from

$$\sigma_p(t) = \frac{ne^2}{m} \int \frac{\nu(\varepsilon)}{\Omega^2 + \nu^2(\varepsilon)} f(\varepsilon,t)\, \varepsilon^{1/2} d\varepsilon \tag{10a}$$

$$\sigma_h(t) = \frac{ne^2}{m} \int \frac{\Omega}{\Omega^2 + \nu^2(\varepsilon)} f(\varepsilon,t)\, \varepsilon^{1/2} d\varepsilon \tag{10b}$$

$$\sigma_z(t) = \frac{ne^2}{m} \int \frac{1}{\nu(\varepsilon)} f(\varepsilon,t)\, \varepsilon^{1/2} d\varepsilon \tag{10c}$$

where σ_p, σ_h, σ_z are the Pederson, Hall and parallel conductivities and n is the electron density. As noted in the introduction a kinetic analysis is an absolute requirement for exploring high power densities. The initial $f(\varepsilon, t = 0)$ was taken as Maxwellian at T_e = 0.025 eV. For the studies reported below $\omega_o = 1.8 \times 10^7$ rad/sec which corresponds to a heater frequency of 2.8 MHz.

We report below results for daytime ionospheric conditions corresponding to altitudes between 70-120 km. The ionospheric model used is shown in Fig. 3.

The need for a kinetic description at high power and high altitude is obvious from the distribution function shown in Fig. 4. Figure 4a-c show the initial and steady state distribution functions for ionospheric heating at 75, 90 and 100 km altitude and at values of $S = 10^{-3}$, 10^{-2} W/m^2, correspondingly. The time required to reach steady state was in all

cases much shorter than 10^{-3} sec. This implies that steady state is reached at times much shorter than the relevant modulation frequencies. It is seen that at low altitude and low power density (i.e. 75 km, 10^{-3} W/m^2) f(ε) does not deviate much from Maxwellian and the fluid description is a good approximation. This, however, is not true for the other two cases where the high energy tails of the distribution functions become the dominant part..

Figures 5-6 show the time dependence of the Hall and Pedersen modulation for the above three cases. At 75 km and 10^{-3}W/m^2 the Hall conductivity modulation is about $7 \times 10^3 sec^{-1}$ which is consistent with the value quoted in Section 2 for the Tromso experiments. The Pederson conductivity modulation is significantly smaller. This is reversed for the 90 and 100km cases at 10^{-2} W/m^2. The Hall conductivity modulation becomes progressively smaller and is negligible at 100 km. Furthermore the level of the Pederson conductivity modulation is about 3×10^4 sec^{-1} at 90 km and 6×10^4 sec^{-1} at 100 km. It is clear that if the size L, which is controlled by the antenna gain was the same for all three cases and the increase in the power density was entirely due to an increase in P_{HF} by a factor of 10, the radiated P_{ELF} would increase by a factor of 20 and 10^2 for the 90 and 100 km cases over the 75 km case. Notice that as noted before steady state is established for all cases much earlier than the low frequency oscillation period,the values of $\Delta\sigma$ are independent of ELF frequency. In order to determine the scaling of conductivity modification with power density and altitude, we conducted a survey of the level of steady conductivity modification for three altitudes (70, 100, 120 km) and values of S in the range of 10^{-4} - 1 W/m^2. The results for the Hall and Pederson conductivities are shown in Figs. 7 and 8 The boundary altitudes were chosen in a way that they reflect the range of variation of the Pedersen and Hall conductivities with altitude. A more detailed analysis of the consequences of the results shown in Figs. 7 and 8 and of the efficiency optimization at intermediate altitudes will be presented elsewhere. We restrict our discussion here to the consequences of the general trends derived from Figs.7 and 8. These are:

(i) For low altitudes (~ 70-75 km) the Hall conductivity provides the dominant contribution. The value of $\Delta\sigma_h$ increases very weakly with power density ($\alpha < 1/2$) and saturates at a value of S about $2 \cdot 10^{-3}$ W/m^2. Further increase in the power density does not produce any increase in the modulated current density. According to the discussion after Eq.(7), optimization of the conversion efficiency requires increase in L under constant S.

(ii) For high altitude (> 90 km) heating the modification of the Pederson conductivity dominates. The value of $\Delta\sigma_p$ increases as S^2(i.e. $\alpha = 2$), up to power density of 10^{-2} W/m^2 and saturates slowly afterward . There is an obvious premium in increasing P_{HF}, since in this case $P_{ELF} \sim P^4_{HF}$, while keeping $S = 10^{-2}$W/m^2.

(iii) Maximum value of $\Delta\sigma$ is achieved for high altitude heating.

4. EFFICIENCY OF HF TO ELF CONVERSION

In this section we combine the results of Barr and Stubbe (1984) as shown in Fig. 2 with the results reported in Section 3, and use them to determine the HF to ELF conversion efficiency and techniques by which it can be optimized. Based on Hall conductivity modulation of the polar electrojet at 70-75 km altitude Barr and Stubbe (1984) estimate a power conversion efficiency of 5-10 mW per MW of HF at 200 Hz. This implies an overall conversion efficiency of about 10^{-8}, compared with 10^{-6} conversion achieved by the Wisconsin Test Facility. For low altitude heating the results of Section 3 indicate that increasing the power does not have any significant effect in the ELF power. However, as shown in Eq. (3) for constant power density and therefore constant $\Delta\sigma$, $P_{ELF} \sim L^4$. An increase in area while maintaining the same approximately power density can be achieved by using phasing to sweep the antenna beam over an area spanned by a maximum tilt of θ_m degree in each direction at a rate faster than the cooling rate, which for 75km is approximately 50-100 μsec. The P_{ELF} then increases according to Eq. (3) by a factor of $(\sin\theta_m/\sin\theta_o)^4$ where θ_o is the antenna half-width. Taking $\theta_o = 7.5°$ and $\theta_m = 35°$, we find an increase in P_{ELF} by a factor of 400. Namely modified the to sweep angle to a 30 ° cone at the Tromso or HIPAS facility over 50-100 μsec is expected to produce 2-4W and have an efficiency of 10^{-6}, comparable to the Wisconsin Test Facility.

Alternately, higher efficiency as well as higher P_{ELF} can be produced by high altitude heating. If HF heating localized in the 95-100 km region can be achieved with power density of the order 10 mW/m^2, the resultant conductivity modification according to Figs. 7 and 8 increases by a factor of 100 over that for low altitude heating. According to Eq. (3) this will produce a factor of 10^4 more power than the 5-10 mW , which results in 50-100 W in ELF even in the absence of sweeping. The system efficiency increases by a factor of 10^3 giving an overall conversion efficiency of 10^{-5}. Incorporating a similar sweep as for the low altitude heating will result in further increase of the efficiency by a factor of 400 giving an overall efficiency better than 4×10^{-3}. The practical difficulty in realizing the high altitude scheme, especially under day time conditions, is the fact that self absorption at lower heights could prevent the achievement of power densities of 10 mW/m^2 at 95-100 km altitude for frequencies of 2.8 MHz used in our calculations. Such heating can be achieved by using higher frequencies, beating two HF waves at the local plasma frequency, or using short pulses that allow the power to "sneak through" to high altitudes. These possibilities are currently under study. The enormous increase in efficiency achieved in high altitude heating places a large premium in realizing them even if their efficiency is by an order of magnitude lower.

5. SUMMARY AND CONCLUSIONS

We presented a detailed kinetic study of local heating of the ionospheric plasma by modulated radiowaves, of the resultant conductivity modulation and of the associated modulated current density in the presence of an ionospheric electric field in the ELF region (50 - 500 Hz). Regimes where the conductivity modulation is a strong or weak function of the incident HF power density were identified. Combining these results with the recorded observations in this ELF region and assuming that to zero order the ELF power density is proportional to $(\Delta\sigma)^2 L^4$ we found that the HF to ELF power conversion efficiency can be increased by more than two orders of magnitude if the heater could be swept over a 30° cone on timescales faster than the plasma cooling rate (~ 100 μsec) for low altitude heating. Heating techniques that can preferentially deposit their energy at higher altitude (~ 90-100 km) where the dominant modulated current is the Pederson current, can further increase the efficiency by a factor of 10^4, although part of this increase can be negated by the potential inefficiency of high altitude heating as well as by a more inefficient coupling to the waveguide. We are currently examining these issues theoretically and expect to resolve them in combination with the Penn State HIPAS experimental campaigns

ACKNOWLEDGMENTS

The work was supported by ONR through Penn State subcontract ONR-TPSU-SAIC 0677-388. Discussions with Professors Ferraro and Lee of Penn State and Dr. Ossakow of NRL are gratefully acknowledged.

REFERENCES

Barr, R. and P. Stubbe, J. Atmos. Terr. Phys., 46, 315, 1984a.

Barr, R. and P. Stubbe, Radio Sci., 19, 1111, 1984b.

Barr, R., M.T. Rietveld. P. Stubbe, and H. Kopka, J. Geophys. Res., 90, 2861, 1985

Belustin, N.S., and S.V. Polyakkov, Radiophys. Wuantum Electron., 20(1), 57, 1977.

Belyaev, P.P., D.S. Kotik, S.N. Mityakov, S.V. Polyakov, V.O. Rapoport and V. Yu. Trakhtengerts, Radiophysics 30, 248, 1987.

Chang, C.L., V. Tripathi, K. Papadopoulos, J. Fedder, P.J. Palmadesso, and S.L. Ossakow, Effect of the Ionosphere on Radiowave Systems, edited by J. M. Goodman, p. 91, U.S. Government Printing Office, Washington, D.C., 1981.

Ferraro, A.J., (this issue) 1988.

Ferraro, A.J., H.S. Lee, T.W. Collins, M. Baker, D. Nerner, F.M. Zain, and P.J. Li (this issue) 1988.

Ferraro, A.J., H.S. Lee, R. Allshouse, K. Carroll, A.A. Tomko, F.J. Kelly, and R.G. Joiner, J. Atmos. Terr. Phys. 44, 1113-1122, 1982.

Galejs, J., J. Geophys. Res., 73, 339-352, 1968.

Galejs, J., Radio Sci., 6(1), 41-53, 1971.

Germantsev, G.G., N.A. Zuikov, D.S. Kotik, L. F. Mironenko, N.A. Mityakov, V.O. Rapoport, Yu. A. Sazonov, V. Yu. Trakhtengerts, and V. Ya. Eidman., JETP Lett. 20, 229, 1974.

Gurevich, A.V., Nonlinear Phenomena in the Ionosphere, Springer-Verlag, New York, 1978.

James, H.G., J. Atm. Terr. Phys. 47, 1129, 1985.

James, H.G., R.L. Dowden, M.T. Rietveld, P. Stubbe and H. Kopka, J. Geophys. Res., 89, 1655, 1984.

Kotik D.S., and V. Yu. Trakhtengerts, JETP Lett., 21, 51-52, 1975.

Migulin, V.V. and A.V. Gurevich, J. of Atm. and Terr. Phys. 47, 1181, 1985.

Papadopoulos, K. and C.l. Chang, Geophys. Res. Lett., 12, 279, 1985.

Papadopoulos, K., R. Sharma, and V. Tripathi, J. Geophys. Res., 87, 1491, 1982.

Papadopoulos, K., K. Ko, and V. Tripathi, Phys. Rev. Lett., 51, 463, 1983.

Stubbe, P., and H. Kopka, J. Geophys. Res., 82, 22319-2325, 1977.

Stubbe, P., and H. Kopa, J. Geophys. Res., 82, 2319, 1977.

Stubbe, P., H. Kopa, and R.L. Dowden, J. Geophys. Res., 86, 9073, 1981.

Stubbe, P., H. Kopa, H. Lauche, M.T. Rietveld, A. Brekke, O. Holt, and R.L. Dowden, J. Atmos. Terr. Phys., 44, 1025, 1982a.

Stubbe, P., H. Kopka, M.T. Reitveld, and R.L. Dowden, J. Atmos. Terr. Phys., 44, 1123, 1982.

Tomko, A.A., Rpt. PSU-IRL-SCI-470, Ionospheeere Research Laboratory, Pennsylvania State University, University Park, PA, 1981

Tripathi, V.K., C.L. Chang, and K. Papadopoulos, Radio Sci., 17(5), 1321-1326, 1982.

FIGURE CAPTIONS

Fig. 1 Typical experimental results in the ELF region generated by the Max Planck Tromso facility (Stubbe et al., 1982).

Fig. 2 ELF paper vs frequency for the Tromso facility as determined by the analysis of Barr and Stubbe (1984a). The ELF power scale has been multiplied by $(3 \times 10^3/\Delta\sigma) \times (20 \text{ km/L})^4$ to emphasize the scaling with size L and conductivity $\Delta\sigma$. For the Tromso results this factor is unity (i.e. $\Delta\sigma \approx 3 \times 10^3$, $L \approx 20$ km).

Fig. 3 Ionospheric profile used in the Fokker-Planck runs.

Fig. 4 Initial and steady state electron distribution for

(a) 75 km, $S = 10^{-3}$ N/m^2

(b) 90 km, $S = 10^{-2}$ W/m^2

(3) 100 km, $S = 10^{-2}$ W/m^2

Fig. 5 Hall conductivity modification for the cases of Fig. 4.

Fig. 6 Same as Fig. 5 for the Pederson conductivity.

Fig. 7 Hall conductivity modulation vs S for 70, 100 and 120 km.

Fig. 8 Pederson conductivity modulation vs S for 70, 100, and 120 km.

APPENDIX

The inelastic term of the Fokker-Planck equation (Eq. (8)) is composed from the following terms (Gurevich 1978)

(i) The excitation of rotational levels is taken into account by a term

$$S_R(f) = \frac{1}{2v^2}\frac{\partial}{\partial v}[v^2 R_R(v)\frac{T}{m}\frac{\partial f}{\partial v} + v f_o)] \qquad (A1)$$

where $R_R(v) = 8\beta_o\sigma_o N_N/mv$, $\sigma_o = 8\pi a_o^2/15$, $a_o = h^2/me^2$ is the Bohr radius, $B_o = 2.5 \times 10^{-4}$ eV is the rotational constant and N_N is the N_2 number density.

(ii) The excitation of vibrational and optical levels

$$S_{v,o}(f) = 2/mv \sum_k N_N[(\varepsilon + \varepsilon_k) f_o (\varepsilon + \varepsilon_k) \sigma_k(\varepsilon + \varepsilon_k) - \varepsilon f(\varepsilon)\sigma_k(\varepsilon)] \qquad (A2)$$

where ε_k is the energy of the k-state and σ_k is the cross section for that state.

(iii) Attachment

$$S_a = - N_o v \sigma_a f$$

where σ_a is the attachment cross section and N_o is the O_2 number density.

Although the code includes ionization processes the energy range for the powers under consideration in this study did not energize the electrons sufficiently to initiate it.

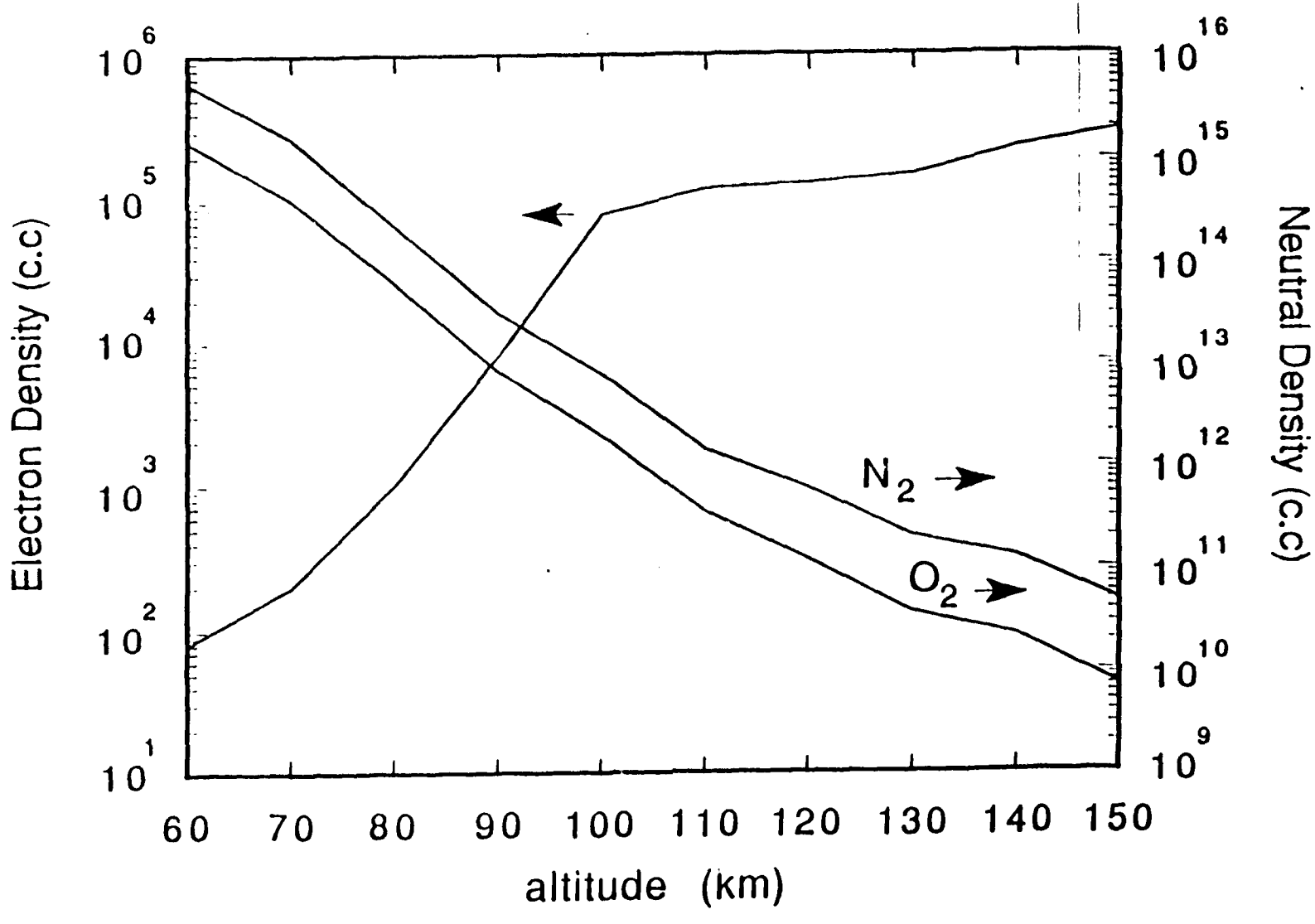
Electron Density (c.c)
10^6
10^5
10^4
10^3
10^2
10^1
Neutral Density (c.c)
10^{16}
10^{15}
10^{14}
10^{13}
10^{12}
10^{11}
10^{10}
10^9
N_2
O_2
60 70 80 90 100 110 120 130 140 150
altitude (km)

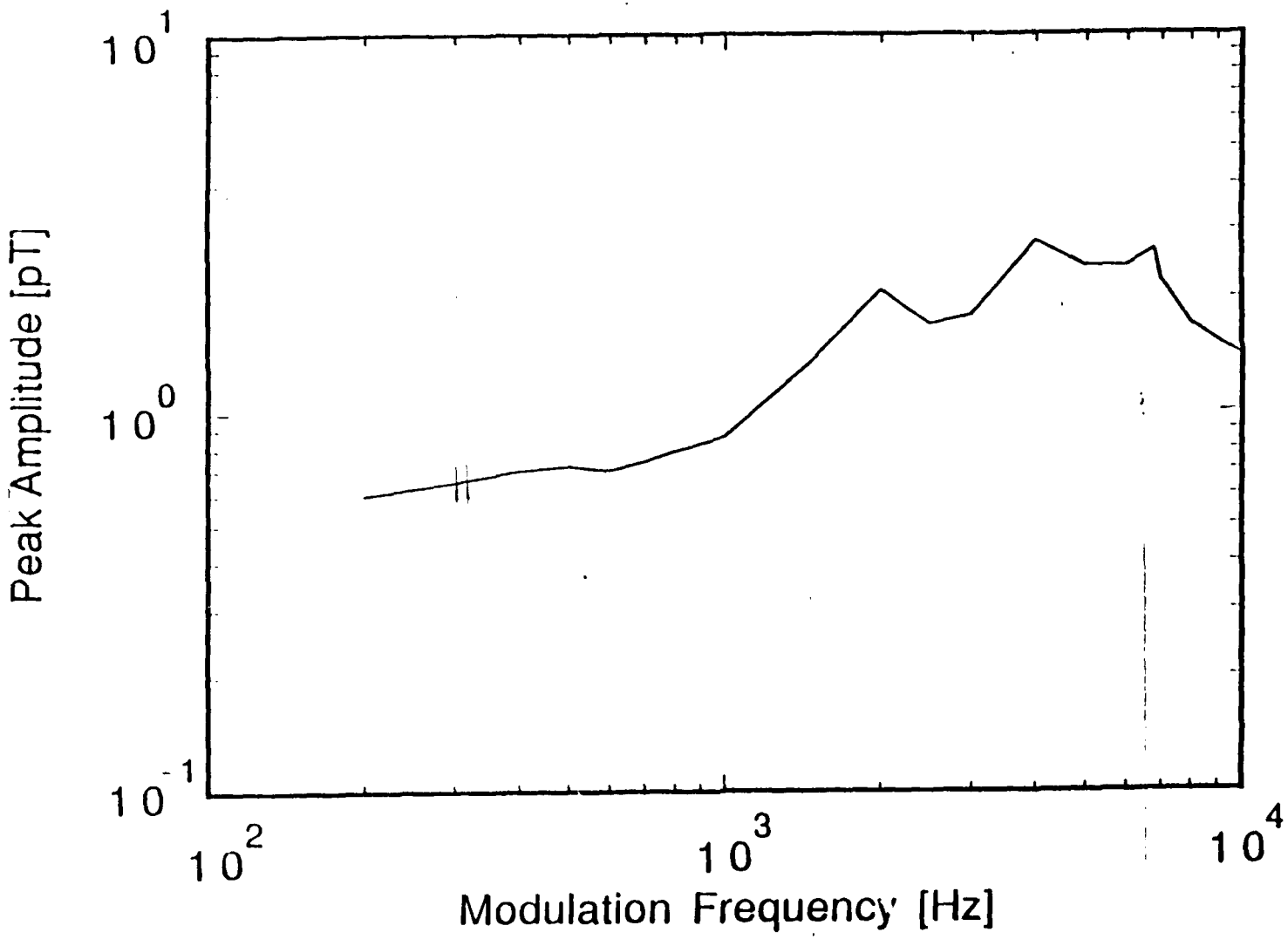
10^1
10^0
10^{-1}
Peak Amplitude [pT]
10^2
10^3
10^4
Modulation Frequency [Hz]

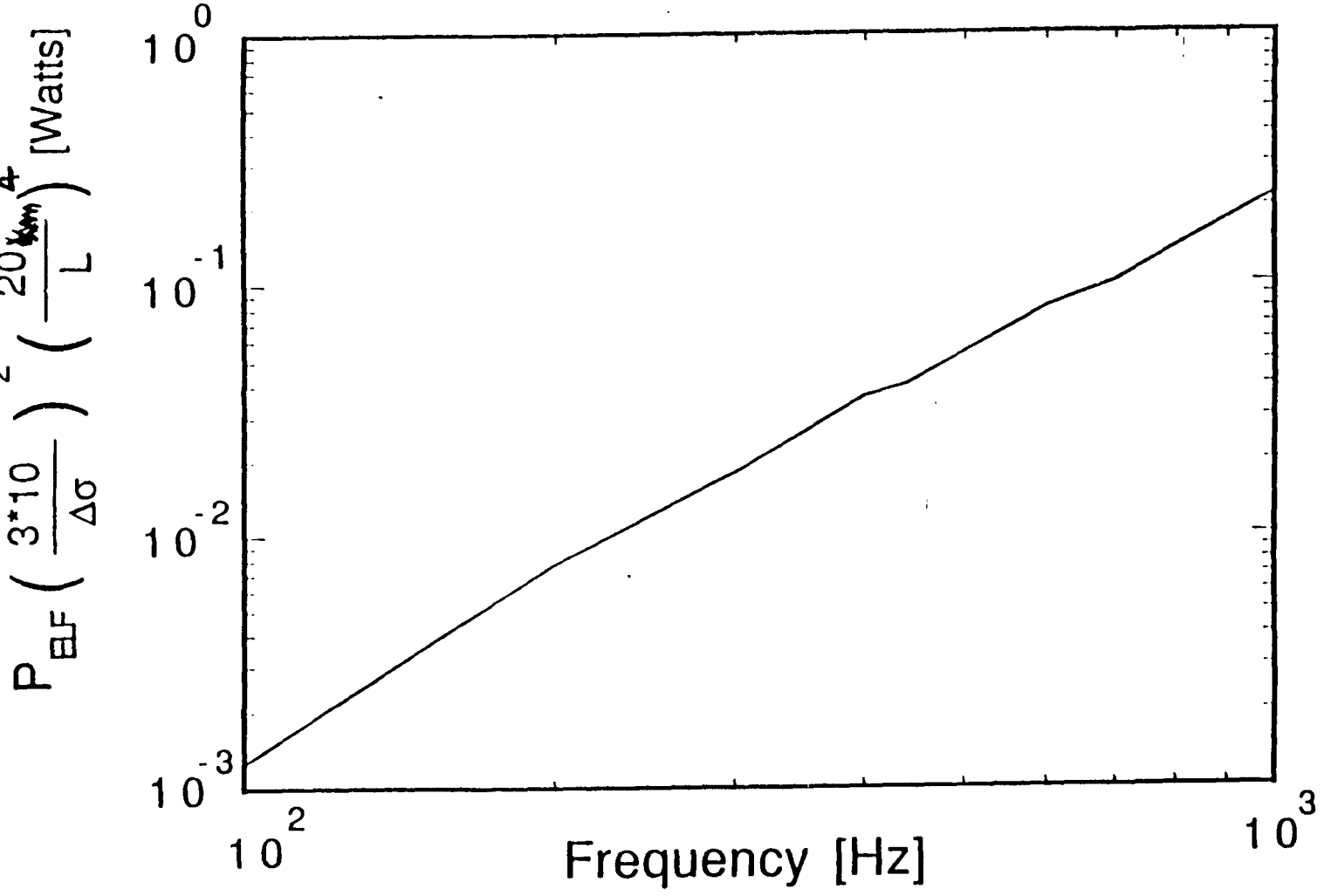
$P_{ELF}\left(\frac{3*10^{3}}{\Delta\sigma}\right)^{2}\left(\frac{20_{km}}{L}\right)^{4}$ [Watts]
10^{0}
10^{-1}
10^{-2}
10^{-3}
10^{2}
10^{3}
Frequency [Hz]

Fig. 4a

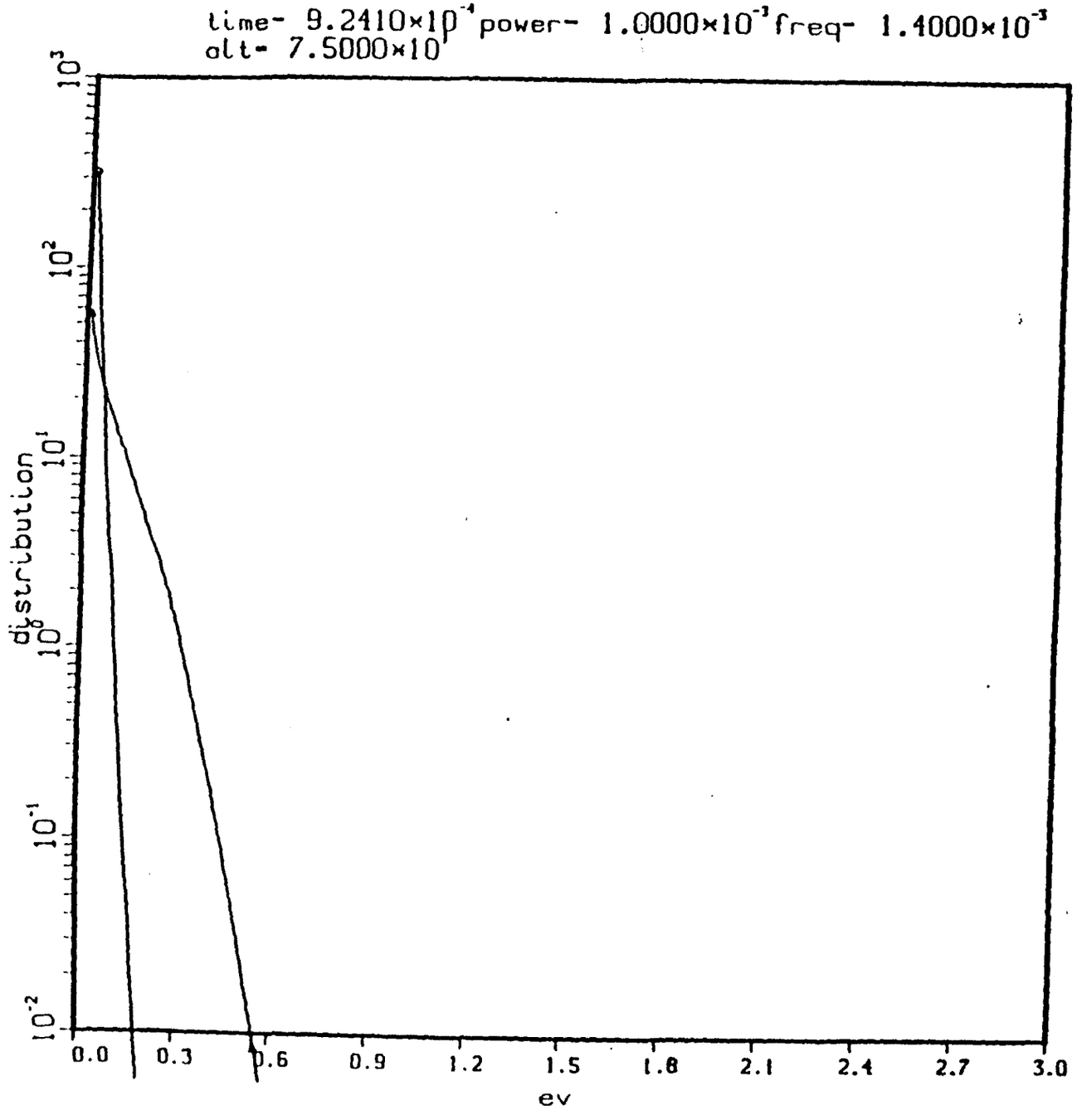
time- 9.2410×10^-4 power- 1.0000×10^-3 freq- 1.4000×10^-3
alt- 7.5000×10
distribution
10^3
10^2
10^1
10^0
10^-1
10^-2
0.0
0.3
0.6
0.9
1.2
1.5
1.8
2.1
2.4
2.7
3.0
ev

4b

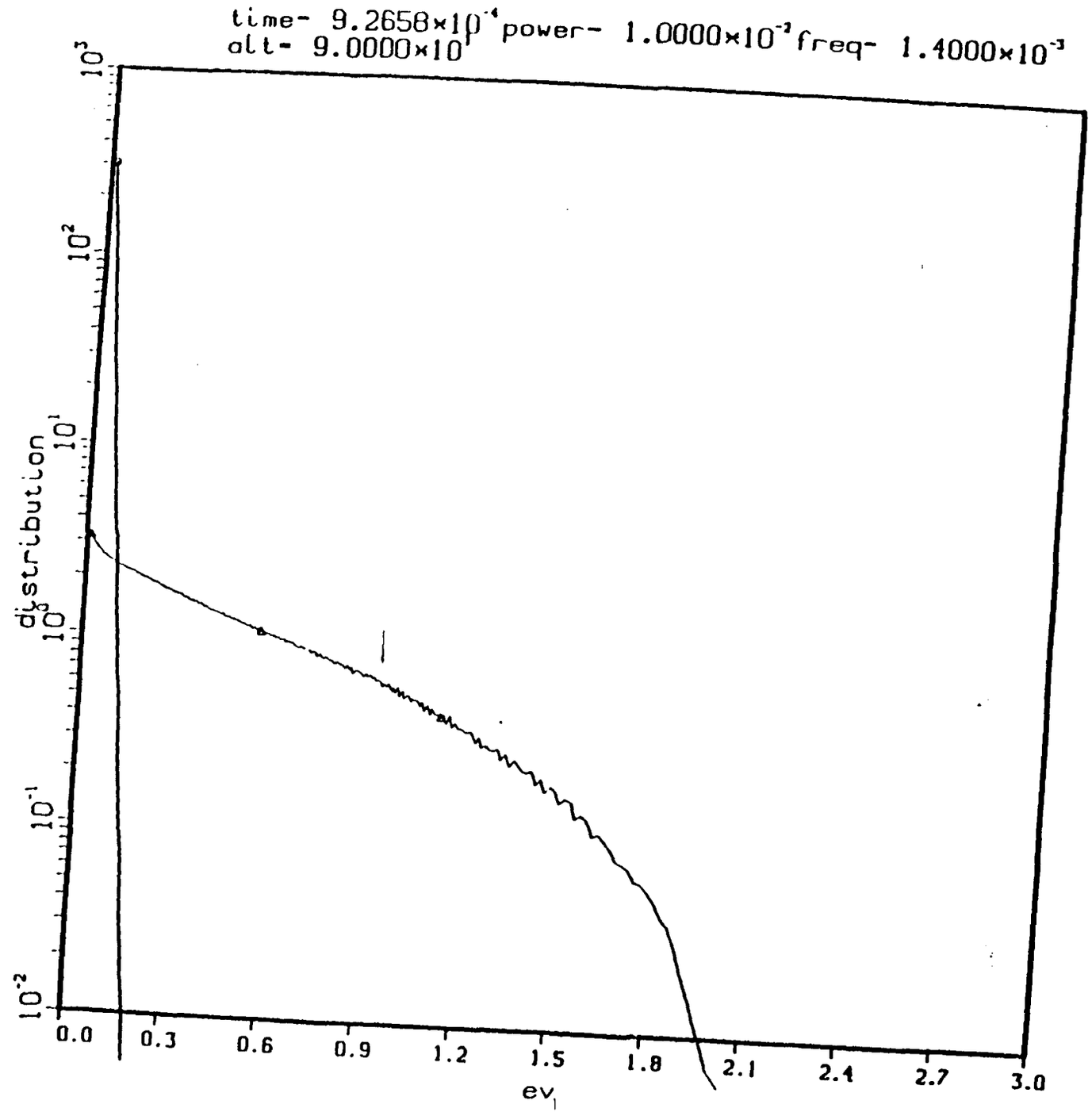
time- 9.2658×10⁻⁴ power- 1.0000×10⁻² freq- 1.4000×10⁻³
alt- 9.0000×10³
distribution
10³
10²
10¹
10⁰
10⁻¹
10⁻²
0.0
0.3
0.6
0.9
1.2
1.5
1.8
2.1
2.4
2.7
3.0
ev

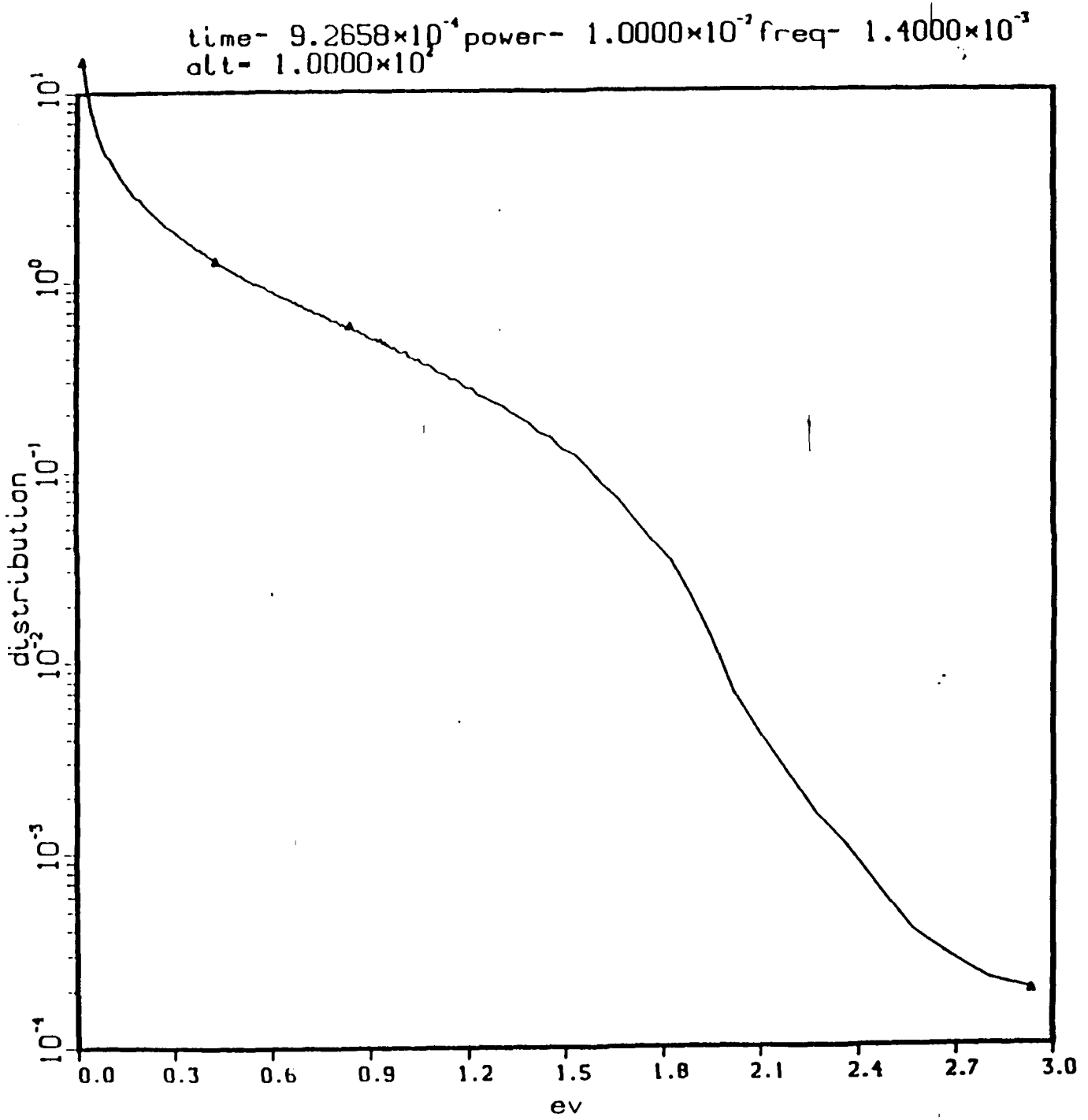
time- 9.2658×10⁻⁴ power- 1.0000×10⁻² freq- 1.4000×10⁻³
alt- 1.0000×10²
distribution
10¹
10⁰
10⁻¹
10⁻²
10⁻³
10⁻⁴
0.0
0.3
0.6
0.9
1.2
1.5
1.8
2.1
2.4
2.7
3.0
ev

Fig-6a

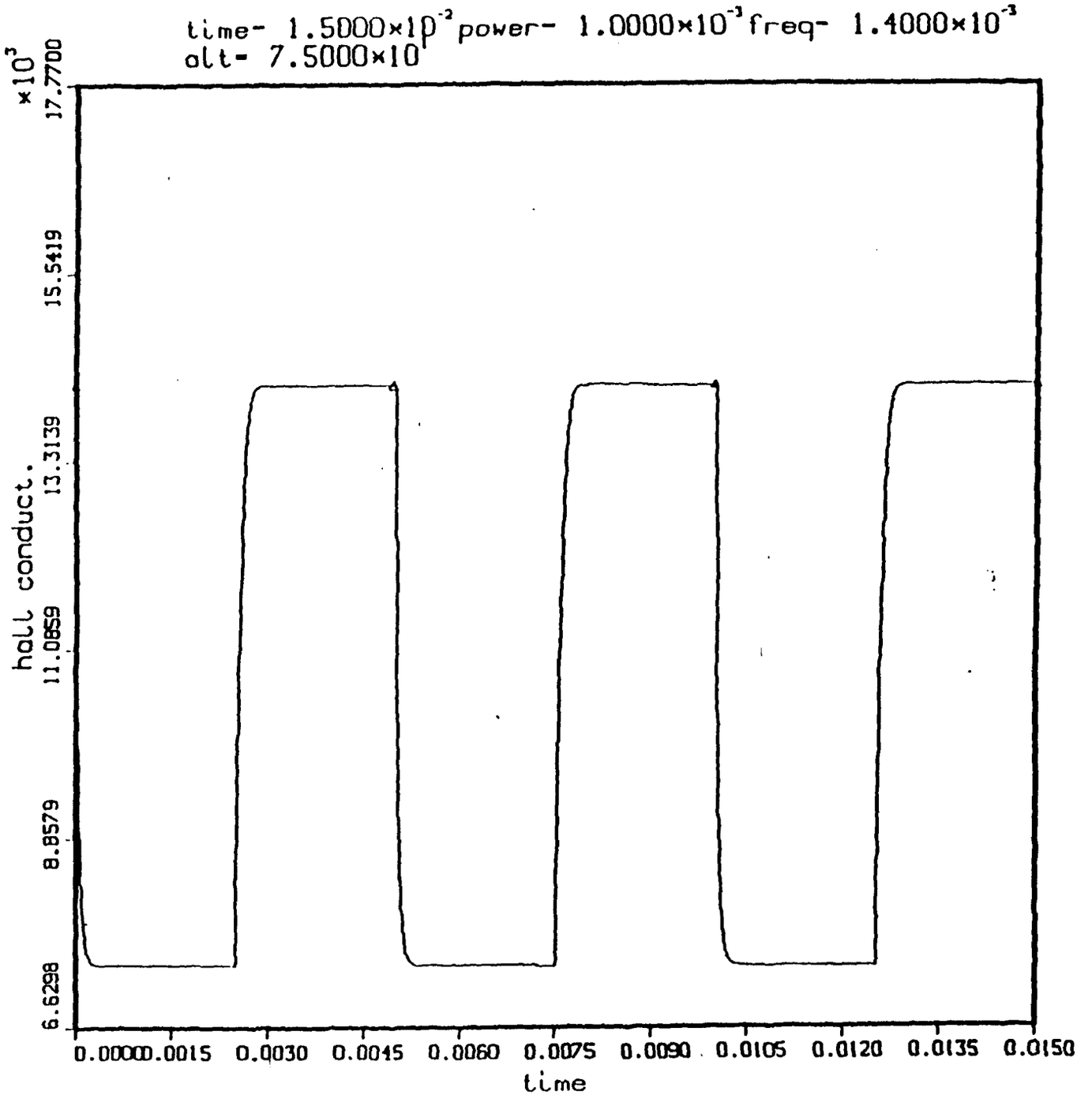
time- 1.5000×10^-2 power- 1.0000×10^-3 freq- 1.4000×10^-3
alt- 7.5000×10^3
×10^3
17.7700
15.5419
13.3139
11.0859
8.8579
6.6298
hall conduct.
0.0000 0.0015 0.0030 0.0045 0.0060 0.0075 0.0090 0.0105 0.0120 0.0135 0.0150
time

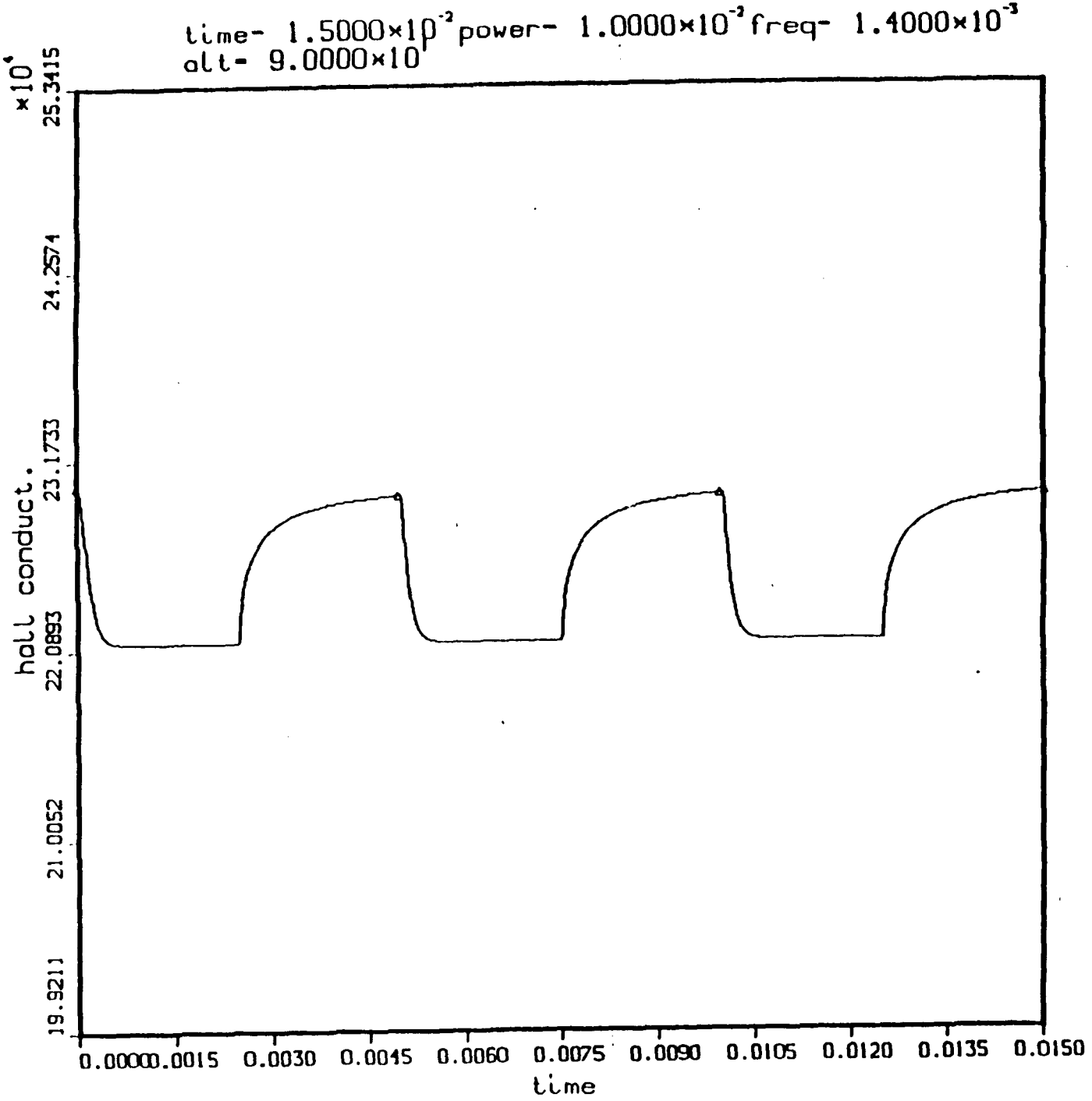
time- 1.5000×10⁻² power- 1.0000×10⁻³ freq- 1.4000×10⁻³
alt- 9.0000×10⁴
×10⁴
25.3415
24.2574
23.1733
22.0893
21.0052
19.9211
hall conduct.
0.0000 0.0015 0.0030 0.0045 0.0060 0.0075 0.0090 0.0105 0.0120 0.0135 0.0150
time

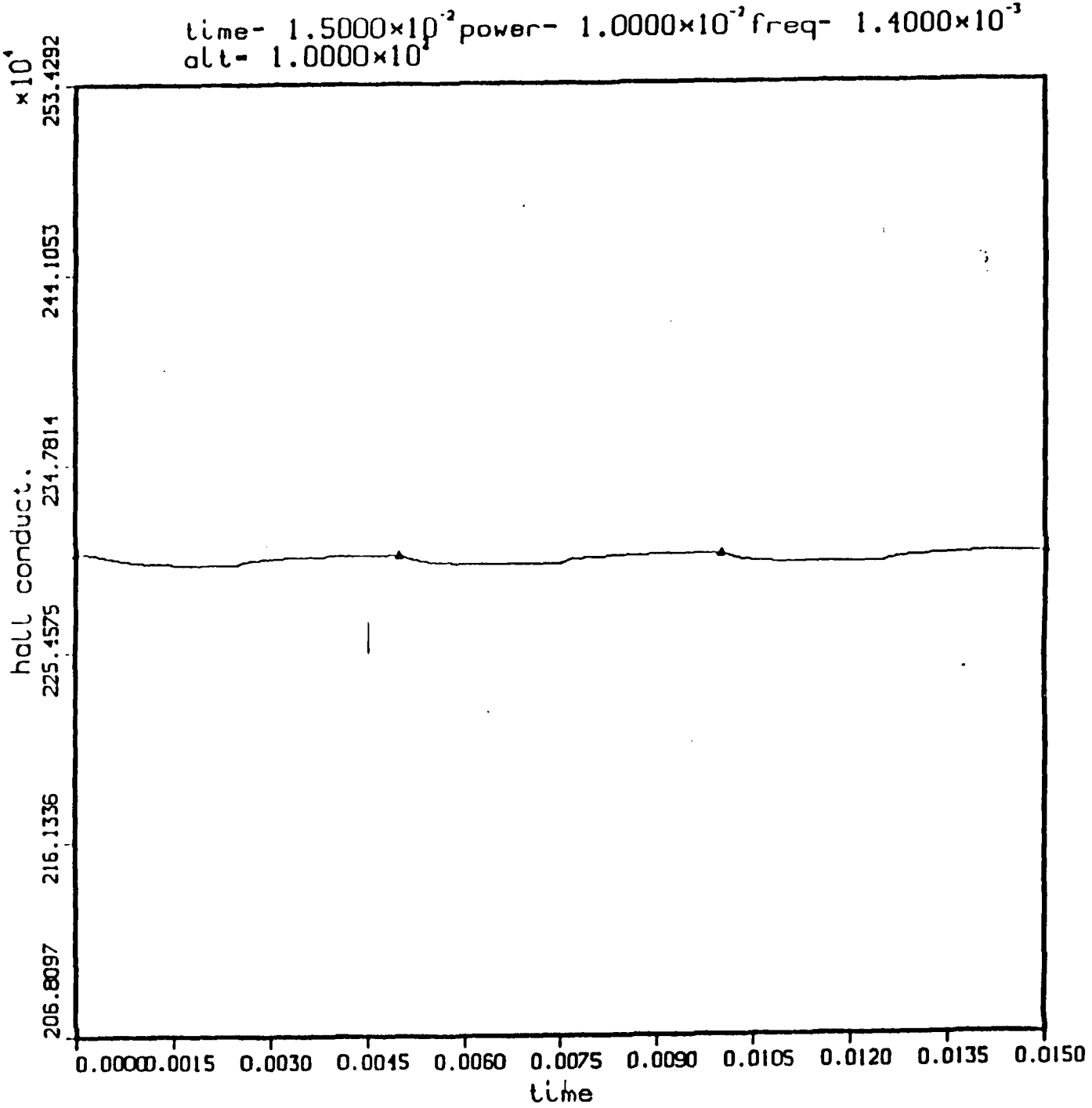
time- 1.5000×10⁻² power- 1.0000×10⁻³ freq- 1.4000×10⁻³
alt- 1.0000×10⁴
×10⁴
253.4292
244.1053
234.7814
225.4575
216.1336
206.8097
hall conduct.
0.0000 0.0015 0.0030 0.0045 0.0060 0.0075 0.0090 0.0105 0.0120 0.0135 0.0150
time

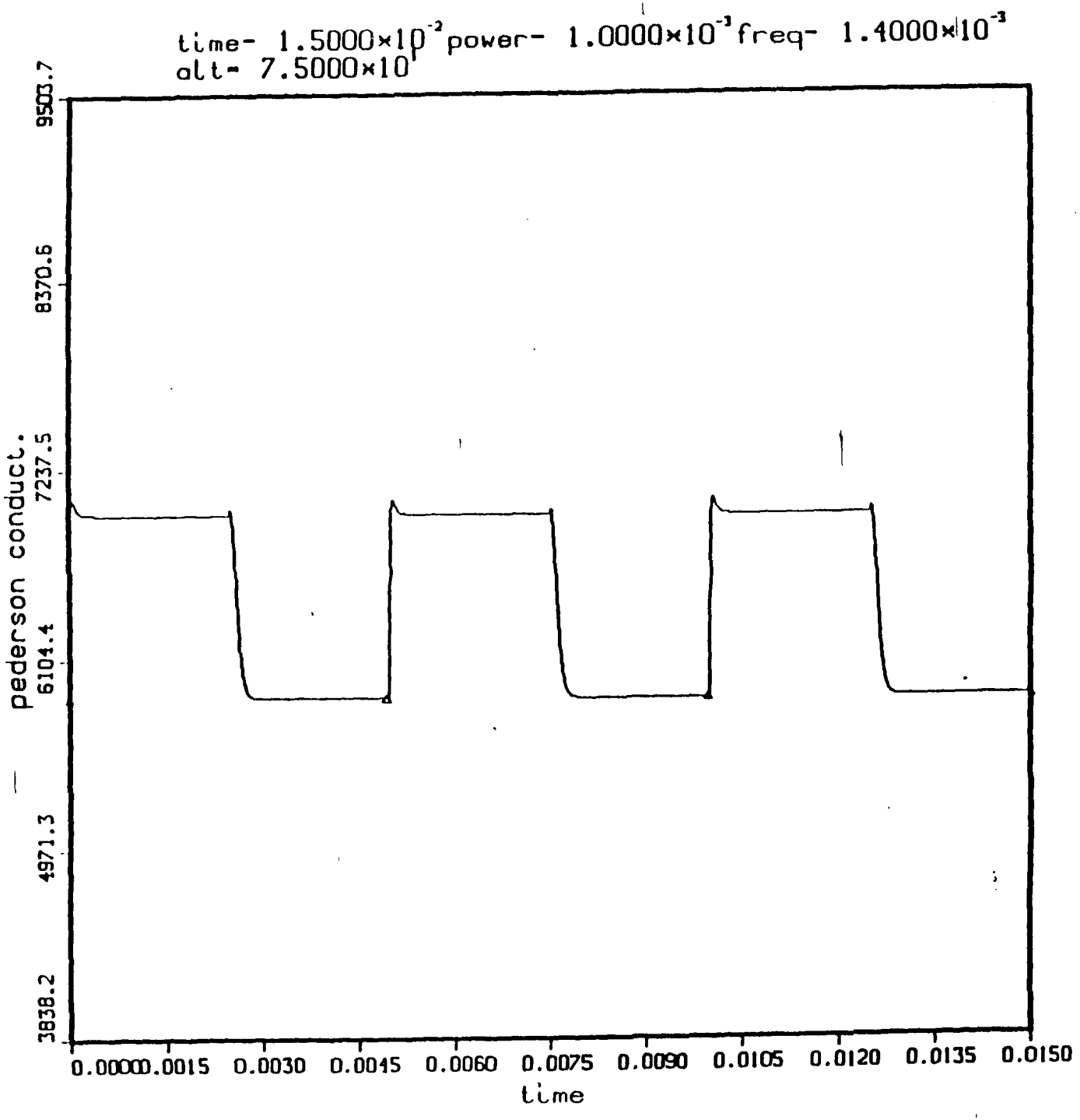
time- 1.5000×10^-2 power- 1.0000×10^-3 freq- 1.4000×10^-3
alt- 7.5000×10^
pederson conduct.
9503.7
8370.6
7237.5
6104.4
4971.3
3838.2
0.0000 0.0015 0.0030 0.0045 0.0060 0.0075 0.0090 0.0105 0.0120 0.0135 0.0150
time

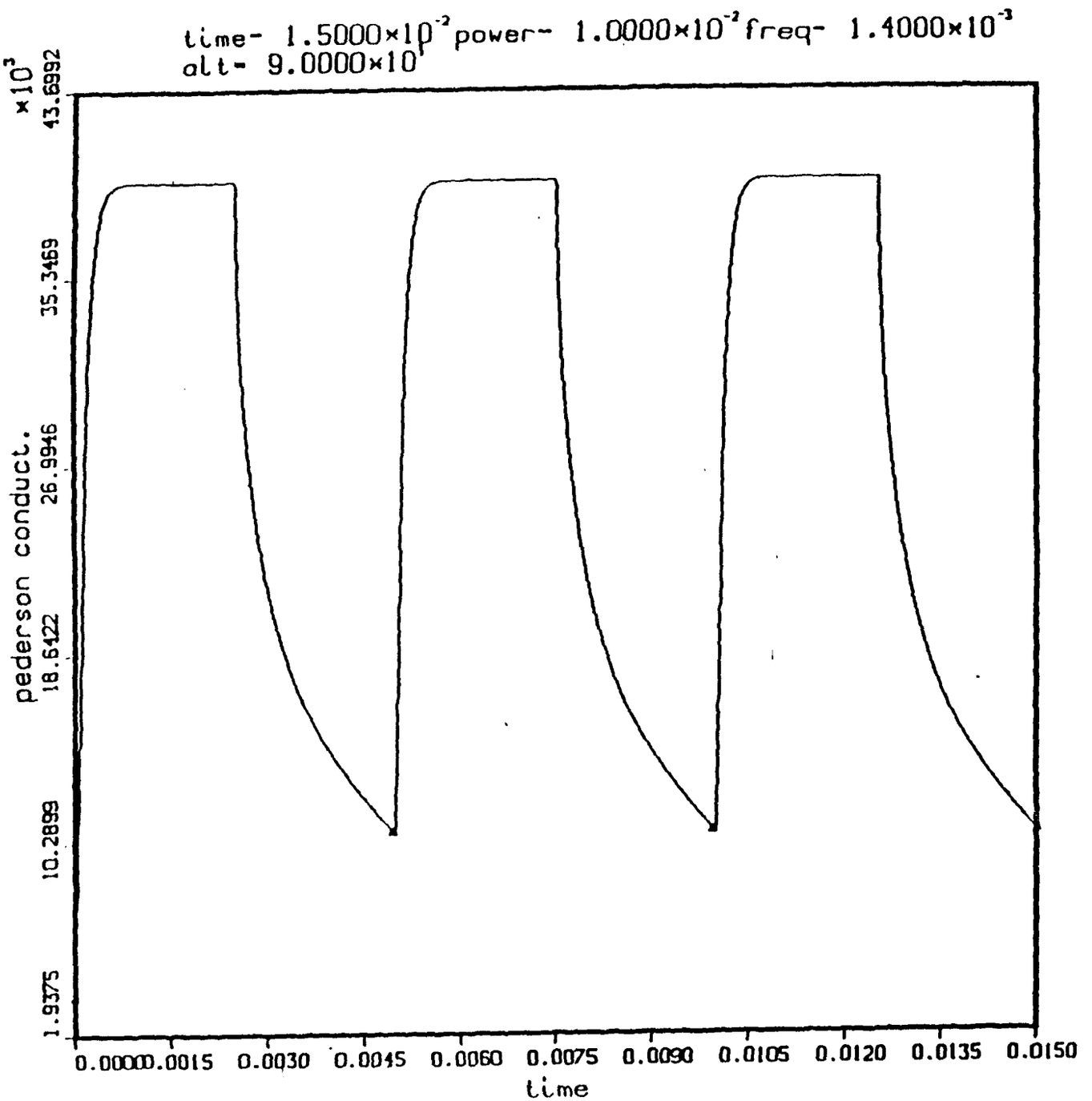
time- 1.5000×10⁻² power- 1.0000×10⁻² freq- 1.4000×10⁻³
alt- 9.0000×10
×10³
43.6992
35.3469
26.9946
18.6422
10.2899
1.9375
pederson conduct.
0.0000 0.0015 0.0030 0.0045 0.0060 0.0075 0.0090 0.0105 0.0120 0.0135 0.0150
time

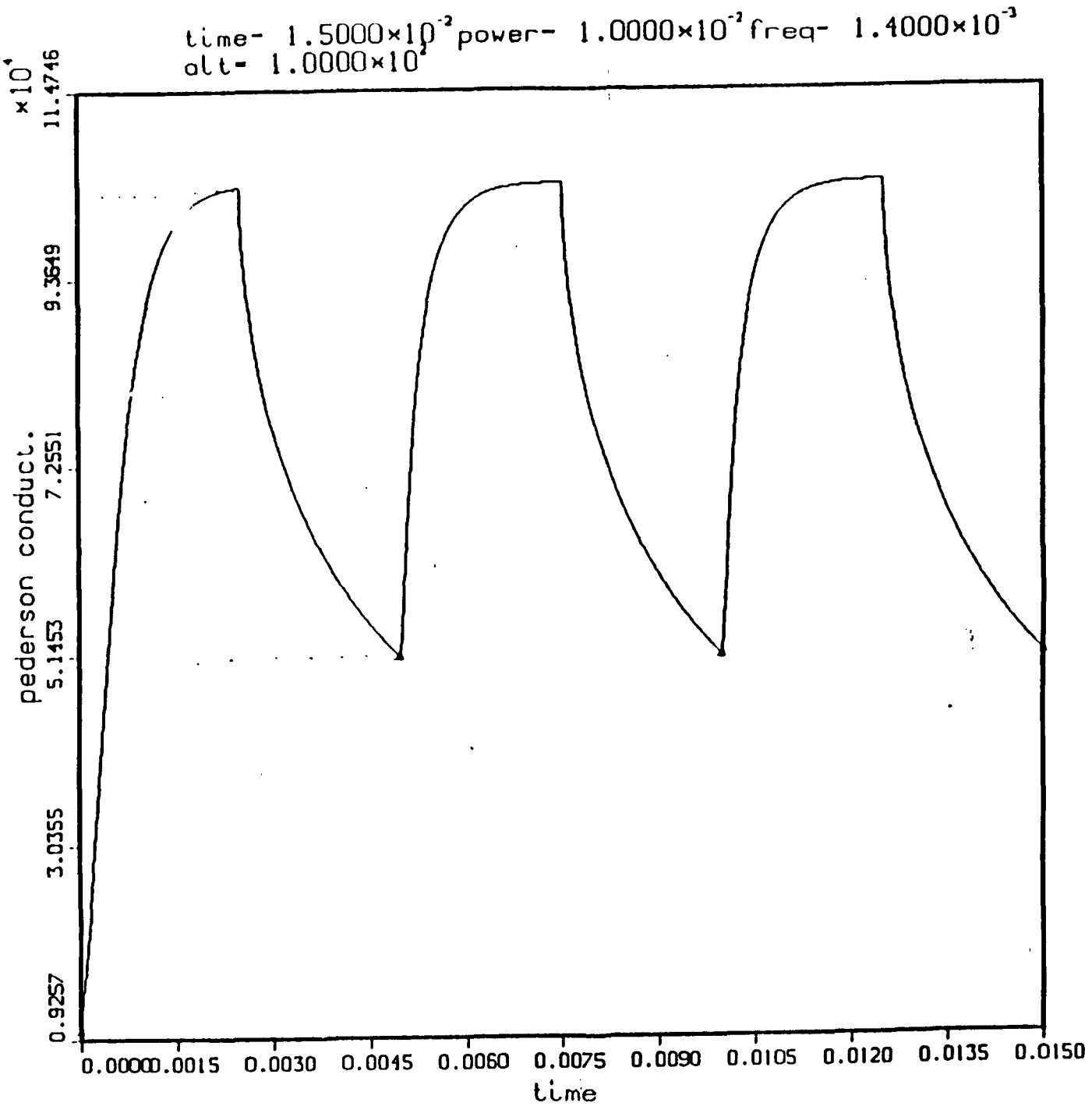
time- 1.5000×10⁻² power- 1.0000×10⁻² freq- 1.4000×10⁻³
alt- 1.0000×10²
×10⁴
11.4746
9.3649
7.2551
5.1453
3.0355
0.9257
pederson conduct.
0.0000 0.0015 0.0030 0.0045 0.0060 0.0075 0.0090 0.0105 0.0120 0.0135 0.0150
time

Fig.7

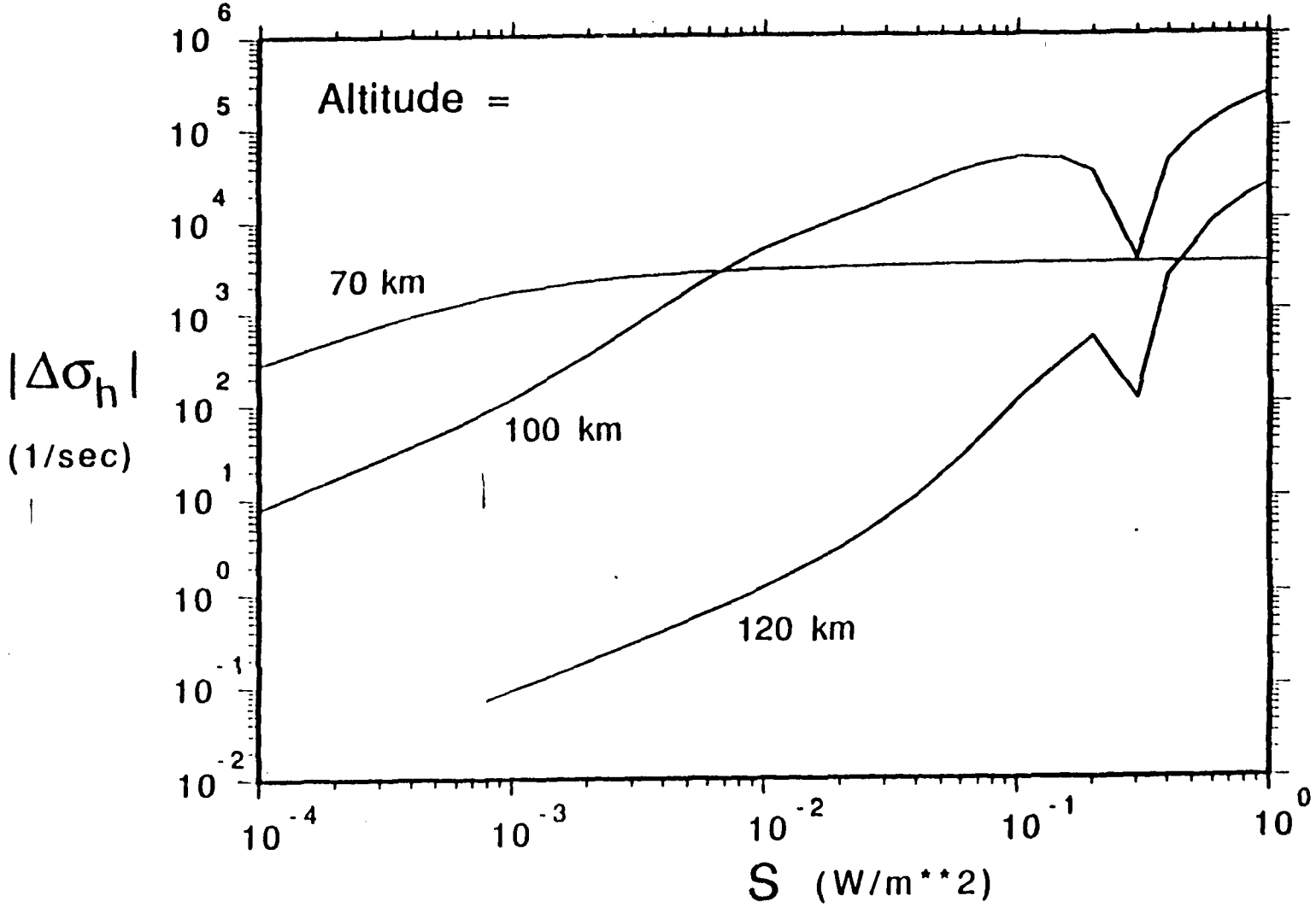
Altitude =
70 km
100 km
120 km
$|\Delta\sigma_h|$
(1/sec)
10^{6}
10^{5}
10^{4}
10^{3}
10^{2}
10^{1}
10^{0}
10^{-1}
10^{-2}
10^{-4}
10^{-3}
10^{-2}
10^{-1}
10^{0}
S (W/m**2)

Fig. 8

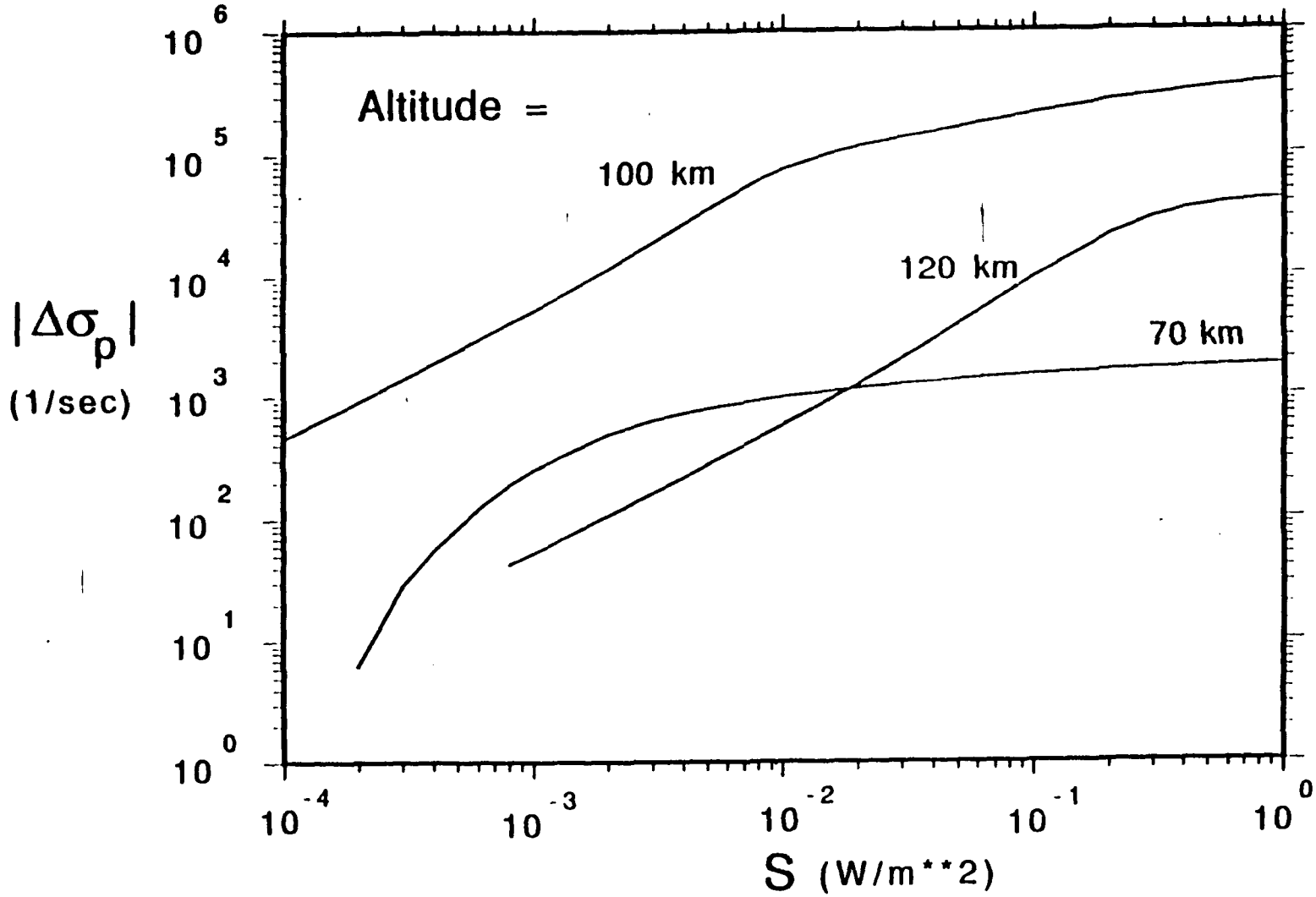
Altitude =
100 km
120 km
70 km
$|\Delta\sigma_p|$
(1/sec)
10^6
10^5
10^4
10^3
10^2
10^1
10^0
10^{-4}
10^{-3}
10^{-2}
10^{-1}
10^0
S (W/m**2)

ON THE EFFICIENT OPERATION OF A PLASMA ELF ANTENNA DRIVEN BY MODULATION OF IONOSPHERIC CURRENTS

K. Papadopoulos[1,2], A. S. Sharma[1] and C. L. Chang[2]

Department of Physics and Astronomy[1]
University of Maryland
College Park, Maryland 20742

and

Science Applications International Corporation[2]
McLean, Virginia 22102

March 1989

Abstract

Low frequency electromagnetic waves have been repeatedly generated when the flow of the polar electrojet current is modified by amplitude modulated heating from ground based HF transmitters. The modified current flow is equivalent to a low frequency plasma antenna known as Polar Electrojet (PEJ) antenna. Current results indicate that the radiation efficiency of the PEJ in the ELF range is by almost two orders of magnitude lower than the ground based ELF facility. It is shown that by matching the operation of the HF heater to the nonlinear response of the ionospheric plasma the efficiency of the PEJ can be increased by almost three orders of magnitude, thus making the PEJ a unique plasma device for studying many geophysical problems.

1. Introduction

The ionosphere is an active, strongly non-linear plasma medium containing free energy sources in the form of ambient currents and density gradients maintained by the input of the solar energy and the earth's rotation. Tapping these free energy sources is a long time goal of space plasma physics. The best known non-linear effect caused by the ionospheric plasma is the so called "Luxemburg effect" in which an amplitude modulated high power HF wave propagating through the ionosphere causes modulation transfer (cross modulation) to other waves passing through the same ionospheric medium. The ionospheric plasma, thus, acts as a non-linear frequency transformer.

Manifestations of the frequency transforming properties of the ionosphere have been confirmed in a series of experiments conducted during the past decade in the U.S.[1-5], the U.S.S.R.[6-11] and Norway[20-21]. The majority of the experiments demonstrated downconversion of HF power in the 1.5-10 MHz region to the VLF-ELF-ULF range (i.e. 10 kHz - 1 mHz). The most comprehensive experiments were performed with the "Heater" facility at Tromso, Norway operated by the Max Planck Institute[12-21]. A summary of the ground measurements of the magnetic field amplitude vs. frequency are shown in Fig. 1. An analysis of the "Heater" results[16,17] gave conversion efficiencies that varied from 10^{-5} at a frequency of 2 kHz to 10^{-8} at 200 Hz. Due to mechanical resonances of their diesel generators data were not taken in the 20 - 200 Hz regime. As seen from Fig. 1 the field amplitude of the 1-20 Hz waves is comparable to the 200 Hz amplitude. The technique of generating low frequency (Ω) waves from HF waves has been called "Combination Frequency Signal" (CFS) in the U.S.S.R. literature because the low frequency Ω could be selected by using two carrier HF waves with frequencies ω_1, ω_2 such that $\omega_1 - \omega_2 = \Omega$ instead of amplitude modulating the HF carrier. The "Heater" experimenters

have called the technique "Polar Electrojet" (PEJ) antenna. In this note we will use the name PEJ.

Electromagnetic (em) waves in the ELF-ULF (1-500 Hz) range are excellent diagnostic tools for geophysical probing due to their long underground penetration range. In fact low frequency em techniques are often used in oil exploration instead of seismic methods. Their large skin depth in sea water combined with their low attenuation rate (1 db/Mm) made ELF the major technique for communicating with submarines. Finally, waves in the ELF/ULF range are excellent diagnostic probes of the magnetosphere.

In attempting to generate ELF/ULF waves from the ground, one is faced with the problem of the long antenna. The free space wavelength of these waves is well in excess of 1000 km, requiring antennae of totally unrealistic lengths and accompanied by major ohmic losses. In the ELF range a Navy transmitter named ELF located in Michigan uses a frequency modulation centered at 76 Hz for almost worldwide communications with submarines. The transmitter has very low efficiency ($\lesssim 10^{-6}$) using over 2 MW of ground power to produce less than 2 W of radiated ELF power[22]. The PEJ antenna offers a simple solution to the size issue. Due, however, to the low efficiency (i.e. 10^{-3}) quoted above, it has been discarded as a potential ionospheric plasma device and is only thought of as a diagnostic tool of D-region ionospheric conditions. It is the purpose of this comment to demonstrate that, while the theoretical analysis of the PEJ efficiency is correct, the conclusion that PEJ constitutes an inefficient plasma device is incorrect. As will be shown below all the current PEJ antennae failed to match their operating procedures to the non-linear ionospheric plasma response. Adjusting their operation to match the ionopsheric plasma response results in an efficiency increase of almost

three orders of magnitude. As a result PEJ can serve as a unique ionospheric plasma device for studying a broad class of geophysical problems.

2. Physics of the PEJ Antenna

PEJ antennae have been studied systematically over the last ten years and a quantitative understanding of its physical principles well validated by experiments has emerged. The free energy source for its operation is the auroral current system. This system is powered by the flow of the solar wind plasma intercepting the polar magnetic field lines. The resultant emf drives currents along the magnetic field lines of the collisionless magnetospheric plasma (Birkeland currents) which close across the magnetic field lines at an altitude between 70-100 km in the collision dominated ionospheric plasma. This DC cross field current is called the auroral electrojet current and is confined around the auroral oval. The auroral oval is a ring around the geomagnetic pole, where the ionospheric conductivity is enhanced by the continuous precipitation of keV electrons. The total power of the electrojet current system is 10^5 MW and its ohmic dissipation results in an increase of the ionospheric temperature by 100° K. The electrojet current I_o is driven by an ionospheric electric field E_o which results from mapping along the magnetic field lines of the emf induced by the solar wind. The average observed value of E_o is about 25 mV/m, although at times it can reach 150 mV/m or be as low as 5-10 mV/m.

The PEJ antenna operates on the following principle. An HF transmitter amplitude modulated at a frequency Δ or, equivalently, two HF transmitters with frequencies $\omega_1 - \omega_2 = \Delta$ are incident on the lower ionosphere. Absorption of the HF power by the electrons that carry the electrojet currents results in local heating and modifies the temperature dependent value of the local

conductivity. For values of ω such that $\omega\tau_c \ll 1$, where τ_c is the electron cooling time, the conductivity modulation $\Delta\underline{\sigma}$ reflects the shape of the envelope imposed by the heater modulation (for the lower ionosphere $\tau_c \approx .1$ ms). The associated variation of the current density $\Delta\underline{j}$ is be given by

$$\Delta\underline{j} = \Delta\underline{\sigma} \cdot \underline{E}_o \tag{1}$$

This constitutes a primary source of modified current. For low frequencies the total current is divergence free. As a result a secondary current is set up consistent with the divergence free condition. The total current consists of the current I_1 flowing through the heated volume, a current I_2 flowing around the modified volume, and a field aligned current I_3 flowing through the magnetosphere to the conjugate ionosphere. The equivalent circuit shown in Fig. 2 was proposed by Stubbe, et al.[14] to describe the radiative loop. It is easy to see for the ELF range (10-500 MHz) the radiating current is essentially due to I_1 and only the $R_1, \mathcal{L}_1$ part of the circuit is active. For the ULF part (1-10 Hz) I_2 becomes relevant. For our frequency range, the field aligned currents do not respond ($\mathcal{L}_M = 50$ H) and the radiating currents are essentially due to the locally modified currents. We refer the reader interested in more details to Refs. 1, 12-20, 23.

For our purposes it is sufficient to consider that the ELF source in the ionopshere is an horizontal magnetic dipole source with moment

$$M = IL \tag{2}$$

where I is the value of the modulated current and L is the horizontal linear

size of the modified region. For the high latitude case

$$I = \Delta j \Delta z L = E_o \Delta\sigma \Delta z L \tag{3}$$

where Δj is the modified current density and Δz the vertical extent of the effective radiating layer. Combining (2) and (3), we find that

$$M = (E_o \Delta z) \Delta\sigma L^2. \tag{4}$$

The value of the ELF field on the ground depends on the value of M and the efficiency at which the field couples to the earth ionosphere waveguide (excitation factor). For the ELF range, the excitation factors varies as Ω. The ELF power on the ground would then be

$$P_{ELF} \sim (E_o \Delta z)^2 \, \varepsilon^2(\Omega) \Delta\sigma^2 L^4 \tag{5}$$

where $\varepsilon(\Omega)$ is the waveguide excitation factor[16,24-25]. The HF to ELF conversion efficiency η is then given by

$$\eta(\Omega) = \frac{P_{ELF}}{P_{HF}} = (E_o \Delta z)^2 \varepsilon^2(\Omega) \frac{\Delta\sigma^2 L^4}{P_{HF}} \tag{6}$$

where P_{HF} is the average ground based HF power. For the case analyzed by Barr and Stubbe[15,17], a square heating pulse was used. The value of P_{HF} was 1 MW and at the ELF generation region the value of $L \approx 10$ km corresponding to heater beam width of 7.5^o.

3. Summary of Current Observations

An analysis of the PEJ efficiency has been presented in Barr and Stubbe[16,17]. The purpose of our comment is to examine if the efficiency η can be increased over the one determined in the above reference by matching the operation characteristics of the HF heater to the nonlinear response of the ionosphere. We thus write Eq. (6) as

$$\eta = K \frac{\Delta\sigma^2 L^4}{P_{HF}} \tag{7}$$

where K is a constant that incorporates factors beyond our control (i.e. E_o, Δz, ε etc). Furthermore in order to be specific, we consider the particular case of 200 Hz, ($\Omega = 1.2 \times 10^3$ sec^{-1}).

The particular observations were made using an HF frequency f = 2.76 MHz, effective radiated power ERP = 150 MW, and antenna beam width $2\vartheta_o = 15^o$; the estimated ELF power was 6-8 mW, giving an efficiency of $\eta \approx 10^{-8}$. The observations were consistent with a modified Hall current density of 10^{-8} A/m^2, which corresponds to a conductivity modification of $\Delta\sigma_o = 4 \times 10^{-7}$ mhos at an altitude h_o = 78-80 km, and a value of E_o = 25 mV/m. The value of T_e corresponding to the modified conductivity was saturated at $T_e \approx 2000\ ^oK$. The power density at 78-80 km was of the order of 2 mW/m^2. For the ELF/ULF frequency range of interest, the observed ELF power was consistent with a horizontal dipole in the ionosphere with magnetic moment

$$M = 3.5 \times 10^4 \text{ A-m}.$$

As is well known from the work of Galejs[24,25] horizontal dipoles are inefficient exciters of the earth ionosphere waveguide at 100-200 Hz, having

excitation efficiency ε of the order of 10^{-2} compared to that of comparable ground based electric dipole. Notice that ground based ELF sources are also very inefficient with typical efficiencies ε of the order of 10^{-3} or less for horizontal magnetic dipoles. From Eq. (7), the measured efficiency and the values discussed above, we can rewrite Eq. (7) as

$$\eta = 10^{-8} \left(\frac{\Delta\sigma}{\Delta\sigma_o}\right)^2 \left(\frac{P_{HF,o}}{P_{HF}}\right) \left(\frac{L}{L_o}\right)^4 \tag{8}$$

where $\Delta\sigma_o = 4 \times 10^{-7}$ mhos, $L_o = h_o \tan \theta_o \approx 10$ km, and $P_{HF,o} = 1$ MW are the values of the reference case. The on-off heater time τ_{H_o} is half of the wave period of 200 Hz. Furthermore, we should remember that the $\Delta\sigma_o$ modification over an L_o^2 area was accomplished with an incident power flux $S_o = 2$ mW/m^2 at h_o.

4. Modulated HF Heating and Associated Conductivity Modulation

The modulated heating of the ionosphere by an X-mode HF field of frequency ω and peak amplitude E_o is given by

$$\frac{3}{2}\frac{dT_e}{dt} = 2\tilde{\varepsilon}\,\nu_{en}\frac{1}{1+\nu_{en}^2/\omega_o^2} - \nu_{er}(T_e - T_o) - \nu_{ev}\exp\left(f\frac{T_e - 2000}{2000\,T_e}\right) \tag{9}$$

where $\tilde{\varepsilon}$ is the quiver energy defined as

$$\tilde{\varepsilon} = \frac{1}{2}m\frac{e^2E_o^2}{m^2\omega_o^2} \tag{10}$$

and ω_o is the effective frequency

$$\omega_o = \omega - \omega_e \tag{11}$$

Also Ω_e is the electron cyclotron frequency, ν_{en} is the electron neutral collision frequency for momentum transfer, ν_{er} the rate of inelastic electron neutral collisions resulting in excitation of the rotational levels of N_2, the term with ν_{ev} is the vibrational loss and $T_o = 100^oK$ is the ambient temperature of the neutrals. For the range of electron energies of interest here

$$\nu_{en} = 2.3 \times 10^{-9} N \left(\frac{T_e}{100^oK}\right) \equiv \nu_o \left(\frac{T_e}{100^oK}\right) \tag{12a}$$

$$\nu_{er} = 3.2 \times 10^{-11} N \left(\frac{T_e}{100^oK}\right)^{-1/2} \equiv \nu_R \left(\frac{T_e}{100^oK}\right)^{-1/2} \tag{12b}$$

$$\nu_{ev} = 3.5 \times 10^{-8} N \equiv 1068\ \nu_R.$$

where N is the number density of the neutrals. Defining

$$y \equiv T_e/T_o, \quad \tau \equiv \nu_R t$$

$$\tilde{K} \equiv 2 \left(\frac{\tilde{\varepsilon}}{T_o}\right) \frac{\nu_o}{\nu_R}, \quad \alpha^2 \equiv \nu_o^2/\omega_o^2 \tag{13}$$

we can cast Eq. (9) in a dimensionless form as

$$\frac{3}{2}\frac{dv}{d\tau} = K \frac{v}{1 + \alpha^2 y^2} - \frac{v - 1}{\sqrt{y}} - 10.68 \exp\left[f \frac{y - 20}{y}\right] \tag{14}$$

where $f = 5.3 + 3.755 \tanh[0.11\ (y - 18)]$. The modification of the temperature results in changes in the conductivity of the medium. For the ionosphere the conductivity tensor $\underline{\underline{\sigma}}$ transverse to the magnetic field is given by

$$\underline{\sigma} = \begin{pmatrix} \sigma_p & \sigma_H \\ -\sigma_H & \sigma_p \end{pmatrix} \tag{15}$$

were σ_p is the Pedersen conductivity, i.e. the conductivity along the electric field $\underline{E}_o$, and σ_H is the Hall conductivity. In our dimensionless units they are given by

$$\sigma_p = \Gamma \frac{\beta\nu}{1 + \beta^2 y^2} \tag{16a}$$

$$\sigma_H = \Gamma \frac{1}{1 + \beta^2 y^2} \tag{16b}$$

where ω_e is the plasma frequency and

$$\beta = \nu_o/\Omega_e = 3.8 \times 10^{-2} \left(\frac{N}{10^{15}}\right) \tag{17}$$

$$\Gamma = \frac{\omega_e}{4\pi} \frac{\omega_e}{\nu_R} \tag{18}$$

From the above equations we note that the values of the dimensionless quantities α and β, Γ and τ are altitude dependent, while the value of K depends only on the incident HF power density. Equations (9-18) can and have been solved numerically under several conditions. Important insight is provided by considering some limiting cases.

(i) The regime of interest corresponds to $\beta \ll 1$, i.e. neutral densities $N \ll 10^{16}$ #/cm^3, so that for $y = 1$, $\sigma_p/\sigma_H \approx \beta \ll 1$. Furthermore heating always decreases σ_H forcing the Hall current to flow outside the heated volume. The Pederson conductivity has a different dependence on y. For values of $\beta y \leq 1$, σ_p increases with y, producing

currents in antiphase with the Hall currents, while for $\alpha y > 1$ it decreases with y and the currents are in phase with the Hall currents. Notice that since the ambient electrojet current flows at an angle

$$\delta = \tan^{-1} 1/\beta$$

with respect to the ambient $\underline{E}_o$, it is a Hall current. For $\alpha y = 1$ it flows at a 45^o angle with respect to $\underline{E}_o$. This implies that the induced polarization electric field $\underline{E}_p$ has the same value as $\underline{E}_o$. Finally for $\alpha y >> 1$ the Pedersen current becomes dominant.

(ii) Inspection of the heating equation (Eq. 14) shows the presence of a strong barrier for values of $y \approx 20-30$ due to the third term on the r.h.s. of Eq. (14). This term is due to the high value of the inelastic electron-N_2 cross section for vibrational excitation. It implies a heavy energy penalty in achieving temperatures past $y \approx 20$.

(iii) Equation (14) shows that for values of $\alpha y < 1$ and $y < 20$ the heating rate is exponential with τ while the cooling rate which in this regime is due to rotational energy transfer has a weaker (τ^2) dependence.

These observations will be utilized in the next section in our attempt to optimize the efficiency of the PEJ antenna.

5. Efficient Operation of the PEJ Antenna

In order to be concrete we consider the benchmark case discussed in Section 3. Following Barr and Stubbe[16-17] we assume that the source height is at 78-80 km, which corresponds to a neutral density $N \approx 2 \times 10^{14}$ #/cm^3. For this value of density $\alpha = .05$ and $\beta = .05$. The value of the quiver energy

in ^{o}K is given by

$$\tilde{\varepsilon} = 22 \left(\frac{S}{mW/m^2}\right) \left(\frac{MHz}{f_o}\right)^2 {}^{o}K \qquad (19)$$

For $f = 2.76$ MHz, $\Omega_e/2\pi = 1.35$ MHz, ERP of 150 MW which corresponds to 2 mW/m^2 and $T_o \approx 100\ {}^{o}K$, $\tilde{\varepsilon}/T_o \approx .22$. Using Eq. (13), we find that $K = 30$. Finally for ELF frequency of 200 Hz the dimensionless ELF time is $\tau_{ELF} = 34$. Figure 3a shows the waveform of y for a square wave heater operation with period half the period of the ELF wave. It clearly demonstrates the inefficient fashion in which the heater power is utilized. First, more than 95% of the power utilized to maintain the temperature at its saturated value, while the absorbed energy is transferred to the excitation of N_2 vibrations which, of course, do not contribute to the conductivity modification. Second, we are overheating the plasma. There is little, if anything, to gain by heating past the value of $y = 1/\beta$, as is obvious from Eqs. (16). Figure 3a, however, also suggests the operating procedure which can lead to improved efficiency, which is discussed next.

Let us consider a facility with the same average power as the Tromso "Heater" facility but equiped with the capability to scan fast over an area up to a cone of 37.5^{o} (Fig. 4). The ratio of this area to that modified by the 7.5^{o} half-beamwidth HF antenna is

$$\xi = \left(\frac{\tan 45^{o}}{\tan 7.5^{o}}\right)^2 \approx 60$$

If using the same average power as the "Heater" facility we could modify the conductivity of the accessible area A at the desired ELF frequency the efficiency according to Eq. (8), will increase by a factor ξ^2 which corresponds to 3.3×10^3. It will, however, be reduced by the relative

modification of conductivity. The quadratic dependence ξ^2 on the area is a consequence of the fact that a larger area produces a simultaneous increase in total current as well as flux. Techniques by which this can be accomplished are demonstrated below.

We next compute the power enhancement over the standard case that can be accomplished by dividing the area A into a number of smaller areas A_o and sweeping the transmitter so that during the half cycle $\tau_{ELF/2} = 17$ it stays on each spot only A_o/A of the time. The expected enhancement R of the ELF power over that of the standard case is given by the ratio of the efficiencies obtained from Eq. (7) for the two cases. The antenna with beamwidth of 15° irradiates each area A_o for the duration τ_{ON} with a revisit time τ_{OFF} and so the total heated area is $A = (\tau_{ON} + \tau_{OFF})\, A_o$. Further if the antenna gain K is reduced from the value of 30, the heated area is increased by the factor 30/K. Thus for the same power P_{HF}, we get

$$R = \left(\frac{30}{K}\right)^2 \left(\frac{\tau_{ON} + \tau_{OFF}}{\tau_{ON}}\right)^2 \left(\frac{\overline{\Delta\sigma}}{\Delta\sigma}\right)^2 \qquad (20)$$

where $\overline{\Delta\sigma}$ is the final conductivity modification averaged over all the spots and $\Delta\sigma = .72$ is the conductivity modification of the standard case (Fig. 3a). The heated area can be increased by choosing small τ_{ON} and τ_{OFF}, whose limits are set by the heating and cooling timescales. The heating timescale is given by Eq. (14), which for $y \gtrsim 1$ yields $y = y(\tau = 0) \exp(\tau/\tau_o)$ with $\tau_o = 3/2K$. To achieve a 20% rise in the temperature in one heating cycle we need $\tau_{ON} = .2\, \tau_o$, which is 0.01 for K = 30. A value τ_{ON} smaller than this will lead to a weak heating. Since the idea of the proposed scheme is to avoid the strong vibrational losses by keeping $T_e \lesssim 2000°K$, the relevant cooling time is that due to the rotational losses. In the normalized units this has a value

~ 1 and so τ_{OFF} should be $\lesssim$ 1 to prevent excessive cooling. With these considerations different cases are examined as follows.

We first take the case where the full power (K = 30) of the antenna irradiates each area A_o over a time τ_{ON} = .02 with a revisit time τ_{OFF}. The procedure was repeated three times till τ = 17. The enhancements for different values of τ_{OFF} are given in Table 1a, which shows that increasing the total area, i.e., the ratio τ_{OFF}/τ_{ON} results in an increase of R. This is however accompanied by a decrease in $\overline{\Delta\sigma}$ because the distribution of the power into a much larger area limits the heating. This latter effect overcomes the advantage of the increase in area and beyond τ_{OFF}/τ_{ON} = 40 the value of R decreases. There is thus a balance between these two effects that gives an optimum value of τ_{OFF} for a given τ_{ON}. The value of $\overline{\Delta\sigma}$ is the average obtained in the last $(\tau_{ON} + \tau_{OFF})$ before the power was turned off at τ = 17. The peak enhancement for this case was 455 corresponding to τ_{OFF}/τ_{ON} = 40 and the heating profile of the temperature of a typical spot is shown in Fig. 3b. With the same K value and different values of τ_{ON}, the enhancement R will be optimum at different values of τ_{OFF}/τ_{ON}. The reason for the relatively low enhancement compared to the theoretical maximum of 3 x 10^3, is due to the reduction in the conductivity modulation, giving a low value for the $(\overline{\Delta\sigma}/\Delta\sigma)^2$ factor.

Figures 3c and d indicate the results of a trade off study in which the antenna gain was reduced by a factors of 2 and 3 so that the area of each spot was $2A_o$ and $3A_o$ respectively. This, of course, results in a reduction of the corresponding value of K. In the case presented in Fig. 3c, the antenna gain is reduced by a factor of 2 so that K = 15 and the area of each spot is $2A_o$. This requires a longer τ_{ON} to achieve significant heating of a spot and also the total number of spots that can be covered is reduced (Table 1b). Unlike

Table 1a, which shows the enhancement for a wide range of τ_{OFF}/τ_{ON}, Table 1b shows the sensitive dependence of R on τ_{OFF}/τ_{ON} around the case of maximum enhancement. Figure 3d shows the case with K = 10 where the maximum enhancement 524 in efficiency was achieved. In this case only 15 spots each with area $3A_o$ were heated. In all the three cases K = 10, 15 and 30 shown in Figs. 3b,c and d enhancements ~ 500 are easily achieved and the waveforms of y in these cases are similar to each other.

6. Summary and Conclusions

In this comment we have demonstrated that operating the PEJ antenna in a mode consistent with the nonlinear properties of the ionospheric plasma can increase the HF to ELF conversion efficiency by a factor of 500 efficiently than the current facility, without any increase in the ground HF power or the antenna gain. Furthermore, this is close to one order of magnitude more efficient than the Navy ELF facility. Under strong auroral conditions the efficiency can increase dramatically. Comparable or even higher efficiencies can be achieved for other ELF frequencies. To summarize, we believe that the current experimental evidence indicates that the PEJ antenna constitutes the first practical device based on tapping the free energy of the ionospheric plasma. Adjusting its operation to the high efficiency mode, requires only phase shifting or other electronic means for scanning the HF antenna at a relatively high speed. With this complement PEJ can be a unique geophysical exploration tool.

Acknowledgements

The work was supported by ONR N00014 86 K2005 (K.P., C.C.) and by APTI-DM-88-C-05 (A.S.). Discussions with Drs. D. Brandt and T. Ferraro are greatfully acknowledged.

References

1. C.L. Chang, V. Tripathi, K. Papadopoulos, J. Fedder, P.J. Palmadesso, and S.L. Ossakow, Effect of the Ionosphere on Radiowave Systems, edited by J.M. Goodman, p. 91, U.S. Government Printing Office, Washington, DC, 1981.

2. A.J. Ferraro, H.S. Lee, R. Allshouse, K. Carroll, A.A. Tomko, F.J. Kelly, and R.G. Joiner, J. Atmos. Terr. Phys., 44, 1113, 1982.

3. A.A. Tomko, Rpt. PSU-IRL-SCI-470, Ionospheric Research Laboratory, Pennsylvania State University, University Park, PA, 1981.

4. A.J. Ferraro, Radio Sci., 24, 1989, (in press).

5. A.J. Ferraro, H.S. Lee, T.W. Collins,M. Baker, D. Nermer, F.M. Zain, and P.J. Li, Radio Sci., 24, 1989 (in press).

6. G.G. Getmantsev, N.A. Zuikov, D.S. Kotik, L.F. Mironenko, N.A. Mityakov, V.O. Rapoport, Yu. A. Sazonov, V. Yu, Trakhtengerts, and V. Ya. Eidman, JETP Lett., 20, 229, 1974.

7. D.S. Kotik and V. Yu. Trakhtengerts, JETP Lett., 21, 51, 1975.

8. N.S. Belustin and S.V. Polyakkov, Radiophys. Quantum Electron, 20, 57, 1977.

9. A.V. Gurevich, Nonlinear Phenomena in the Ionosphere, Springer-Verlag, New York, 1978.

10. M.V. Migulin and A.V. Gurevich, J. of Atm. and Terr. Phys., 47, 1181, 1985.

11. P.P. Belyaev, D.S. Kotik, S.N. Mityakov, S.V. Polyakov, V.O. Rapoport and V. Yu. Trakhtengerts, Radiophysics, 30, 248, 1987.

12. P. Stubbe and H, Kopka, J. Geophys. Res., 82, 2319, 1977.

13. P. Stubbe, H. Kopka, and R.L. Dowden, J. Geophys. Res., 86, 9073, 1981.

14. P. Stubbe, H. Kopka, H. Lauche, M.T. Rietveld, A. Brekke, O. Holt, and R.L. Dowden, J. Atmos. Terr. Phys., 44, 1025, 1982.

15. P. Stubbe, H. Kopka, M.T. Reitveld, and R.L. Dowden, J. Atmos. Terr. Phys., 44, 1123, 1982.

16. R. Barr and P. Stubbe, J. Atmos. Terr. Phys., 46, 315, 1984.

17. R. Barr and P. Stubbe, Radio Sci., 19, 1111, 1984.

18. R. Barr, M.T. Rietveld, P. Stubbe, and H. Kopka, J. Geophys. Res., 90, 2861, 1985.

19. H.G. James, J. Atm. Terr. Phys., 47, 1129, 1985.

20. H.G. James, R.L. Dowden, M.T. Rietveld, P. Stubbe and H. Kopka, J. Geophys. Res., 89, 1655, 1984.

21. P. Stubbe, private communication.

22. P.B. Bannister, J. Oceanic Eng. OE-9, 179, 1984.

23. V.K. Tripathi, C.L. Chang, and K. Papadopoulos, Radio Sci., 17, 1321, 1982.

24. J. Galejs, J. Geophys. Res., 73, 339, 1968.

25. J. Galejs, Radio Sci., 6, 41, 1971.

Figure Captions

Figure 1 A typical magnetic field amplitude vs. frequency measured on ground at the Max Planck Tromso "Heater" facility (Stubbe)[21].

Figure 2 Equivalent circuit system to describe the modulation current. Current I_1 is flowing through the modified volume, I_2 around the modified volume, I_M along the magnetic field lines through the conjugate ionosphere, and I_z is the current flowing in the wave (Stubbe et al.[15]).

Figure 3 The ionospheric electron temperature (in units of 100 ^{o}K) under various scenarios of heating the PEJ and producing ELF. a: All power delivered to an area corresponding to a beam half-width of 7.5^{o}. b-d: The power is delivered over a wider area consisting of many spots. R is the enhancement of the ELF power over that of the case a.

Figure 4 Scheme for the enhancement of ELF power by sweeping over an area within the beaming angle of 37.5^{o}.

Figure Caption

Table 1 Enhancement of the ELF generation for different antenna gains (K) and τ_{OFF}/τ_{ON} ratios. a. The enhancement R for K = 30 and a wide range of values of τ_{OFF}/τ_{ON}. The gain from increasing τ_{OFF}/τ_{ON} is offset by the accompanying decrease in $\bar{\alpha}$, giving the peak value of R = 455. b. For half the full antenna gain (K = 15) the variation of the enhancement around the peak value (R = 458) is shown.

Table 1

a. K = 30 and τ_{ON} = 0.02

τ_{OFF}/τ_{ON}	$\Delta\sigma$	R
20	.49	204
30	.44	353
35	.41	417
40	.37	455
45	.31	396
50	.21	224

b. K = 15 and τ_{ON} = .03

16	.42	399
17	.41	424
18	.40	445
19	.38	458
20	.36	452
21	.34	439
22	.31	397

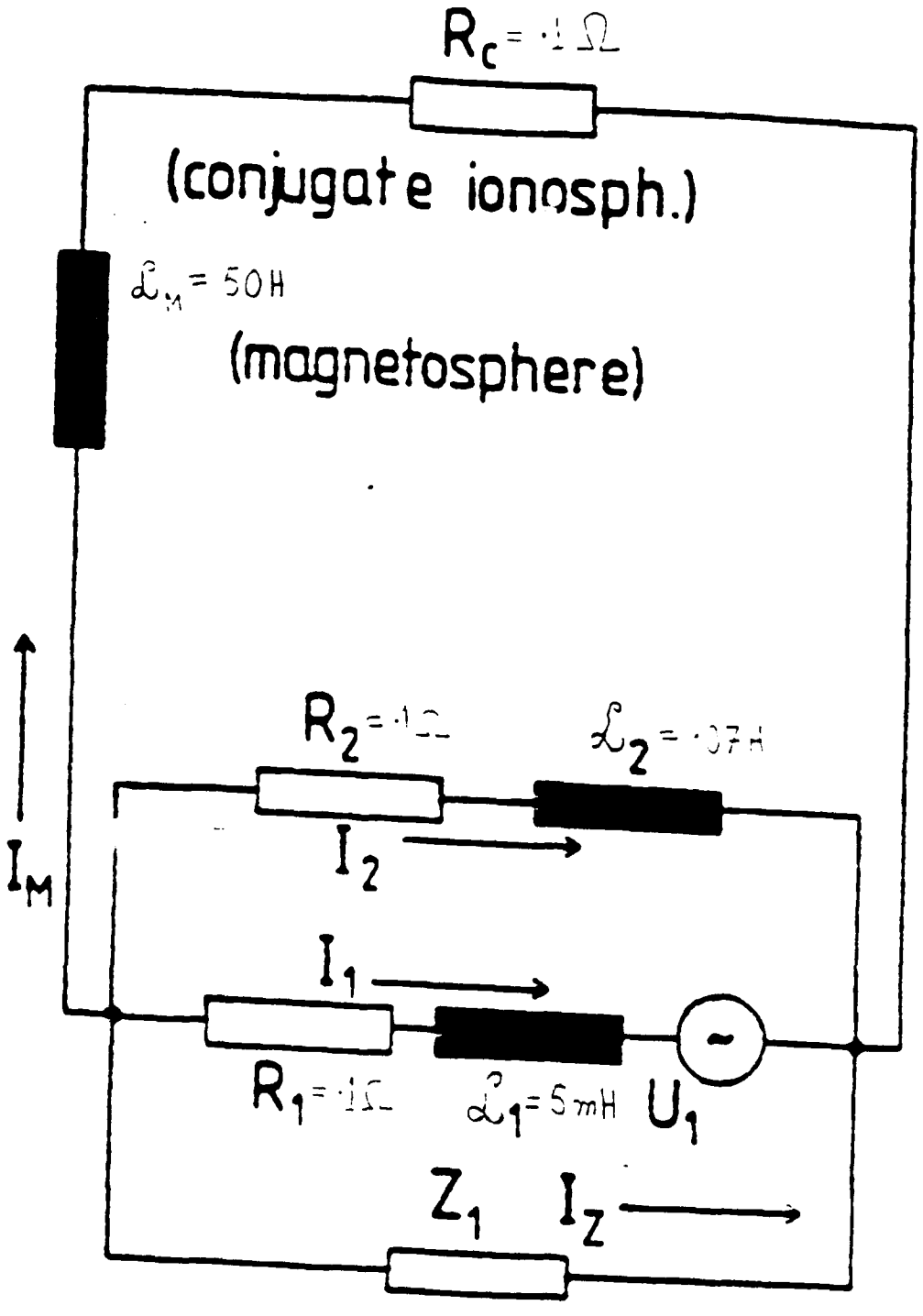
$R_c = \cdot 1\ \Omega$
(conjugate ionosph.)
$\mathcal{L}_M = 50H$
(magnetosphere)
I_M
$R_2 = \cdot 1\Omega$
$\mathcal{L}_2 = \cdot 07H$
I_2
I_1
$R_1 = \cdot 1\Omega$
$\mathcal{L}_1 = 5mH$
U_1
Z_1
I_Z
(wave impedance)

a.
K = 30

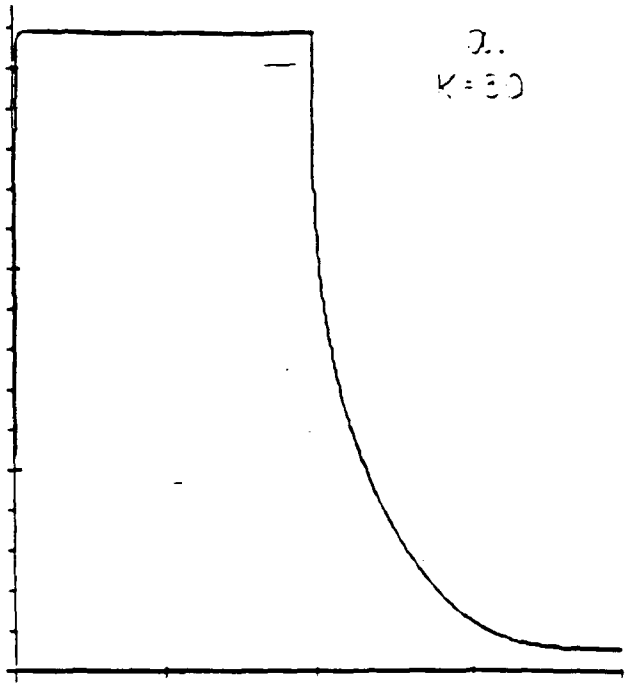

b.
K = 30, τ_{on} = ·0… & τ_{off} = ·2
R = 55

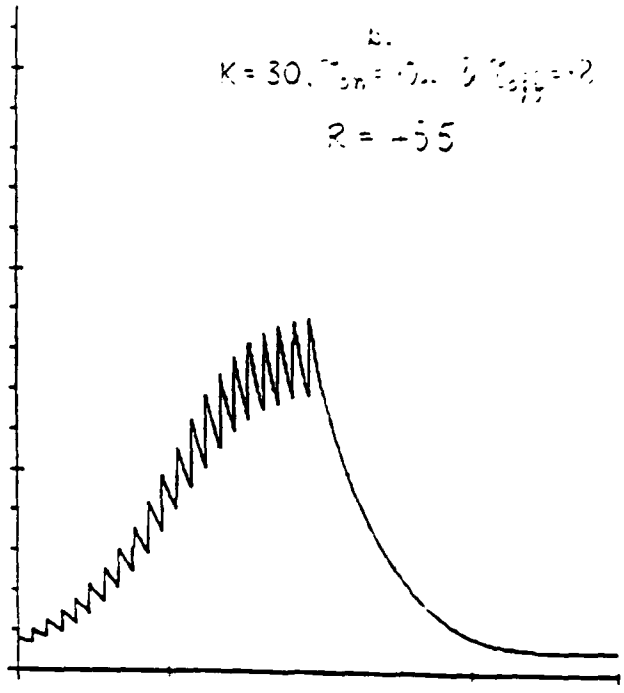

c.
K = 15, τ_{on} = ·03 & τ_{off} = ·57
R = 458

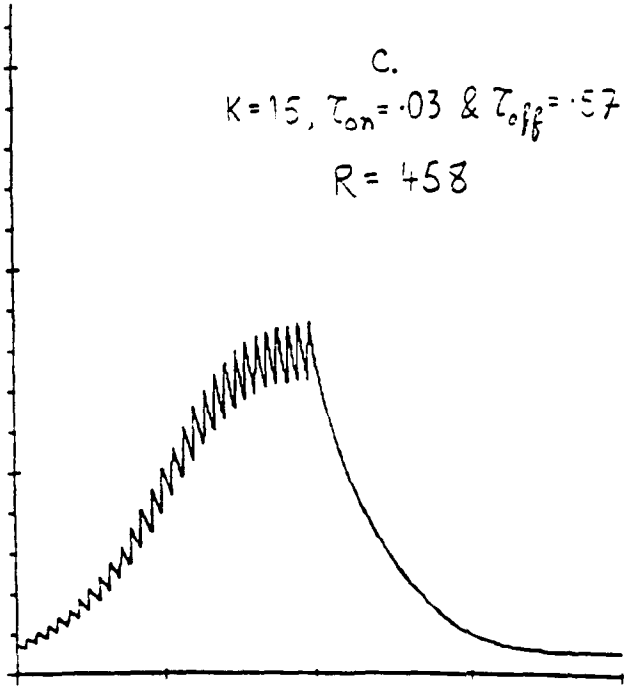

d.
K = 10, τ_{on} = ·06 & τ_{off} = ·84
R = 524

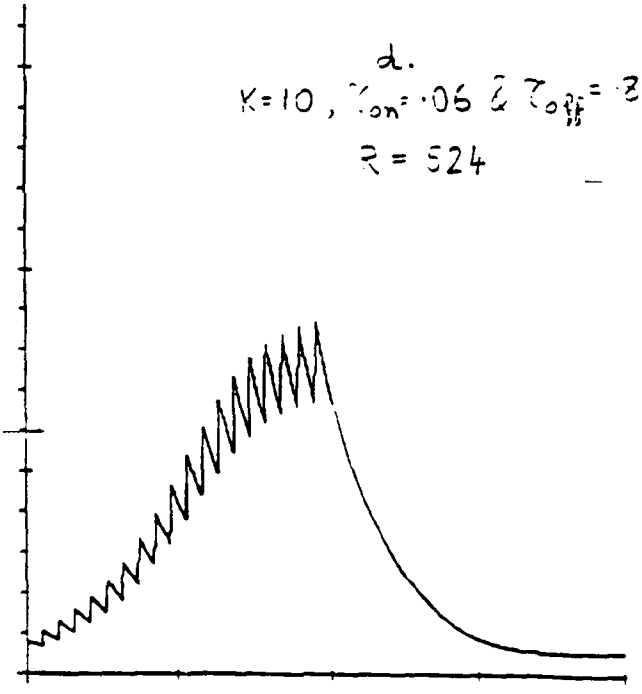

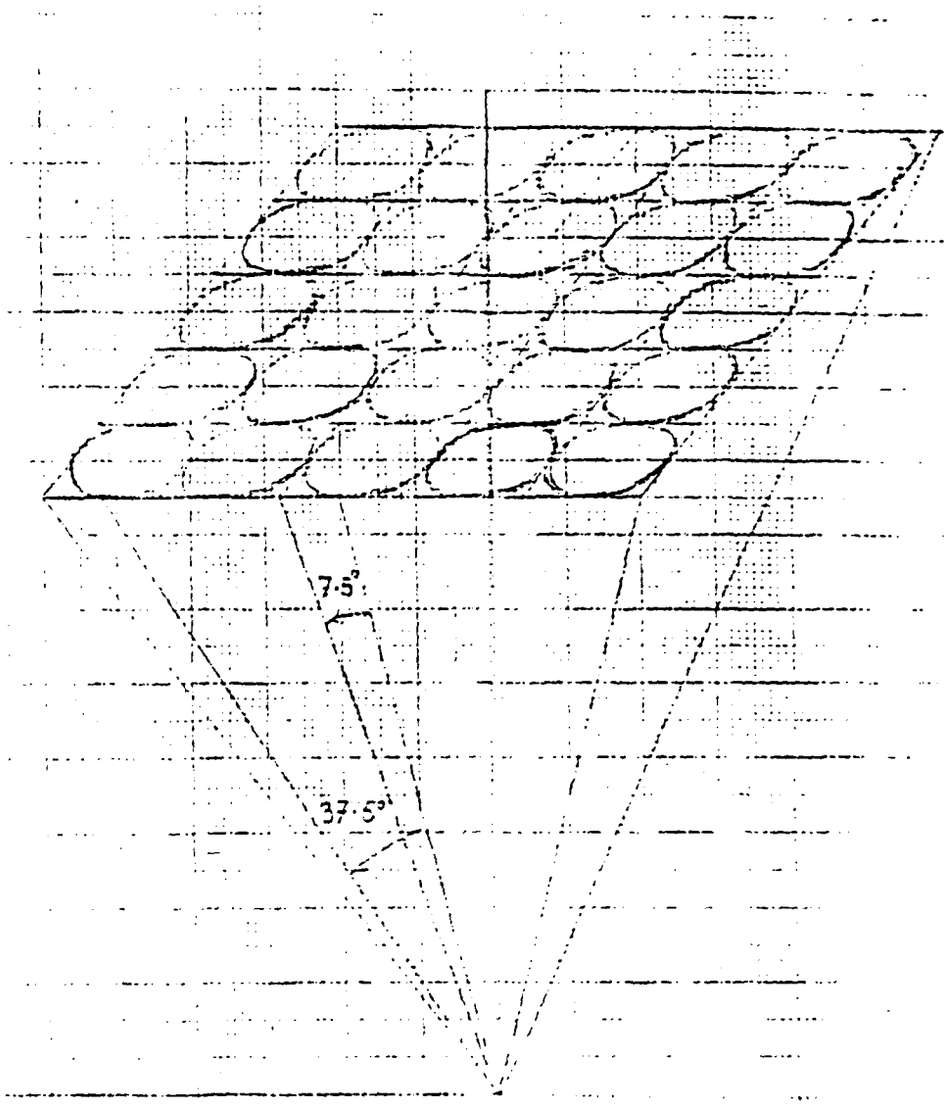
7·5°
37·5°

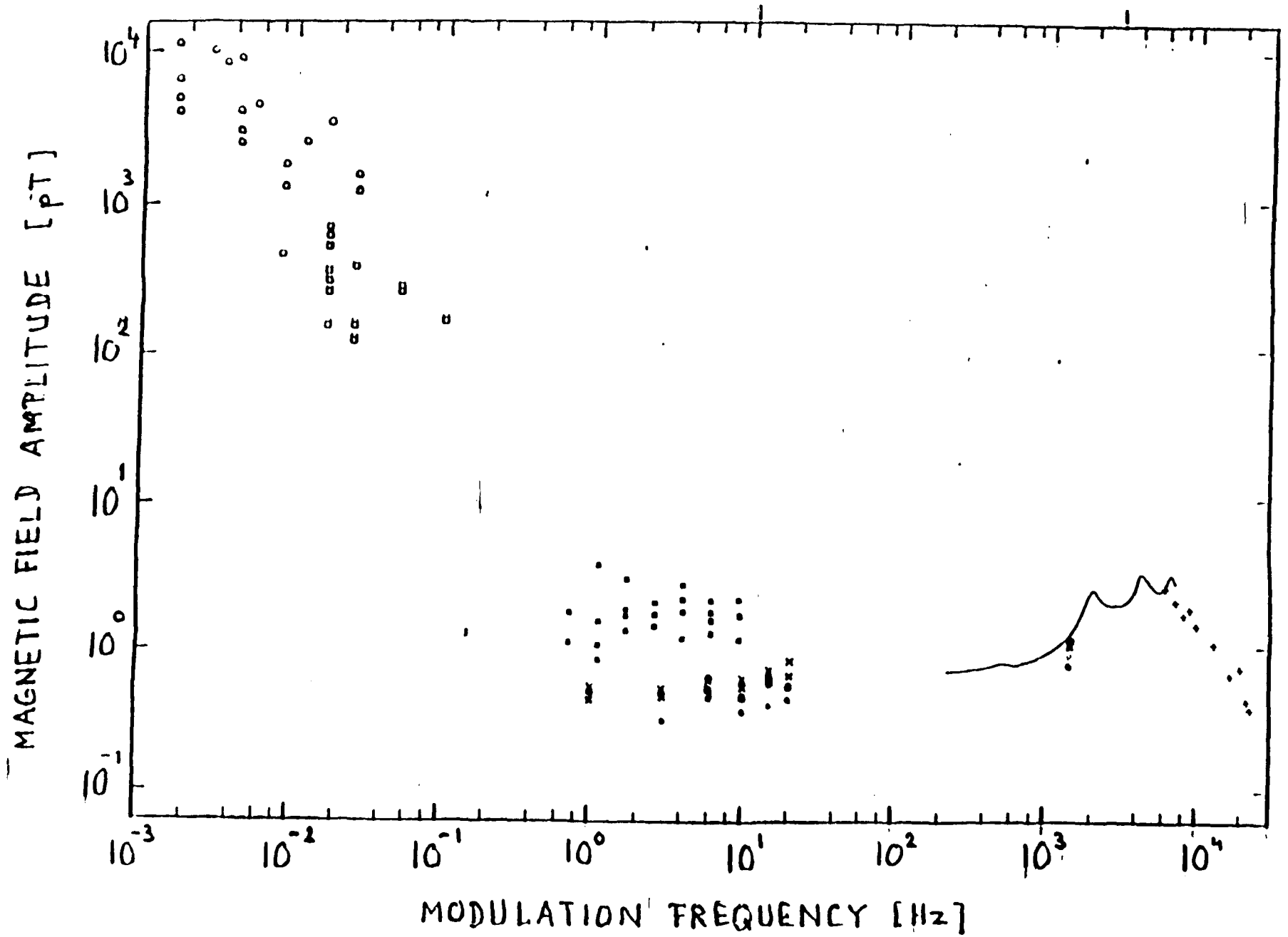
MAGNETIC FIELD AMPLITUDE [pT]
10^4
10^3
10^2
10^1
10^0
10^{-1}
10^{-3}
10^{-2}
10^{-1}
10^0
10^1
10^2
10^3
10^4
MODULATION FREQUENCY [Hz]